

The Impacts of Droughts, Local Land-Use Policies, and
Anthropogenic Activities against Water Resources in the
Upstream Sesan River Basin, Central Highlands of Vietnam

2022, September

VO NGOC QUYNH TRAM

Graduate School of Environmental and Life Science

(Doctor's Course)

OKAYAMA UNIVERSITY

ABSTRACT

Water resources management is considered based on quantitative and qualitative aspects. Managing water resources comprehensively requires an understanding of the vulnerability and sustainability of the current status of water resources. To develop water resources strategies, their impacts on water resources and agriculture should be discussed in the long-term period. With the increasing uncontrolled land-use changes, some land use policies were established to efficiently manage and reduce the negative effects impacting water quality downstream. The ineffectiveness of land-use change policies could impact dramatically the agricultural watershed's health. In recent years, the fast population growth leads to serious issues including deforestation, agricultural expansion, and urbanization in Southeast Asia. During the rainy season, excess discharge combined with intensive rainfall contributed to accelerating surface erosion and increasing nutrient losses deposited downstream. In the dry season, droughts coupled with water scarcity have increased pressure on water resources in these countries depending heavily on agriculture. The poorer farmers are more vulnerable when they had to struggle with drought condition in the dry season and erosion and water quality degradation in the rainy season.

The overall objective of this research is to assess the impacts of droughts, local land-use policies, and anthropogenic activities against water resources in the upstream Sesan river basin, Central Highlands of Vietnam. The specific objectives are as follows: (1) Evaluation of historical drought features in the Dakbla watershed, Central Highlands of Vietnam; (2) The impacts of land-use input conditions on flow and sediment discharges in the Dakbla watershed, Vietnam; (3) Effects of local land-use policies and anthropogenic activities against water quality in the upstream Sesan river basin, Vietnam.

At first, the historical drought features in the DBW were evaluated in terms of severity, duration and lag time, and drought frequency based on a combination of hydrological modeling and drought indices. Previously, much more attention to meteo-hydrological drought assessment was paid in Vietnam. While agricultural drought was rarely assessed because of the lack of observed agricultural data on the watershed scale. The important role of agricultural drought along with meteo-hydrological droughts was emphasized because of their larger impacts on agricultural productivity in the long-term period. The higher drought risk was found in the southwestern area, especially in agricultural drought. Rice is one of the main crops in these drought-prone agricultural areas. Also, the other agricultural crops grown in these areas are peanut, corn, soybean, pepper, cabbage, potato, cassava, sugarcane, and coffee. According to the Vietnamese National standard, the total water requirement for rice in the Central Highlands is

normally 600-700 mm/season. For coffee, the total water requirement is about 200-265 mm/season. Corn, peanut, soybean, and cabbage require about 120-200 mm/season. Nevertheless, these crops in drought-prone areas require a higher water requirement compared to the threshold of the national standard. These results can evaluate and visualize drought impacts on agriculture on a watershed scale in detail and support long-term drought management strategies (2021-2030), crop conversion and irrigation system planning. Farmers can understand drought characteristics in specific drought-prone areas to choose suitable crop types, soil characteristics, and irrigation methods.

Secondly, surveying and assessing land of the whole country and regions have been evaluated once every five years in Vietnam because of the dramatic changes in the relatively short period. Previously, the impacts of land-use changes have been evaluated by using a single static land use map in different periods. In another case, the delta approach is applied to analyze the land-use change impacts in two periods by using the simulation results derived from different static land use data. Nevertheless, the frequent land-use changes in a relatively short-term period could not be assessed appropriately in the watershed by these approaches. Also, one of the most challenges is lack of the spatial location information for these LUC policies leading to insufficient long-term land use planning and watershed management strategies. The impacts of land-use input conditions on flow and sediment discharge in the DBW were assessed by updating the different land-use conditions in the hydrological model. The best performance scenario with updating the four land-use conditions was chosen for further analysis. It means updating different land use input conditions had led to more realistic conditions in the modeling instead of using a single static land use map. Differences in flow and sediment simulation will affect the long-term land use plan in the target area.

Lastly, the effects of local land-use policies and anthropogenic activities on water quality in the upstream Sesan river basin were evaluated by updating land-use conditions following the local policy decision and local agricultural practices information into the model in the different periods. Applying the different local land-use change policies along with the extensive anthropogenic activities from 2005 onwards had significant effects on the aquatic environment downstream compared to before applying land use policies. The annual sediment, TN and TP loads were higher than in the northwestern area where the range land predominated, and in the southwestern area where arable land and permanent cropland predominated. If the changes in the 2005-2009 period do not apply, the huge amount of sediment, TN, and TP in the southwestern area will not estimate leading to significant impacts on the local land use strategies. Similarly, if the changes in the 2010-2014 period continuously apply for the 2015-2018 period, the large

amount of sediment, TN, and TP in the northwestern and southwestern areas will consider leading to the inaccuracy assessment of water quality downstream.

This dissertation is divided into six chapters. Chapter I illustrates the general introduction of some remarkable issues in water resources management in Southeast Asia. This part focuses on what the main issues are, what the existing difficulties are, how to tackle these phenomena, and which these approaches to solve these issues. The objectives for each issue were also mentioned in this part. Chapter II reviews the literature on the drought status and the characteristics of different droughts on a global/ regional scale. Understanding the impacts of drought on meteorology, hydrology, and agriculture in the different regions in Vietnam were summarized in this chapter. Another important part is that the impacts of local land-use policies and anthropogenic activities on the aquatic environment downstream were discussed. And then, the important role of updating multiyear land-use changes policies and agricultural practices in the hydrology modeling and its advantages were emphasized. Chapter III characterizes the historical drought features on meteorological, agricultural and hydrological aspects, and understands their spatial distribution on each subbasin. Chapter IV concentrates on establishing different updated land-use input conditions by using the developed land-use maps and then evaluates to what extent the updating land-use input conditions can improve the flow and sediment outputs of the model. Chapter V expands the scale of the target area including the PKW and DBW belonging to the upstream Sesan river basin. The impacts of different land-use policies and agricultural practices on the aquatic environment in the different periods were evaluated and then determined how to improve erosion and water quality in the target river basin. Chapter VI draws out the general conclusions based on these above results before proposing the recommendation on water resource management for the target area in particular and the Central Highlands region in general.

In summary, an image of popular issues concerning water resources and agriculture aspects in the upstream of the Sesan river basin was shown based on the spatio-temporal analysis on the watershed scale. The specific areas occurring the different issues such as droughts, erosion, and nutrient losses were described in this dissertation. These findings could support policy-decision makers in implementing more effective local drought management strategies, land-use planning policies, soil conservation plans, and water resource management strategies for the watershed in the future accordingly by considering local water resource availability and suggesting crop conversion planning for the local farmers.

ACKNOWLEDGEMENTS

I would wish to thank all my teachers, family, and friends for motivating and supporting me throughout my academic career for a while. I feel very fortunate to possess had the chance to work with some great mentors during my time at Okayama University. First, I touch my heartfelt gratitude to my supervisor Assoc. Professor Hiroaki Somura for accepting me as his student, for his wonderful guidance, freedom, and creativity in my research, and for thoroughness in reviewing my research which will help my future career tremendously. Without his patience, valuable comments, and prompt feedback, it had been impossible to complete my research during my three years in Japan.

I would like to send my sincere thanks to my co-supervisors Professor Toshitsugu Moroizumi and Professor Morihiro Maeda for their participation in my research, and their valued feedback throughout the tutorial counseling per annum and other research activities for three years.

Also, I wish to extend my sincere thanks to the committee members for their encouragement in my dissertation committee and their valued feedback in improving the research.

I especially thank Professor Nguyen Kim Loi for always finding time from his busy schedule to provide the academic knowledge and helping me follow my research career. Many thanks to all my colleagues at the Research Center of Climate Change, Nong Lam University for supporting and encouraging me to overcome the obstacles with the distance below.

I would also like to thank Professor Célia Joaquim-Justo and Professor Bernard Tychon at Liege University, Belgium for being the reason I started enjoying the research and for identifying the potential in me to pursue Ph.D.

I am deeply indebted to my family and friends for serving as my emotional support system during my ups and downs in these past three years. Special thanks to all my colleagues in our lab for their personal and professional help and for making my office a happy place.

Lastly, I am grateful to my parents and my relatives for believing in me more than I believed in myself, for always putting up with me during my stress-filled days, and for being a mentor for life. Without you by my side, this Ph.D. would not have been possible. Above all, I am trying to learn new knowledge and improve my personal skills day by day to become a more perfect person in the future.

TABLE OF CONTENTS

ABSTRACT	i
ACKNOWLEDGEMENTS	iv
TABLE OF CONTENTS	v
LIST OF FIGURES.....	ix
LIST OF TABLES	xii
LIST OF ABBREVIATIONS	xiv
CHAPTER 1. INTRODUCTION	1
1.1. Background	1
1.2. Research objectives	4
CHAPTER 2. LITERATURE REVIEW	6
2.1. The drought status and the characteristics of different droughts	6
2.1.1. Global scale.....	6
2.1.2. Regional scale: Vietnam	7
2.2. Evaluating the impacts of land-use change policies and anthropogenic activities on the aquatic environment downstream.....	11
2.2.1. Impacts of land-use change policies and human activities on the aquatic environment downstream.....	11
2.2.2. Importance of updating multiyear land-use changes policies and agricultural practices in the hydrology modelling.....	14
CHAPTER 3. EVALUATION OF DROUGHT FEATURES IN THE DAKBLA WATERSHED, CENTRAL HIGHLANDS OF VIETNAM.....	17
3.1. Introduction	17
3.2. Materials and methods	18
3.2.1. Study area.....	18
3.2.2. Methods.....	19
3.3. Results	22
3.3.1. Reproducibility of river discharge	22
3.3.2. Temporal variation of historical drought features.....	23
3.3.3. Spatial distribution of historical drought features.....	26

3.4. Discussion	27
3.4.1. The importance of drought evaluation in agriculture in the Central Highlands of Vietnam	27
3.4.2. Contribution to future drought mitigation in the Central Highlands of Vietnam	28
3.5. Conclusions	29
3.6. Limitation and recommendation	29
CHAPTER 4. THE IMPACTS OF LAND-USE INPUT CONDITIONS ON FLOW AND SEDIMENT DISCHARGES IN THE DAKBLA WATERSHED, VIETNAM.....	30
4.1. Introduction	30
4.2. Materials and methods	31
4.2.1. Study area.....	31
4.2.2. Input data.....	33
4.2.3. Methods.....	34
4.2.4. Uncertainty analysis method.....	39
4.3. Results	39
4.3.1. Reproducibility of flow and sediment in the calibration period (2000–2009)..	39
4.3.2. The influence of land-use update on flow in the validation period (2010–2018)	41
4.3.3. The influence of land-use update on sediment in the validation period (2010–2018).....	42
4.3.4. The responses of flow and sediment to the different land-use input conditions	43
4.4. Discussion	46
4.4.1. Importance of land-use update for improving modeling performance	46
4.4.2. Influence of land-use update for flow and sediment simulation.....	47
4.4.3. Land-use policies in the region for the future, including the DBW, and the contribution from the model simulation.....	48
4.5. Limitation of the study	49
4.6. Conclusions	50

CHAPTER 5. EFFECTS OF LOCAL LAND-USE POLICIES AND ANTHROPOGENIC ACTIVITIES ON WATER QUALITY IN THE UPSTREAM SESAN RIVER BASIN, VIETNAM.....	51
5.1. Introduction	51
5.2. Data and methods	53
5.2.1. Study area.....	53
5.2.2. Methods.....	55
5.3. Results	63
5.3.1. Sensitivity analysis for model simulation with updates to land-use changes and agricultural practices information	63
5.3.2. Reproducibility of river discharge, sediment, and nutrient loadings during the 2000–2018 period.....	65
5.3.3. The changes in river discharges, sediments, and nutrient loading at the outlets (Poko outlet and Dakbla outlet)	71
5.3.4. Spatial distribution of annual sediment, TN, and TP loads in each subbasin...	74
5.3.5. The changes in sediment, TN, and TP loadings for each land use during the four periods	76
5.3.6. The changes in total annual sediment, TN, and TP loadings at the inflow to the lake	77
5.4. Discussion	80
5.4.1. Impacts of different land-use policies and agricultural practices on river discharge, sediment, and nutrients	80
5.4.2. Spatial changes in river discharge, sediment, and nutrient loadings during the different periods	81
5.4.3. Impacts of different land-use policies and agricultural practices on the downstream aquatic environment, particularly Yaly lake	82
5.4.4. Land use and crop conversion policies for the future in the Central Highlands of Vietnam, including the target watersheds	83
5.5. Limitation of the study	84
5.6. Conclusions	85
CHAPTER 6. CONCLUSIONS AND RECOMMENDATION	87

APPENDIX	91
REFERENCES.....	97

LIST OF FIGURES

Figure 3.1. Location of the DBW.....	19
Figure 3.2. Simulated and observed river discharges at the Kon Tum station in the calibration period (2000-2009) and validation period (2010-2018)	23
Figure 3.3. Drought severity for the <i>SPI</i> , <i>SDI</i> , and <i>SSI</i> (3-, 6-, 12- month time scales). The inward tick of each year starts from September. The years and duration of the El Niño events were referred from FAO (2014), CCAFS-SEA (2016), Phong and Chinh (2017), and Williams et al. (2019)	24
Figure 3.4. Drought frequency of <i>SPI</i> , <i>SSI</i> , and <i>SDI</i> indices between the different time scales	26
Figure 3.5. Spatial distribution of the 12-month time scale drought frequency in the DBW	27
Figure 4.1. Location of the DBW. The model performance was evaluated at Kon Tum hydrological station.....	32
Figure 4.2. The 2005, 2010, 2015, and 2018 land-use maps in the DBW. The major changes in land use are shown in the legend for the 2010, 2015, and 2018 maps. AGRC: agricultural land, non-row crops; AGRR: agricultural land row crops; COFF: coffee; FRSE: forestry land; F46: mixed forest (400–600 m); F68: mixed forest (600–800 m); F810: mixed forest (800–1,000 m); FRST: mixed forest; ORCD: orchard; RICE: rice; RNGB: rangeland; RUBR: rubber; URBN: urban; WATR: water.....	37
Figure 4.3. Land-use map input conditions in simulation scenarios 1–4. S1 represents the static input condition and S2, S3, and S4 represent the three updated input conditions	38
Figure 4.4. The correlation between the observed and simulated flow (a) and sediment (b) in the calibration period. S1 represents the simulation result when using the 2005 land-use map for the entire calibration period. S2, S3, and S4 represent the simulation results when using the two land-use condition types, namely, the 2005 land-use map from 2000 to 2004, and the linearly interpolated map for the 2010 land-use condition during the calibration period.....	40
Figure 4.5. The correlation between the observed and simulated flow discharges in the validation period. S1 represents the simulation results when using the 2005 LU map for	

the entire validation period. S2 represents the simulation results when using the 2010 LU condition for the entire validation period. S3 represents the simulation results when using two LU condition types for 2010 and 2015, and then linearly interpolating toward 2015 after 2010, where the 2015 LU condition is employed for the 2015–2018 simulation. S4 represents the simulation results when using three LU condition types during the validation period and linearly interpolating between two LU conditions.....41

Figure 4.6. The correlation between the observed and simulated sediment discharges in the validation period. S1 represents the simulation results when using the 2005 LU map for the entire validation period. S2 represents the simulation results when using the 2010 LU condition for the entire validation period. S3 represents the simulation results when using two LU condition types for 2010 and 2015 and then linearly interpolating toward 2015 after 2010, where the 2015 LU condition is then employed during the 2015–2018 simulation. S4 represents the simulation results when using three LU condition types during the validation period and then linearly interpolating between two LU conditions42

Figure 4.7. The differences of the total annual flow between the different updated land-use scenarios.....44

Figure 4.8. The differences of the total annual sediment between the different updated land-use conditions.....44

Figure 4.9. Change of cumulative sediment discharge between the scenarios (2000-2018)46

Figure 5.1. Location of the PKW and DBW. River discharges were observed at Dak Mot station in PKW and Kon Tum station in DBW. SPCs 1, 2, 3, and 4 represent the four monitoring points of water quality in the PKW, while SDLs 2 and 3 represent the two monitoring points of water quality in the DBW.....55

Figure 5.2. The land use maps for 2005, 2010, 2015, and 2018 in the target river basin. The main land-use types include AGRC: agricultural land, non-row crops; AGRR: agricultural land, row crops; COFF: coffee; FRSE: forestry land; F46: mixed forest (400–600 m); F68: mixed forest (600–800 m); F810: mixed forest (800–1,000 m); FRST: mixed forest; ORCD: orchard; RICE: rice; RRGB: rangeland; RUBR: rubber; URBN:

urban; and WATR: water. The symbol “+/-” indicates the increased/decreased percentage of land use categories of that period compared to the previous period.....60

Figure 5.3. Global sensitivity analysis of river discharge, sediment, and nutrients simulations.....64

Figure 5.4. The relationship between the observed and simulated daily river discharge, TN, TP, NO₃-N, and NH₄-N loadings in the PKW. The model was calibrated from 2000 to 2015 and validated from 2016 to 2018 for river discharge. The calibration and validation periods for the remaining variables were from 2014 to 2015 and from 2016 to 2018, respectively.....67

Figure 5.5. The relationship between the observed and simulated daily river discharge and sediment loading in the DBW. The model was calibrated from 2000 to 2015 and validated from 2016 to 2018 for river discharge and sediment68

Figure 5.6. The relationship between the observed and simulated daily TN concentration at the five monitoring points in the PKW (SPC1, SPC3, and SPC4) and DBW (SDL2 and SDL3). The average observed and simulated values are described under each graph ...69

Figure 5.7. The relationship between the observed and simulated daily TP concentration at the five monitoring points in the PKW (SPC1, SPC3, and SPC4) and DBW (SDL2 and SDL3). The average observed and simulated values are described under each graph ...70

Figure 5.8. Total annual river discharge, sediment, TN, and TP loadings at the outlets from 2000 to 2018.72

Figure 5.9. Average monthly total river discharge, sediment, and nutrient loadings at the outlets during the 2000–2018 period.....73

Figure 5.10. Total cumulative sediment, TN, and TP at the outlets during the whole period74

Figure 5.11. Spatial distribution of annual sediment, TN, and TP loadings in each subbasin.....75

Figure 5.12. Changes of sediment, TN, and TP loadings into the reach according to land-use type during the four periods.....77

Figure 5.13. Changes in the total annual sediment, TN, and TP loadings at the inflow to the lake during the four periods. The total average annual rainfall (mm) was calculated using the Thiessen method.79

LIST OF TABLES

Table 2.1. Research of drought characteristics in the different regions of Vietnam.....	10
Table 2.2. Research of the impacts of LUC and anthropogenic activities on flow, sediment, and nutrients in the different regions of Vietnam.....	14
Table 2.3. Updating multiyear land-use input conditions and agricultural practices in the original SWAT model by different approaches over the world.....	15
Table 3.1. Input data information for the SWAT.....	20
Table 3.2. Eight sensitive parameters selected by the SUFI-2 algorithm and their ranges for the parameter value optimization. The calibrated values are used for modifying the original values in the SWAT by relative changes.....	23
Table 3.3. The correlation R^2 between SPI and SSI or SDI for the 0-, 1-, and 2- month lag periods. Bold values represent the highest correlation between SPI and SSI or SDI (3-, 6-, 12- month time scales)	25
Table 3.4. The drought duration, minimum and maximum drought severity of drought events recorded by SPI -12, SSI -12, and SDI -12 during a 2001-2018 period (indices ≤ -1)	25
Table 4.1. Statistical summary of the observed river flow and total suspended sediment (TSS) concentration at the Kon Tum station (2000–2018). Min/Max: minimum and maximum values; SD: standard deviation.....	34
Table 4.2. The statistical values of R^2 , NSI, and PBIAS in the static land-use condition (S1), featuring the 2005 land-use map during entire simulation period of 2000–2018, and the updated land-use conditions (S2, S3, and S4). R^2 : coefficient of determination; NSI: Nash–Sutcliffe index; PBIAS: percent bias	40
Table 4.3. Relative difference (RD) values of the target components with the updated land-use input conditions vs. static input condition.....	44
Table 5.1. Necessary input data of the model	57
Table 5.2. Sensitive parameters selected for the calibration of river discharge, sediment, and nutrients and their final optimal values	58
Table 5.3. Agricultural practices information	61

Table 5.4. Criteria of performance evaluation for river discharge, sediment, nitrogen, and phosphorus on the watershed scale according to Moriasi et al. 201563

Table 5.5. The results of three statistical values (R^2 , NSI , and $PBIAS$) in the calibration period and validation period. The model was calibrated from 2000 to 2015 and validated from 2016 to 2018 for river discharge and sediment. The calibration and validation periods for the TN, TP, NO_3-N , and NH_4-N variables were from 2014 to 2015 and from 2016 to 2018. The sediment, TN, TP, NO_3-N , and NH_4-N variables were calibrated and validated by load66

Table 5.6. The highest and lowest total annual river discharge, sediment, TN, and TP loadings at the outlets from 2000 to 2018.....71

Table 5.7. Comparisons of rainfall, total annual sediment, TN, and TP loadings at the inflow to the lake between pre- and post- land-use policy application, and between land-use policy period 3 and period 4. The first period, from 2000 to 2004, represents a base period without the implementation of land-use policies (period 1). The remaining periods illustrate the following changes in land-use policies: the second period (2005–2009), conducted for afforestation, agricultural expansion, and urbanization (period 2); the third period (2010–2014), crop conversion policy involving a shift from mixed forests to rubber forests (period 3); and the fourth period (2015–2018), crop conversion policy involving a shift from insufficient rubber forests to orchards (period 4). The total annual loadings during the target period per 1,000 mm of rainfall (thousand ton/period/ 10^3 mm) were calculated at the inflow to the lake for the annual sediment, TN, and TP to evaluate the influence of land-use policies.....79

LIST OF ABBREVIATIONS

AD	Agricultural drought
CCAFS-SEA	CGIAR Research Program on Climate change, Agriculture and Food Security-Southeast Asia
DBW	Dakbla watershed
ESCAP and ASEAN	The Economic and Social Commission for Asia and The Association of the Southeast Asian Nations
FAO	Food and Agriculture Organization
GLDARD	Gia Lai provincial Department of Agriculture and Rural Development
GSO	General Statistics Office of Vietnam
HD	Hydrological drought
HRU	Hydrological Response Unit
JICA	Japan International Cooperation Agency
KTDARD	Kon Tum provincial Department of Agriculture and Rural Development
KTDONRE	Kon Tum provincial Department of Natural Resource and Environment
KTGSO	Kon Tum General Statistics Office
LUC	Land use changes
MARD	Ministry of Agriculture and Rural Development
MD	Meteorological drought
OECD	Organisation for Economic Cooperation and Development
PKW	Poko watershed
SDI	Streamflow Drought Index
SPI	Standardized Precipitation Index
SSI	Standardized Soil Moisture Index
SWAT	Soil and Assessment Tool
SWAT-CUP	Calibration Uncertainty Program
TN	Total nitrogen
TP	Total phosphorus

UNESCO	United Nations Educational, Scientific and Cultural Organizations
VAWR	Vietnam Academy for Water Resources
WRD	Directorate of Water Resources
WHO	World Health Organization
WMO and GWP	World Meteorological Organization and Global Water Partnership

CHAPTER 1. INTRODUCTION

1.1. Background

Water resources management is considered based on quantitative and qualitative aspects. Managing water resources comprehensively requires an understanding of the vulnerability and sustainability of the current status of water resources. To develop water resources management strategies, their impacts on different aspects should be considered in the long-term period. The rapid population growth and anthropogenic activities are increasing the pressure on water resources. In recent decades, the percentage of pollution from the agriculture aspect was higher than in the first two-thirds of the twentieth century (Holden et al., 2015). Some rivers in Southeast Asia are faced with water quality degradation, mainly from agricultural practices although this region belongs to the tropical monsoon climate with a plentiful water supply (World Health Organization: WHO, 2010). To efficiently manage and reduce these negative effects impacting water quality downstream, some policies were established by the governments and local governments based on the increasing uncontrolled land-use changes and agricultural practices. The land-use change policy is one of the most noticeable policies concerning water resource management. The policies in each country are quite different because it depends on the cultural identity, soil and land use characteristics, and climatic condition as well as their self-conception and self-perception.

In Vietnam, surveying and assessing land of the whole country and regions have been evaluated once every five years because of the dramatic changes in the relatively short period (National Assembly of Vietnam, 2013). Among different regions in Vietnam, Central Highlands seems to be a hot spot for intense land-use conversion in recent years. Although the information of land-use change occurs on the local scale, its effects can damage the larger scales including the regional or global scales for a long time (Zhao et al., 2006). Along with urbanization, many anthropogenic activities including deforestation, agricultural expansion, and crop conversion have strongly occurred in this region. The agricultural expansion towards the steep-slope regions and the indiscriminate deforestation for agricultural purposes to ensure food and feed demand has been increasing vulnerability in the mountainous regions, especially in the intensive-farming areas (Pierret et al., 2011; Frohlich et al., 2013). The ineffectiveness of land-use change policies and anthropogenic activities impacted dramatically to the agricultural watershed's health was indicated. Evidence revealed that conversion from forests to agricultural land impacted streamflow (Cung et al., 2022), the soil

and nutrient losses downstream (Altdorff et al., 2017), and hydrological processes (Affessa et al., 2022).

An illustration is that many projects have been conducted to convert mixed forests into rubber forests in Kon Tum and Gia Lai provinces to create jobs and generate income for local people, especially ethnic minorities since 2010 (Prime Minister, 2009); nevertheless, most of the new rubber trees have not grown in Gia Lai Province after two or three years of planting because of inappropriate soil with low fertility and poor organic compounds. From 2015 onwards, the conversion of inefficient rubber areas to other crops has been conducted in Gia Lai Province to solve these obstacles. Additionally, excess discharge combined with intensive rainfall during the rainy season, contributed to accelerating surface erosion and then increasing nutrient loss deposited downstream (Shi et al., 2012; Folliott et al., 2013). The pollutant discharges from the point and non-point sources increase the loads in the watershed with significant impacts on crop productivity (Alexander et al., 2008). Previously, the impacts of land-use changes have been evaluated by using a single static land use map in different periods (Son et al., 2015; Li et al., 2019; Munoth and Goyal, 2020; Makhtoumi et al., 2020). In another case, the delta approach is applied to analyze the land-use change impacts in two periods by using the simulation results derived from different static land use data. Nevertheless, the frequent land-use changes in a relatively short-term period could not be assessed appropriately in the watershed by these approaches. Also, one of the most challenged to evaluate the impacts of land-use changes in a watershed is lack of the spatial location information for these LUC policies leading to insufficient long-term land use planning and watershed management strategies.

While droughts coupled with water scarcity have exacerbated issues during the dry season. The water shortage in 2030 is forecasted by approximately 40% over the world in comparison between predicted water demand and available water supply (World Bank, 2017). Prolonged water shortage, hydrological instability along with extreme weather events will threaten global stability. If drought prolongs for a long time, it creates an enormous threat to agriculture leading to the decline of regional socio-economic development in some countries depending heavily on agriculture (World Meteorological Organization and Global Water Partnership: WMO and GWP, 2016). Approximately four-fifths of the economic impact of drought is absorbed by agriculture during the past 30 years in Southeast Asia (The Economic and Social Commission for Asia and the Pacific and The Association of Southeast Asian Nations: ESCAP and ASEAN, 2020). Agriculture can rebound or be impaired within a very short period depending upon the strength of drought conditions or precipitation events.

Central Highlands of Vietnam is also one of the most affected regions by water shortage and drought against crop production (CGIAR Research Program on Climate Change, Agriculture and Food Security - Southeast Asia: CCAFS-SEA, 2016). Rainfall in the dry season was normally only 10-15% of that of the whole year in this region (Vietnam Academy for Water Resources: VAWR, 2012). In strong drought events such as 2004-2005, 2010, and 2015-2016 events, prolonged droughts occurred across a large area. The rainfall was 30-50% lower than the average for many years from 2000 to 2016. Thus, the area irrigated directly from irrigation projects was only 30% of the cultivated area (Directorate of Water Resources: WRD, 2016). The water volume of irrigation reservoirs in the Central Highlands fell to 10-50% of their designed capacity in early April 2016 (CCAFS-SEA, 2016).

The irrigation efficiency was less than 60% and 70% of the designed irrigation capacity in Kon Tum and Gia Lai Provinces, respectively (Kon Tum provincial Department of Agriculture and Rural Development: KTDARD, 2018; Gia Lai provincial Department of Agriculture and Rural Development: GLDARD, 2019). Many drought damages have been recorded and the solutions have been enforced. In the face of droughts that are more severe in recent years, the local government organized many action programs to allocate water resources appropriately and mobilized local people to irrigate crops but still needed to maintain clean water for domestic aspects. Accordingly, some action programs are conducted such as cleaning and dredging wells, digging wells, utilizing water economically, and sharing water resources. For some water scarcity areas, water resources are transferred from other regions to respond to water demand leading to people's lives not being turned upside down. However, in some areas without dams, irrigation water is mainly utilized from ponds, lakes, or streams, but prolonged heat makes them become exhausted. Moreover, the expenses of drilling wells and transferring crops are enormous. Short-term strategies were implemented by the local government each year to mitigate drought issues and water shortages (Kon Tum People's Committee, 2019). Nevertheless, assessing drought impacts on agriculture to how agricultural productivity can improve in the dry condition was not fully mentioned in these policies. Also, the improvement of agricultural productivity in the drought condition is not efficiently discussed. Since 2020, a "Project on drought management in Kon Tum Province during the 2021–2030 period" was approved to mitigate the impacts of prolonged droughts on agriculture, which involved building a set of tools for drought management and promoting irrigation infrastructure investment (Kon Tum People's Committee, 2020). As for local farmers, switching crops in the drought areas was not fully efficient because of the lack of detailed drought information for crop cultivation and irrigation. The poorer farmers are most

vulnerable as they had to struggle with drought conditions in the dry season as well as erosion and water quality degradation in the rainy season. The current irrigation, reservoirs, and crop conversion projects along with advanced agricultural applications are carried out to support local farmers. Nevertheless, some farmers still choose the traditional farming methods instead of converting advanced technology because of the expensive cost of equipment, operating, and maintenance costs. Changing human awareness to reduce fertilizer use and limit indiscriminate crop conversion in a short period is an obstacle for local authorities in implementing local policies accordingly.

Understanding the drought characteristics and evaluating the effects of local land use policies and anthropogenic activities on the aquatic environment downstream is extremely essential in water resources management, which plays a key role to determine available strategies for soil conservation, land-use changes, drought and water resource management based on local specific set policies and regulations.

1.2. Research objectives

The overall objective of this research is to assess the impacts of droughts, local land-use policies, and anthropogenic activities against water resources in the upstream Sesan river basin, Central Highlands of Vietnam. The specific objectives are as follows:

- *Objective 1: Evaluation of historical drought features in the Dakbla watershed (DBW), Central Highlands of Vietnam.*

Tasks in Objective 1 were (1) to characterize meteorological (Standardized Precipitation Index: *SPI*), agricultural (Standardized Soil Moisture Index: *SSI*), and hydrological (Streamflow Drought Index: *SDI*) droughts on different temporal scales, and (2) to understand the distribution of historical drought features on each subbasin in the DBW.

- *Objective 2: The impacts of land-use input conditions on flow and sediment discharges in the DBW, Vietnam.*

Tasks in Objective 2 were (1) to create land-use maps following local statistical information in a watershed, where GIS-based information of land-use changes is infrequently updated while in the context of complicated local land-use policy changes, (2) to establish updated land-use input conditions by using the developed land-use maps, and then (3) to evaluate to what extent the updating land-use input conditions can improve the flow and sediment outputs of the model.

- *Objective 3: Effects of local land-use policies and anthropogenic activities against water quality in the upstream Sesan river basin, Vietnam.*

Tasks in Objective 3 were (1) to evaluate the impacts of different land-use policies and agricultural practices on discharge, sediment, and nutrients in the different periods based on the temporal and spatial distributions; (2) to understand the effects of terrestrial activities by each policy on the aquatic environment downstream and (3) to determine how to improve the erosion and water quality in the target river basin.

CHAPTER 2. LITERATURE REVIEW

2.1. The drought status and the characteristics of different droughts

2.1.1. Global scale

Drought is known as a natural phenomenon creating negatively affects food security and farmers' livelihood through reducing crop production and economic growth. Droughts can appear from hydrometeorological processes that are caused by precipitation deficit leading to reduce surface water or groundwater, creating significantly drier conditions than normal as well as limiting moisture availability to probable damage on a large scale (WMO and GWP, 2016). In recent years, there had a significant contrast in rainfall among wet/dry regions and wet/dry seasons. Droughts became more intensive, more extensive, and longer than in the past. Droughts could not be caused by climate change, however, climate change may exacerbate and expand their extent, especially in the subtropical dry regions (Trenberth et al., 2014).

Understanding the drought features is necessary throughout utilizing drought detection and monitoring indices. Similar to other hazards, droughts are characterized by the severity, duration and timing, and frequency (WMO and GWP, 2016). Meteorological drought is one of the common types of drought that is assessed based on rainfall. However, it is not enough just with rainfall information to assess drought characteristics as meteorologic indices describe the anomalies of climate separately from their hydrologic conditions while hydrology-based indices can directly describe the effects of climate anomalies on their hydrologic context (Shukla and Wood, 2008). The strength of the index based on runoff are its forecastability depending on both climate and hydrologic conditions and simulation of calibrated runoff is more reasonable for real-time application than the measured data. In agricultural areas, drought impacts should be evaluated based on several factors as evapotranspiration, soil water content, and crop yield (Łabędzki, 2007). Meteo-hydrological drought was projected to be less severe than agricultural drought, especially in the upstream parts which were expected to increase the severity of agriculture drought (Sun et al., 2019). Nevertheless, the lack of observed data for the long-term periods was one of the difficulties in drought forecasting and operational planning to mitigate the negative effects. Utilizing reliable information on drought is necessary to evaluate the drought characterization more comprehensively throughout the multiple variables (Hao and AghaKouchak, 2013). Understanding and evaluating the impacts of droughts on water resource systems are crucial to prevent the risks and make reasonable strategies.

Kamali et al. (2017) indicated that the probability of severe and extreme drought intensities will increase for meteo-hydrological and agricultural droughts in Iran. By using SPI, it is predicted to decrease the drought duration and frequency while there were expected to decrease using two other indices represented to hydrological and agricultural droughts, and the highest drought exposures were found in agriculture. In India, the drought severity, duration, and frequency had a rising tendency by using the Standardized Precipitation Evapotranspiration Index (SPEI). The drought frequency ranging from severe to extreme levels was increased under the projected climate scenarios (Bisht et al., 2019). As for Southern Africa, the temporal variability of droughts was evaluated through using the four SPI, SPEI, SRI, and SSI indices, of which SPI and SPEI have shown the best performance of all drought events in terms of drought severity. The evaluation using SPEI indicated that there was an increasing tendency of drought severity and SPEI had a higher correlation with hydrological drought (Lweendo et al., 2017). By using Agricultural Drought Intensity (ADI) index, the impacts of meteorological drought on agriculture were found in areas with abundant water resources as the Southwest part of China which was the most vulnerable to droughts (Lu et al., 2017). The role of adjusting the percentage of crop planting was important to increase the water-use efficiency in agriculture and minimize the risks in humid regions. In the important stages of crop growth, drought indices had a strong correlation with crop yields as Narasimhan and Srinivasan (2005) mentioned. The Soil Moisture Deficit Index (SMDI) and Evapotranspiration Deficit Index (ETDI) were the reasonable drought indices for agricultural drought monitoring in the United States.

2.1.2. Regional scale: Vietnam

Viet Nam located in the Southeast Asia region with the typical tropical and tropical monsoon climate led to the diversity of rainfall patterns and the larger volume of rainfall. The rainfall predominated by about 80-90% in the rainy season starting from April to October (VAWR, 2012). Despite the high average rainfall, the distribution of rainfall is uneven caused by the water shortage and droughts in many regions. In recent years, the increase in average temperature and evaporation has led to a more extreme rainfall distribution, especially in the dry season. Consequently, the rainfall decreased significantly in the dry season whereas dramatically increased in the remaining season (Daniel and Ardakanian, 2015). The climatic and drought characteristics of regions in Vietnam are described in more detail in the Regional workshop on capacity development to support national drought management policies for Asia-Pacific countries in 2015 as follows:

➤ Northern region: The dry season starts from September or October, droughts mainly occur in the winter-spring crop season when lack of rainfall and the low water level of reservoirs.

➤ Central coastal lands area: Droughts occur with the highest frequency in both winter-spring and summer-autumn crop seasons compared to other regions. Along with the hot climate, the low water retention capacity of reservoirs and lack of rainfall resulted in droughts

➤ Central Highlands and Southeast areas: Droughts appear in all cropping seasons, in which the winter-spring crop season had the more frequent drought. This phenomenon is mainly impacted by climatic conditions as many farmlands do not depend on the irrigation network.

➤ Southwest area (Mekong Delta): Water scarcity and droughts appear in all cultivation seasons leading to salt intrusion in this area. These issues had impacted crop cultivation in particular and agriculture in general.

The northern region of Vietnam had a dramatic increase in rainfall while there was a decreasing tendency in the Southern region (Hung et al., 2020). Moreover, the temperature had a rising tendency, mainly in the Southern region caused by the higher drought frequency and severity in this region, particularly in the South Central region and the Mekong Delta. At the beginning of the dry season, it can be seen that significant differences in the frequency of onset of drought episodes were found in the south of Vietnam (Stojanovic et al., 2020). The changes in temperature and evapotranspiration are important to drought intensity. Nguyen and Rosbjerg (2007) mentioned that El Niño had a stronger impact in the south of Vietnam. This is also emphasized by Nguyen (2006) that most regions in Vietnam faced the dramatic negative effects of severe drought resulting in a serious impact on people's livelihood and socio-economic development, especially in the central and south regions. The seasonal changes in temperature and precipitation in the Central Highlands and Southern regions were smaller than in others. ENSO was highly sensitive to drought in the South Central and Southern regions (Phong et al., 2019). Vu et al. 2015b mentioned that all the drought events occurred about a year after the strong El Niño years before 2000. The drought corresponding to the El Niño events has been dramatically impacting Vietnam again from 2014 onwards, of which eighteen provinces belonging to the South Central, Central Highlands, and Mekong Delta regions were severely impacted (CCAFS-SEA, 2016). Quang et al. (2021) also confirmed that El Niño had significant effects on extreme drought events as well as all these events are strongly related to El Niño striking events. There was an increasing tendency of drought intensity, duration, and frequency during the 1985-2018 period. In recent years, the

drought events became more severe, and extreme drought events tended to occur in the whole Mekong Delta region. It is expected that the precipitation and temperature will increase leading to rising river discharge in the future from 2071 to 2100. The drought events will increase while the intensity and frequency will decrease in this period. Also, the number of drought months and the drought severity from severe to extreme drought levels will increase (Vu et al., 2017).

Among these regions, Central Highlands is one of the most sensitive regions to the El Niño effect resulting in serious drought in the dry season, which leads to crop damage, productivity decline, and water scarcity in agriculture (CCAFS-SEA, 2016). The highest drought frequency in the Central Highlands area occurred from January to the end of April with a value of over 60%. In April 2016, the irrigation reservoirs had a lower capacity than the designed capacity by 50-60%. The areas irrigated directly from the irrigation works occupied only 30% of the cultivated area. And then, the total area to be stopped in the Winter-Spring crop in the 2015-2016 period was 2,865 ha because of lack of water. (WRD, 2016). The communes of Gia Lai and Dak Lak provinces are the most impacted areas in this area (Tri et al., 2019). The Central Highlands is known as the largely drought-prone region that plays a key role in perennial plantations (Vu et al., 2015a). More than 90 % of the higher drought probabilities were found in January in this region (Hang et al., 2014). Furthermore, the water discharge and soil water content are expected to decrease dramatically and there would be increasing tendencies of the drought severity, duration, and frequency in the 2016–2040 period (Sam et al., 2019). Based on the fast growth of population, lack of arable land and agricultural products occurred strongly in Central Highlands as the change from a part of forest land to arable and residential land. These activities just concentrated on short-term planning without the mention of environmental protection and long-term sustainable strategies. The inefficient land-use change and water management increased the vulnerability of agricultural areas under extreme drought events (Nguyen, 2007). The main factors including meteo-hydrological conditions, forest and water resources management, and the meteo-hydrological forecast network have led to the drought in Vietnam (Daniel and Ardakanian, 2015). It is difficult to indicate the particular drought indices which could be represented by the drought situations in Vietnam (Hang et al., 2014; Thang et al., 2014). Moreover, many research studies has already evaluated the drought impacts on the global scale or regional scale with ignoring the complicated drought impacts on the watershed scale, especially in the upstream areas (Sehgal and Sridhar, 2019).

The impacts of drought on meteorology, hydrology, and agriculture were evaluated in the different regions in Vietnam. Many drought indices were used to understand drought characteristics along with various approaches such as hydrological modeling, rainfall-runoff model, hydroclimate model, or satellite images as shown in Table 2.1.

Table 2.1. Research of drought characteristics in the different regions of Vietnam

Authors	Regions	Periods		Drought types		
		Historical period	Predicted period	Meteorology	Hydrology	Agriculture
Hang et al., 2014	Whole Vietnam	×		de Martonne J, PED, SPI		
Nguyen et al., 2015	Cai river basin (South Central region)	×		SPI, SPEI		SSI
Vu et al., 2015	Central Highlands	×	×	SPI		
Le et al., 2016	Khanh Hoa province (South Central region)	×	×	SPEI		
Nauditt et al., 2017	Vu Gia–Thu Bon river basin (Central region)	×		SPI	SRI	
Vu et al., 2017	DBW (Central Highlands)	×	×	SPI	SRI	
Vu et al., 2017	Vu Gia–Thu Bon river basin (South Central region)	×	×	SPI	SRI	
Nga et al., 2019	Gia Lai province (Central Highlands)	×				Palmer index
Sam et al., 2019	Central Highlands	×	×	SPI	SRI	SSWI
Tri et al., 2019	Ba river basin (South Central region)	×		J, PED, SPI	$K_{Drought}$	
Cuong et al., 2019	Hong-Thai Binh river watershed (Northern region)	×		SPI	SDI	

Hung et al., 2020	Whole Vietnam	×			SPEI	
Stojanovic et al., 2020	Whole Vietnam	×			SPI, SPEI	
Quang et al., 2021	Mekong Delta	×			SPEI	
Tuan and Canh, 2021	Ninh Thuan province (South Central region)	×			SPI	MI
Khoi et al., 2021	Be river basin (Central Highlands and Southeast regions)	×	×		SPI	SDI
Le et al., 2021	Central Highlands and South of Vietnam	×			SPI	VHI, SSM

Note: MD (Meteorological drought), HD (Hydrological drought), AD (Agricultural drought), SPI (Standardized Precipitation Index), SPEI (Standardized Precipitation Evapotranspiration Index), SRI (Standardized Runoff Index), SDI (Standardized Discharge Index), SSWI (Standardized Soil Moisture Index), SSI (Standardised Streamflow Index), J (Drought index), PED (Ped Index), MI (Moisture Index), VHI (Vegetation Health Index), and SSM (Surface Soil Moisture).

2.2. Evaluating the impacts of land-use change policies and anthropogenic activities on the aquatic environment downstream

2.2.1. Impacts of land-use change policies and human activities on the aquatic environment downstream

Changes in anthropogenic processes in the upstream areas could have significant impacts on the aquatic environment downstream. The policies on the regional and local scale were approved to manage and minimize the negative effects impacting water resources based on the fastly changes in reality. Land-use change policies are one of the most noticeable policies in the management of water resources in Asia countries that had great changes in land use in the relatively short-term period, especially the expansion of agricultural land (Zhao et al., 2006). Economic, environmental, and ecological aspects will be damaged on a larger scale although inappropriate land-use changes were conducted at the local scale (S. Zhao et al., 2006). In these policies, land use plans and spatial land use are extremely important for land-use strategies, thus, it requires the consideration of all pollutants and polluters at the national scale and river-basin scale in the water policy framework concerning water resources

management (Mateo-Sagasta et al., 2017). The coherence among policies should be considered to avoid the overlapping responsibilities of agencies and departments (Mateo-Sagasta et al., 2017). The appropriate land-use policies were applied to improve the irrigation adoption as well as reduce sediment and nutrients downstream such as transferring corn/soybeans from cotton (Momm et al., 2019) or converting annual crops to switchgrass (Ha and Wu, 2017; Li and Zipp, 2019). Nevertheless, crop conversion was not always successful in some countries. In Indonesia, the conversion of land use from forest areas to agricultural fields in the upstream accelerating soil erosion rate led to the eroded soil particles accumulation downstream of the watershed (Aflizar et al., 2010). To convert to shrubland or agricultural land, deforestation escalated concerns according to water scarcity in the dry season and increased erosion in the rainy season, especially in the mountainous regions (Khoi and Suetsugi, 2014; Son et al., 2015). An illustration in Thailand is that the transitional zone of forest and agriculture reached the highest erosion with the altitude ranging from 100 m to 400m because of the encroachment of agricultural fields on forest areas, where the extreme high soil erosion occurred on the sloping farmland by about 90% (Tingting et al., 2008). These issues are popular in Southeast Asia where agriculture plays a key role in socio-economic development. The local policies were not fully updated yet in the long-term watershed management strategies related to water resources and agriculture.

Additionally, deforestation, agricultural expansion, and urbanization in Southeast Asia countries are becoming serious phenomena along with the fast population growth in recent years. The increase in food demand led to more intensive use of current agricultural land and agriculture expansion toward more marginal land could increase significant effects on hydrology (Li et al., 2019; Aghsaei et al., 2020), evapotranspiration (Son et al., 2020), water yield, and sediment yield (Son et al., 2015; Munoth and Goyal, 2020) on the watershed scale. During the period between 1961 and 2001, there was an increasing tendency of fertilizer use in Southeast Asia by about 684% of ammonium phosphate and 292% of urea (FAO, 2022). Even though the expansion of land for agriculture aspect had positive effects on crop yields, its impacts on water resources, aquatic environment, and ecology were significant (Holden et al., 2015). Besides fallow land, agricultural land was one of the most crucial elements for accelerating erosion (Morgan, 2005; Zhang et al., 2015). The soil became drier after the harvesting period and before the cropping season because vegetables did not cover a large area meaning that discharge and soil erosion increased significantly during these years (Morgan, 2005). Nevertheless, after finishing the dry season, intensive rainfall has damaged farmlands and accelerated soil erosion from the area throughout the rainy season combined

with the hillslopes characteristics in the mountainous area leading to excess discharge, particularly on upland agriculture fields. And then the amount of sediment load and the nutrients loss deposited downstream increased (Stott and Mount, 2004; Morgan, 2005; Sidle et al., 2006; Folliott et al., 2013) leading to accelerating the extent of eutrophication in the aquatic environment (Carpenter et al., 1998; Somura et al., 2012). Over 70% of the delivered nitrogen and phosphorus was added from the different non-point and point sources in agricultural processes in the watersheds (Yang et al., 2018). The sediment yields in the agricultural watersheds were higher than in the non-anthropogenic activities areas by approximately a hundredfold (Stallard, 1998). Turkelboom et al. (2009) emphasized that soil fluxes increased dramatically on slopes over 70%, and the rates on an upland field having the 30-50% slope and the 30-50m slope length varied between 8 to 18 tons/ha tillage erosion which is a crucial factor to the total soil loss.

Khoi et al. (2019) indicated that the water discharge and water quality components became less sensitive to climate change instead of land-use change in Vietnam. Afforestation and conducting soil conservation practices were valuable solutions to decrease the runoff and sediment yield in Vietnam (Son et al., 2015). Vezina et al., 2006 mentioned that more than half of the area was hillslopes and mountainous terrain that converted to inappropriate agricultural fields with high soil erosion vulnerability. Rainfall intensity and land cover have a tight correlation with runoff and sediment yields if plant covers surpassed the plot surface on the hillslope areas upstream by a value of 40% (An et al., 2012). Dung et al., (2008) revealed that erosion and runoff were two principal factors of total nutrient losses throughout the cropping and fallow periods. The nutrient imbalances and soil erosion became two momentous issues in these upland regions when the fallow periods were shorter from 4 to 6 years. It is obvious that rainfall patterns and hillslopes are the main factors of erosion affecting agricultural fields among various characteristics in Southeast Asia countries and the Central Highlands of Vietnam is typical evidence. Nevertheless, human beings only reduced soil erosion intensity through suitable crop conversion, land use improvement, and irrigation planning because the change of rainfall patterns was impossible. The pollutant discharges from point and non-point sources should be controlled to minimize the erosion and nutrient loadings in the watershed without a significant impact on crop productivity (Jha et al., 2007; Alexander et al., 2008). Some research mentioned the impacts of land-use change and anthropogenic activities on flow, sediment, and nutrients in the different regions of Vietnam as shown in Table 2.2. Even though it is undeniable that anthropogenic activities have a great

influence on water quality downstream, the magnitude of these impacts would be greatly increased if the crop conversion is inappropriate.

Table 2.2. Research of the impacts of LUC and anthropogenic activities on flow, sediment, and nutrients in the different regions of Vietnam

Authors	Regions	Impacts of LUC and anthropogenic activities		
		On flow	On sediment	On nutrients
Khoi and Suetsugi, 2014	Be river basin (Central Highlands and Southeast regions)	×	×	
Quyên et al., 2014	Srepok river basin (Central Highlands)	×		
Khoi and Thom, 2015	Srepok river basin (Central Highlands)	×		
Son et al., 2015	Da river basin (Northwest Vietnam)	×	×	
Loi et al., 2016	Srepok river basin (Central Highlands)	×	×	
Tran et al., 2017	Cau river basin (Northern Vietnam)			×
Huyen et al., 2017	Srepok river basin (Central Highlands)	×	×	
Khoi et al., 2019	La Buong river basin (Southern Vietnam)	×		×
Son et al., 2020	Nam Rom river basin (Northwest Vietnam)	×		
Son et al., 2022	Nam Rom river basin (Northwest Vietnam)	×		
Son et al., 2022	Nam Rom river basin (Northwest Vietnam)	×	×	
Cung et al., 2022	Upstream Dong Nai river basin	×		

2.2.2. Importance of updating multiyear land-use changes policies and agricultural practices in the hydrology modelling

As for the Central Highlands of Vietnam, the water quality monitoring network was scattered and the observation data and the necessary information on the point and non-point pollution sources were limited to evaluating the pollution extent in the watershed scale. The approaches including paired catchment, statistical analysis, and hydrological modeling (Li et al., 2009) were utilized to tackle these obstacles and evaluate the impacts of local land-use change policies and anthropogenic activities on water quality in detail. One of the popular approaches is the modeling method, the SWAT (Soil and Water Assessment Tool) model, a

physically-based semi-distributed hydrological model, was selected to evaluate the impacts of land-use change on runoff and sediment (Munoth and Goyal, 2020), or assess the impacts of river discharge, hydrology, sediment, and nutrients (Huang et al., 2009; Abbaspour et al., 2015; Hanief and Laursen, 2017; Malagó et al., 2017; Keraga et al., 2019) in the large watersheds where had the limitation of measuring stations similar to the target area. The SWAT model had been widely applied to identify and prioritize particular subwatersheds for management strategies (Tripathi et al., 2003). Thus, the impacts of land-use policies and human practices should be considered in-depth on the watershed scale. In the watershed scale, simulations have been conducted in the long-term by using the original model with the remaining stable land-use variable leading to unrealistic changes for the agricultural areas (Moriassi et al., 2019). Wagner et al. (2019) indicated that the development following the linear dynamic land use was more appropriate with the static method than those without the linear approach. The incorporation of different land use categories in the model is expected to improve the performance accuracy of hydrological processes based on the temporal and spatial distribution under realistic conditions (Pai and Saraswat, 2011; Yonaba et al., 2020) or the simulation of nitrate (Guse et al., 2015), total nitrogen and total phosphorus (Wang et al., 2018). This approach represented the final conditions in the whole simulation period as well as the intermediate conditions due to the change in crops continuously that affect hydrologic and aquatic systems (Guse et al., 2015). Updating the different land-use changes input into the original model could be considered a useful tool for land-use planning policies (Aghsaei et al., 2020) as well as an integrated modeling framework for decision-makers and water resource managers (Yonaba et al., 2020). The role of updating land use inputs in the original model was also emphasized by Wang et al., 2018 to simulate the non-point source pollution. Updating multiyear land-use input conditions and agricultural practices in the original SWAT model were conducted on the watershed scale based on different approaches as shown in Table 2.3.

Table 2.3. Updating multiyear land-use input conditions and agricultural practices in the original SWAT model by different approaches over the world

Authors	Regions	Simulated variables
Pai and Saraswat, 2011	Ankarsas watershed (The US)	Surface runoff, groundwater, ET
Guse et al., 2015	Treene catchment (Germany)	Nitrate load
Wang et al., 2018	Xiangxi watershed (China)	Flow, Total N, Total P
Wagner et al., 2019	Mula and Mutha catchments (India)	Water yield, ET

Lee et al., 2019	Little Eagles Creek watershed (India)	Flow
Aghsaei et al., 2020	Anzali catchment (Iran)	ET, water yield, sediment yield
Yonaba et al., 2020	Tougou watershed (Africa)	Surface runoff
Wang et al., 2022	Wei watershed (China)	Flow, sediment, Total N

From these arguments, meteorological drought was more popular than other droughts in Vietnam. Agricultural drought was rarely assessed because of the lack of observed data on evapotranspiration, soil moisture, and detailed crop information, especially on the watershed scale. Additionally, water quality risks should be tackled along with water quantity assessment prior to water resources planning. One of the noticeable phenomena is water quality degradation based on the impacts of local land-use change policies and anthropogenic activities. The land-use change policies in the short-term periods for each region were different depending on the actual circumstances. These policies have not been fully updated promptly in the strategies yet making it difficult to estimate the impacts on the downstream comprehensively. The mountainous areas and upstream of large watersheds should be considered and the target area could be seen as a typical illustration. Through different approaches, updating multiyear land-use input conditions and agricultural practices in the hydrological model was conducted in many countries to estimate the hydrology components, sediment, and nutrients. It seemed to be one of the notable directions in recent years even though not so much research was conducted in the Central Highlands of Vietnam. Thus, this study was carried out to evaluate the drought characteristics in more detail as well as the effects of multi-year land-use changes and human activities on water quality downstream to support the water resources management in the upstream Sesan river, Central Highlands of Vietnam more comprehensively.

CHAPTER 3. EVALUATION OF DROUGHT FEATURES IN THE DAKBLA WATERSHED, CENTRAL HIGHLANDS OF VIETNAM

3.1. Introduction

Drought is an insidious natural phenomenon occurring when the levels of rainfall are lower than what is considered normal. If drought lasts for a long time, the environment and people's activities in their daily life, industry, and agriculture will be affected significantly because of water scarcity. A long-lasting drought impacted Southeast Asian countries based on a precipitation deficit inherited from 2019 and an insufficient start to the monsoon season the following year (Barbosa et al., 2020). Agriculture is the sector that is most affected by droughts followed by industrial, and domestic water supply. Over the past 30 years, approximately 80% of the economic impact of drought is absorbed by agriculture in Southeast Asia (ESCAP and ASEAN, 2020). In the 2015-2016 drought events, the total rice production reached the lowest level since 2000, with a decreased value of 27 million tonnes (ESCAP and ASEAN, 2020). The food and feed demands of human beings were impacted by the prolonged droughts. With slower onset, repeated or persistent conditions of low or moderate intensity, droughts are known as extensive risks compared with other intensive risks such as earthquakes and cyclones. They are highly localized hazards and occur with a significant impact on largely dispersed populations over longer timescales (ESCAP and ASEAN, 2020). Nevertheless, the impacts of drought are different depending on the meteorological and agricultural characteristics of each region. If decision makers are unable to deal with local-scale drought impacts, this leads to the implementation of less effective drought planning policies and water resources management strategies in the future. Hence, drought is becoming a noticeable phenomenon, especially in Southeast Asian countries.

The Central Highlands of Vietnam are one of the most sensitive regions to El Niño effects, which have a tropical monsoon climate (CCAFS-SEA, 2016). Rainfall in the dry season was normally only 10-15% of that of the whole year in this region (VAWR, 2012). In the strong drought events such as 2004-2005, 2010, and 2015-2016 events, prolonged droughts occurred across a large area. The rainfall was 30-50% lower than the average of many years from 2000 to 2016. Thus, the area irrigated directly from irrigation projects was only 30% of the cultivated area (WRD, 2016). The water volume of irrigation reservoirs in the Central Highlands fell to 10-50% of their designed capacity in early April 2016 (CCAFS-SEA, 2016). Furthermore, the rapid expansion of urbanization and agricultural activities along with drought conditions has led to severe stress on water resources. As a result, food security issues

have worsened in this region, where poverty rates are high (Grosjean et al., 2016).

Utilizing observed data only, it was not possible to evaluate drought features of severity, duration and lag time, and frequency on the watershed scale comprehensively because of the uneven and sparse distribution of observed stations in mountainous regions. Paired catchments, statistical analysis, and hydrological modeling are the popular approaches to assess the impacts of environmental changes on hydrological processes (Z. Li et al., 2009). Among these approaches, hydrological modeling combined with drought indices is more appropriate to evaluate drought impacts and the relationships between different droughts. Historical drought features were analyzed based on different temporal scales which could support policymakers in the short-/middle-/long-term drought planning. Moreover, understanding the spatial distribution of drought features is very essential for sufficient water resources management in particular drought-prone areas. Droughts were assessed all over the world such as Lweendo et al. (2017), Veetil and Mishra (2020), and Brouziyne et al. (2020). In addition, some research discussed the drought impacts in the Central Highlands of Vietnam, such as the evaluation of regional meteorological droughts – the whole Central Highlands (Vu et al., 2015a); local meteo-hydrological droughts – the DBW (Vu et al., 2015b); or agricultural drought at the district level – Gia Lai province (Nga et al., 2019). To evaluate more detailed drought impacts on the watershed scale, a combination of modeling and drought indices is required, particularly in relation to agriculture. The overall objectives of this study are (1) to characterize meteorological (Standardized Precipitation Index: *SPI*), agricultural (Standardized Soil Moisture Index: *SSI*), and hydrological (Streamflow Drought Index: *SDI*) droughts on different temporal scales, and (2) to understand the distribution of historical drought features on each subbasin in the DBW.

3.2. Materials and methods

3.2.1. Study area

The DBW is one of the main subbasins in the upstream of the Se San River basin. Dakbla River, with an area of 3,507 km², passes through Kon Tum and Gia Lai Provinces, and is located in the Central Highlands of Vietnam (Figure 3.1). The dry season is from December to April and approximately 15% of the rainfall is concentrated in the dry season. Thus, a consistent lack of rainfall and discharge had some significant impacts on cultivation areas.

As for drought status in the study area, the 2015-2016 drought event was the most prolonged drought event in Vietnam in over 90 years and impacted 52 out of 63 provinces (ESCAP and ASEAN, 2020). A state of emergency was declared in Kon Tum and Gia Lai

Provinces in 2015-2016 due to a drought event that presented a high level of danger. This drought event affected 228.5 km² of crops (including 56.2 km² of rice) in Gia Lai Province (GLDARD, 2016). Additionally, 42.0 km² of crops (including 13.7 km² of rice) were destroyed in Kon Tum Province (KTGSO, 2016).

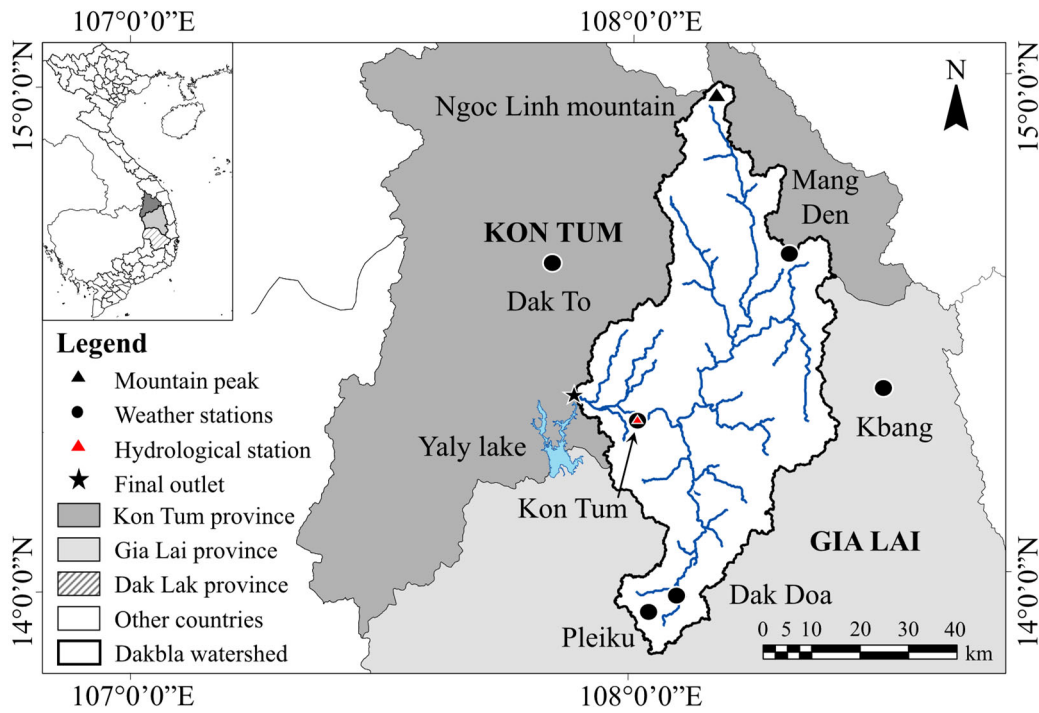


Figure 3.1. Location of the DBW

3.2.2. Methods

❖ SWAT description

The SWAT, a physically based semi-distributed hydrological model, was selected to assess the river discharge as well as to consider the impacts of drought conditions on our target watershed over long time periods. The simulation of water components was based on the water balance equation. Many studies have proved its reliability and wide applicability in mountainous watersheds, such as in simulating runoff (Somura et al., 2009); estimating drought severity (Sehgal and Sridhar, 2019); or evaluating hydrological vulnerability to future droughts (Brouziyne et al., 2020).

Input data information: Spatial and meteorological data are required in order to utilize the SWAT (Table 3.1). A digital elevation model (DEM) was downloaded from the NASA and Japan ASTER Program (2009). A land use map was obtained from the National Institute of Agricultural Planning and Projection (2005). Agricultural land and industrial crops are mainly concentrated in the western and southern areas, making up 20.4% of the total area.

Soil data were downloaded from Food and Agriculture Organization - United Nations Educational, Scientific and Cultural Organization (FAO-UNESCO, 2007), and Ferric Acrisols predominated with a value of 51.9%. Meteorological data were collected by the Central Highlands Region Hydrometeorological Centre during the 1990-2018 period. The Kon Tum and Pleiku stations are two weather stations measuring daily rainfall, daily maximum and minimum temperature, daily mean humidity, daily sunshine hours, and daily mean wind speed. Daily rainfall data were also collected from the four other stations (Dak To, Dak Doa, Kbang, and Mang Den stations) in and around the watershed. Daily mean river discharge at the Kon Tum station was also recorded by the Hydrometeorological Centre from 2000 to 2018.

Table 3.1. Input data information for the SWAT

Data	Description	Sources
Digital Elevation Model	Topography features (resolution 30 m)	NASA and Japan ASTER Program (2009)
Land use map	Land use classification (scale 1:50,000)	National Institute of Agricultural Planning and Projection (2005)
Soil map	Soil types (scale 1:5,000,000)	FAO-UNESCO (2007)
Meteorological data	<ul style="list-style-type: none"> ➤ Kon Tum and Pleiku stations: Daily rainfall, daily maximum and minimum temperature, daily mean humidity, daily sunshine hours, and daily mean wind speed (1990-2018) ➤ Dak To, Dak Doa, Kbang, and Mang Den stations: Daily rainfall 	Central Highlands Region Hydrometeorological Centre
River discharge	Kon Tum station: Daily mean river discharge (2000-2018)	Central Highlands Region Hydrometeorological Centre

SWAT application: The DBW was divided into 73 subbasins and 480 Hydrological Response Units (HRUs) in the SWAT. The first ten years (1990-1999) were set up as a warm-up period. The parameter values were calibrated from 2000 to 2009 and validated from 2010 to 2018. The calibration procedure was conducted utilizing the Sequential Uncertainty Fitting version 2 (SUFI-2) in the Calibration Uncertainty Program for SWAT (SWAT-CUP).

❖ Evaluation of model performance

To evaluate the accuracy of the model performance, three statistical parameters were used, the coefficient of determination (R^2), the Nash–Sutcliffe index (NSI), and the percent bias ($PBIAS$). The R^2 represents the degree of collinearity between simulated and observed data (Santhi et al., 2001). The NSI was utilized to evaluate long-term simulations (Nash and

Sutcliffe, 1970). The model performance was satisfactory if the *NSI* value ranged between 0.5 and 0.65 (Moriasi et al., 2015). The average model simulation bias was identified using the *PBIAS*. The model performance was evaluated as satisfactory if the *PBIAS* value ranged from $\pm 10\%$ to $\pm 15\%$ for monthly flow (Moriasi et al., 2015).

❖ Assessment of drought features

In order to assess drought hazards and to alleviate their impact, severity, duration and lag time, and frequency (Saeid and Faezeh, 2017) were chosen as the drought features in this study. Severity is defined as the degree of the rainfall shortfall. Duration is the time interval from the start to the end time expressed in months and lag time is an interval of time between two droughts. Frequency refers to the number of drought months in a given time period.

Three drought indices of *SPI*, *SSI*, and *SDI* were utilized to calculate meteorological, agricultural, and hydrological droughts, respectively. Drought indices are typically computed as numerical representations of drought severity to measure the qualitative state of droughts using hydrometeorological inputs (WMO and GWP, 2016). Meteorological drought is characterized as a longer period with considerably lower than average rainfall. Agricultural drought is defined as when the available soil moisture is inadequate to fulfil the crops' requirements during the growing season. Hydrological drought is a period of below average water content in streams (Saeid and Faezeh, 2017).

As for meteorological drought, the *SPI* was developed by McKee et al. (1993) to determine the probability distribution of rainfall for particular time scales from the long-term rainfall record. The gamma distribution was developed by Thom (1958) to fit the rainfall time series based on the maximum likelihood estimators. The *SPI* index is calculated as:

$$SPI_{i,k} = \frac{R_{i,k} - \bar{R}_{i,k}}{s_k^R} \quad (3.1)$$

where $R_{i,k}$: The cumulative precipitation for the k -th reference period of the i -th year; $\bar{R}_{i,k}$ and s_k^R are the mean and standard deviation of the cumulative precipitation for the k -th reference period.

The methodology and calculations of *SPI* can also be applied to the *SSI* and *SDI* (Nalbantis and Tsakiris, 2009; Hao and AghaKouchak, 2013). The *SSI* and *SDI* were calculated for agricultural and hydrological droughts using soil water content and discharge from the SWAT. The *SSI* and *SDI* indices are calculated as follows:

$$SSI_{i,k} = \frac{SW_{i,k} - \overline{SW}_{i,k}}{s_k^{SW}} \quad (3.2)$$

where $SW_{i,k}$: The cumulative soil water content for the k -th reference period of the i -th year; $\overline{SW}_{i,k}$ and s_k^{SW} are the mean and standard deviation of the cumulative soil water content for the k -th reference period.

$$SDI_{i,k} = \frac{Q_{i,k} - \overline{Q}_{i,k}}{s_k^Q} \quad (3.3)$$

where $Q_{i,k}$: The cumulative discharge for the k -th reference period of the i -th year; $\overline{Q}_{i,k}$ and s_k^Q are the mean and standard deviation of the cumulative discharge for the k -th reference period.

The 3-, 6-, and 12-month indices were utilized in this study to evaluate the drought features. A drought event is a period in which the index is continuously negative and the index reaches a value of -1.0 or less. The drought severity was classified as follows: (1) mild drought ($-1 < \text{indices} < 0$); (2) moderate drought ($-1.5 < \text{indices} \leq -1$); (3) severe drought ($-2 < \text{indices} \leq -1.5$); (4) extreme drought ($\text{indices} \leq -2$).

3.3. Results

3.3.1. Reproducibility of river discharge

The high accuracy of the river discharge simulation indicates that the SWAT seems to be a reasonable tool for application in mountainous areas. Eight sensitive parameters were calibrated to achieve the highest model performance using the SUFI-2 algorithm. The calibrated values of these sensitive parameters were summarized in Table 3.2. Additionally, the correlation between simulated and observed river discharges at the Kon Tum station in the calibration period (2000-2009) and validation period (2010-2018) was shown in Figure 3.2. The reproducibility of the model was determined with R^2 , NSI , and $PBIAS$ values of 0.84, 0.79, and 16.4% in the calibration period, and 0.72, 0.69, and 15.5% in the validation period, respectively. In the performance evaluation, the $PBIAS$ values were slightly lower than the criterion of Moriasi et al. (2015) because of the reproducibility of the high flows in the rainy season. Overall, the simulation results in both periods were satisfactory.

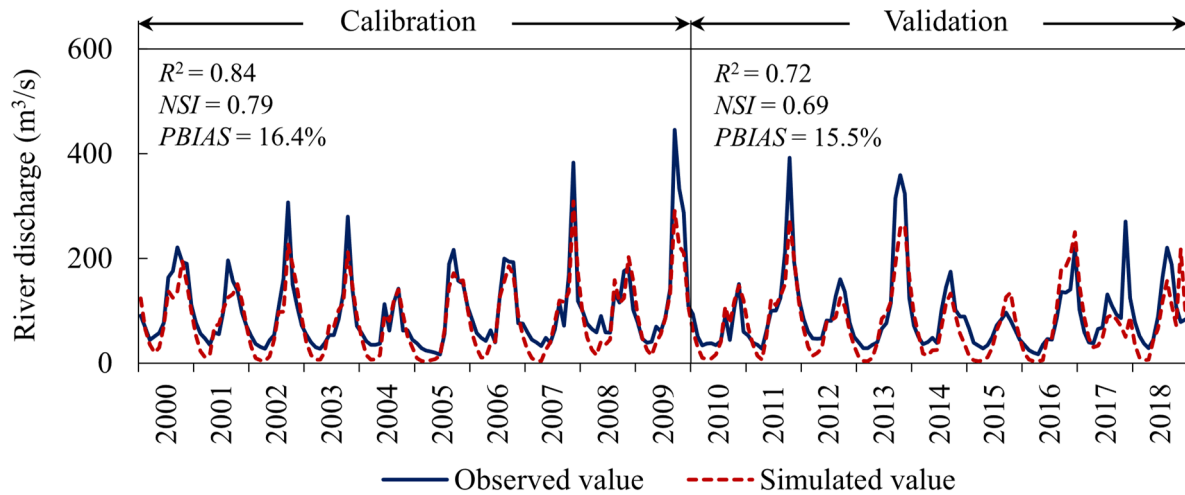


Figure 3.2. Simulated and observed river discharges at the Kon Tum station in the calibration period (2000-2009) and validation period (2010-2018)

Table 3.2. Eight sensitive parameters selected by the SUFI-2 algorithm and their ranges for the parameter value optimization. The calibrated values are used for modifying the original values in the SWAT by relative changes

Sensitivity ranking	Parameters	Description	Range	Calibrated values
1	CN2	SCS runoff curve number factor	(-0.7, -0.5)	-0.59
2	SURLAG	Surface runoff lag time	(-0.2, 0)	-0.02
3	SOL_AWC	Available water capacity of the soil layer	(-0.3, -0.1)	-0.10
4	SOL_K	Saturated hydraulic conductivity	(0.1, 0.2)	0.19
5	CH_N2	Manning's "n" value for the main channel	(-0.2, 0)	0.02
6	ALPHA_BF	Baseflow alpha factor (days)	(0.2, 0.4)	0.36
7	GW_DELAY	Groundwater delay (days)	(0.2, 0.4)	0.21
8	GW_REVAP	Groundwater "revap" coefficient	(0, 0.2)	0.12

3.3.2. Temporal variation of historical drought features

❖ Drought severity

Drought events have a tight relationship with El Niño events (Food and Agriculture Organization: FAO, 2014). Droughts that occurred in Vietnam in the El Niño years were reported in FAO (2014), CCAFS-SEA (2016), Phong and Chinh (2017), and Williams et al. (2019). There were severe droughts in 2004-2005, 2010, and 2014-2016, and moderate droughts in 2002-2003 and 2006-2007. Our results confirmed that, in the DBW, the extreme drought events appeared after the impact of strong El Niño events in the same year as the events. There were nine drought events from 2001 to 2018, in which the 2004-2005, 2010,

and 2014-2016 periods experienced severe droughts, while there were moderate droughts in the 2002-2003 and 2006-2007 periods, as shown in Figure 3.3.

The changes in drought severity in the shorter time scales were more sensitive than those in the longer time scales (McKee et al., 1993). The drought events had a clustering tendency and lasted a long time, leading to a longer duration of drought spells over the longer time scales (L. Zhao et al., 2014), such as the 2004-2005 and 2015-2016 drought events. In some special cases, the *SPI* indicated precipitation spells that were insufficient to relieve agricultural and hydrological droughts. This is reflected in the non-recovery of the *SSI* and *SDI*, such as *SSI-3* and *SDI-3* in the 2002-2003 period. The recovery of the *SPI* to above normal levels was more frequent than for the *SSI* and *SDI* (Shukla and Wood, 2008).

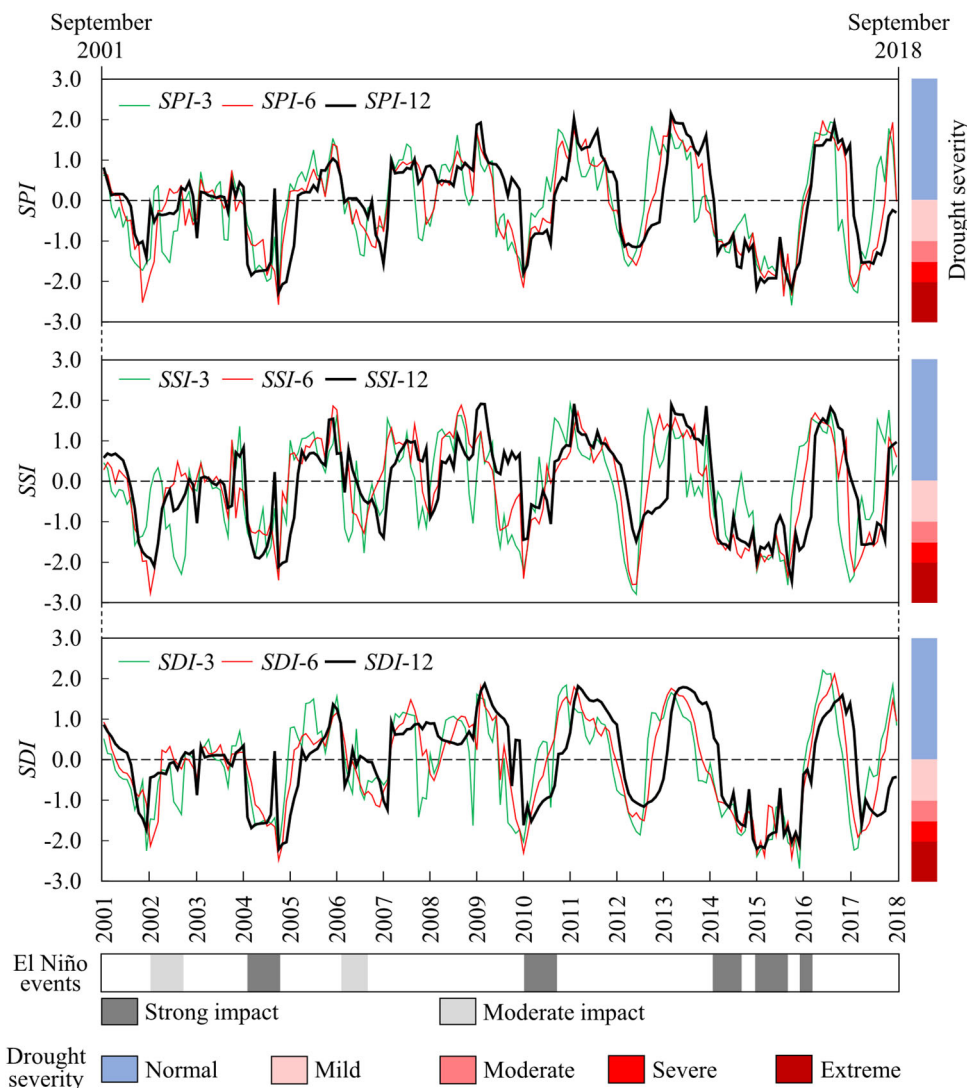


Figure 3.3. Drought severity for the *SPI*, *SDI*, and *SSI* (3-, 6-, 12- month time scales). The inward tick of each year starts from September. The years and duration of the El Niño events were referred from FAO (2014), CCAFS-SEA (2016), Phong and Chinh (2017), and Williams et al. (2019)

The correlation among three drought indices was assessed (Table 3.3). A 12-month time scale was selected to demonstrate the drought features in the target area because of the presence of the highest correlation among the drought indices for this time scale compared to others. The R^2 values were 0.82 for the *SPI-SSI* correlation and 0.89 for the *SPI-SDI* correlation over the 12-month time scale. The 6-month time scale could also be used, although the correlation evaluation was lower than the 12-month time scale. The correlation among these indices over the 6-month time scale was 0.81 for the *SPI-SSI* correlation and 0.84 for the *SPI-SDI* correlation.

Table 3.3. The correlation R^2 between *SPI* and *SSI* or *SDI* for the 0-, 1-, and 2- month lag periods. Bold values represent the highest correlation between *SPI* and *SSI* or *SDI* (3-, 6-, 12-month time scales)

Time lag	R^2 of <i>SPI</i> and <i>SSI</i>			R^2 of <i>SPI</i> and <i>SDI</i>		
	<i>SPI</i> -3 vs. <i>SSI</i> -3	<i>SPI</i> -6 vs. <i>SSI</i> -6	<i>SPI</i> -12 vs. <i>SSI</i> -12	<i>SPI</i> -3 vs. <i>SDI</i> -3	<i>SPI</i> -6 vs. <i>SDI</i> -6	<i>SPI</i> -12 vs. <i>SDI</i> -12
0 months	0.70	0.81	0.82	0.74	0.84	0.89
1 month	0.48	0.67	0.69	0.76	0.85	0.91
2 months	0.11	0.47	0.54	0.35	0.67	0.70

❖ Drought duration and time lag

Agricultural drought had a longer duration than the other types of drought. Drought duration of each drought event during a 2001-2018 period was shown in Table 3.4.

Table 3.4. The drought duration, minimum and maximum drought severity of drought events recorded by *SPI*-12, *SSI*-12, and *SDI*-12 during a 2001-2018 period (indices ≤ -1)

No.	Years of drought events	<i>SPI</i> -12	<i>SSI</i> -12	<i>SDI</i> -12
1	2002-2003	2 ^a (-1.07 ^b , -1.4 ^c)	3 (-1.51, -2.10)	2 (-1.32, -1.72)
2	2004-2005	4 (-1.32, -2.37)	5 (-1.52, -2.42)	4 (-1.36, -2.41)
3	2005-2006	3 (-1.12, -1.54)	4 (-1.38, -1.98)	4 (-1.32, -1.62)
4	2007-2008	1 (-1.05, -1.42)	1 (-1.26, -1.47)	1 (-1.02, -1.43)
5	2010-2011	4 (-1.03, -1.65)	5 (-1.06, -1.62)	4 (-1.04, -1.55)
6	2012-2013	3 (-1.07, -1.15)	3 (-1.17, -1.48)	3 (-1.01, -1.16)
7	2014-2015	6 (-1.04, -2.19)	7 (-1.40, -2.22)	6 (-1.08, -2.20)
8	2015-2016	6 (-1.10, -2.19)	7 (-1.21, -2.47)	7 (-1.14, -2.20)
9	2017-2018	3 (-1.01, -1.56)	4 (-1.03, -1.57)	3 (-1.01, -1.58)

^a: Drought duration of drought events (month); ^b: Minimum drought severity of drought events; ^c: Maximum drought severity of drought events.

The total drought months (indices ≤ -1) among drought events in this period of *SPI*-12, *SSI*-12, and *SDI*-12 were 32, 39, and 34 months, respectively. Agricultural drought followed the pattern of meteorological drought without a time lag, whereas there was a one-month time lag between meteorological and hydrological droughts. The correlation among these indices is shown in Table 3.3. Besides rainfall, the length of the lag time depends on other variables, as a basin's morphological conditions contribute to discharge formation (Kamali et al., 2017). Hydrological drought happened later than meteorological drought, which could be based on the buffering function of the soil layers and the groundwater system to meteorological drought (L. Zhao et al., 2014).

❖ Drought frequency

The drought frequency of the three indices was calculated by the number of drought months from moderate to extreme drought (indices ≤ -1) in total dry months (indices < 0) of 18 target years as shown in Figure 3.4. The *SSI*-12 showed the highest percentage of drought months with a value of 38.2%, which was evaluated higher than by utilizing the *SPI* and *SDI*. In *SPI*-12 and *SDI*-12, the percentage of drought months occupied 37.0% and 32.6% in total dry months, respectively. It is obvious that drought impacts regarding soil moisture could not be evaluated if only the *SPI* and *SDI* were used. Thus, the use of multiple indices in drought assessment is essential to provide comprehensive support for policymakers in the development of realistic local drought policies, especially for agriculture.

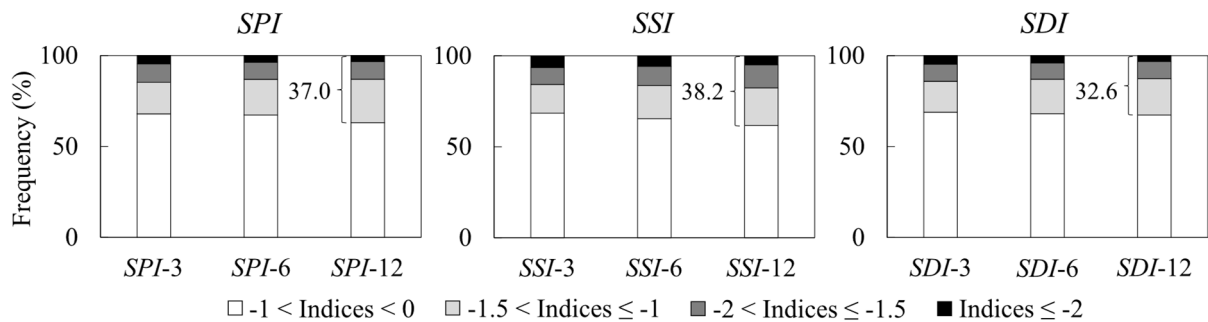


Figure 3.4. Drought frequency of *SPI*, *SSI*, and *SDI* indices between the different time scales

3.3.3. Spatial distribution of historical drought features

The spatial distribution of the 12-month time scale drought frequency from 2001 to 2018 is shown in Figure 3.5. The drought tendency increased, following the north–south and east–west directions. The highest meteorological drought frequency was concentrated mainly in the southern part of the study area. The drought frequency of agricultural and hydrological

droughts tended to expand from the southern to the southwestern areas. The southwestern areas may be more exposed to drought risks than others because agricultural land occupied the largest proportion in these areas, especially rice. The relationship between drought events and rice productivity is understood based on statistical data in Kon Tum Province. In the 2004-2005 drought event, the rice productivity dropped from 0.40 to 0.37 kg/m². There was also a decreasing tendency that occurred in the 2010-2011 period, and a value of 0.42 kg/m² instead of 0.47 kg/m² in the 2009-2010 period. During the severe drought event in 2015-2016, the rice productivity decreased from 0.47 to 0.42 kg/m² (GSO, 2021).

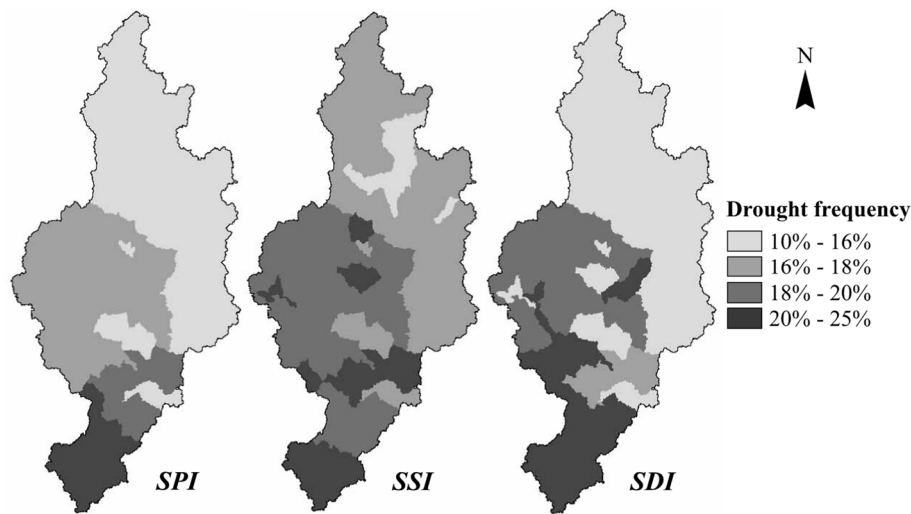


Figure 3.5. Spatial distribution of the 12-month time scale drought frequency in the DBW

3.4. Discussion

3.4.1. The importance of drought evaluation in agriculture in the Central Highlands of Vietnam

Droughts in the Central Highlands have been assessed in previous studies. The *SPI* was frequently chosen to evaluate meteorological droughts in these publications because of its simplicity, and only precipitation was used for assessment at the regional scale (Vu et al., 2015a) or district level (Nga et al., 2019). It is difficult to consider drought impacts on hydrology and agriculture when using only the *SPI* for developing irrigation systems and water resources management strategies, which requires using a combination of modeling and other indices such as the *SSI* and *SDI*. Vu et al. (2015b) assessed droughts in the target area, finding a tight correlation between *SPI* and *SDI*, without considering agricultural drought. In addition, although the agricultural drought impacts were also evaluated by a modeling approach in the different river basins (Dak Lak Province) of the Central Highlands by (Sam et al., 2019), the relationship between drought-prone areas and agricultural land was not

indicated.

A noticeable finding in this study is that the watershed-scale evaluation of drought features can provide more specific information compared to regional-scale/district-level assessments. The evaluation of drought issues within the context of a drought mitigation plan was comprehensively conducted using multiple indices. The number of months, ranging from a moderate to severe drought level, occupied between 25 and 35% of the total dry months from our evaluation of three indices, which indicated a higher risk than the result of Vu et al. (2015a) using only the *SPI* for regional assessment (approximately 20%).

Another important finding is that the drought frequency using the *SSI* was higher than when utilizing the *SPI* and *SDI*. In addition, the drought duration of the *SSI* was longer than that of the others and there was no time lag between the *SPI* and *SSI*. This means drought will affect agriculture significantly when meteorological drought occurs. As for the spatial distribution of the 12-month time scale drought frequency, the northeastern part of the target area was not captured well by the *SPI* and *SDI*. Additionally, the southwestern area is a more exposed, drought-prone area with predominantly agricultural land (paddy fields), leading to higher drought vulnerability in these areas, especially with regard to agricultural drought. Thus, the importance of agricultural drought assessment was emphasized along with meteorological drought.

3.4.2. Contribution to future drought mitigation in the Central Highlands of Vietnam

The inefficiency of irrigation systems is a significant obstacle in the Central Highlands of Vietnam. Until 2018, there were 492 irrigation units in Kon Tum Province and 344 units in Gia Lai Province. The irrigation efficiency was less than 60% and 70% of the designed irrigation capacity in Kon Tum and Gia Lai Provinces, respectively (KTDARD, 2018; GLDARD, 2019). Combined with severe climate conditions, the low irrigation efficiency dramatically affects local agricultural production.

Short-term strategies were implemented by the local government each year to mitigate drought issues and water shortages (Kon Tum People's Committee, 2019). There were no inter/long-term policies for drought before 2020 in this area. In 2020, the "Project on drought management in Kon Tum Province during the 2021–2030 period" was started to mitigate the impacts of prolonged droughts for agriculture, which involved building a set of tools for drought management and promoting irrigation infrastructure investment (Kon Tum People's Committee, 2020). By using the SWAT and multiple drought indices, this study showed that different drought features can be indicated for meteorological and agricultural drought on the

watershed scale with different temporal and spatial distributions. Thus, it is considered that this methodology can support policymakers in irrigation system planning by considering local water resource availability, and/or suggesting crop conversion strategies for local farmers in the area.

3.5. Conclusions

Three indices *SPI*, *SSI*, and *SDI* were utilized to evaluate the drought features in the DBW. The main findings are summarized as follows:

- Extreme drought events appeared in the same year as strong El Niño events in the study area, from the result of drought severity evaluation.
- The total drought months (indices ≤ -1) in the 12-month time scale, according to the *SSI*, was evaluated as 39 months, which is longer than the evaluation of the *SPI* by 7 months and that of the *SDI* by 5 months.
- Agriculture is affected immediately when meteorological drought occurs due to the fact that there is no time lag between the *SPI* and *SSI*.
- The drought frequency between moderate and extreme drought levels was 38.2% in the *SSI*-12, which is higher than in the *SPI*-12 and *SDI*-12.
- The 12-month time scale drought frequency was spatially represented by the *SSI* in more detail than by the *SPI* and *SDI*, particularly for the northeastern areas. The areas with higher drought risk were found in the southwest, which is predominated by agricultural land.

Understanding the drought features of meteo-hydrology and agriculture is important in mountainous areas. Drought impacts should be considered alongside other phenomena in the context of climate changes in the future. The DBW plays an extremely crucial role as the upstream of the Se San River basin. Assessments of the impacts of drought will enable policymakers to mitigate the adverse effects of local-scale drought and contribute to the development of regional policies.

3.6. Limitation and recommendation

It is recommended that a minimum 30-year period of data is used to evaluate the drought indices (McKee et al., 1993). However, eighteen years of the data from 2001 to 2018 were used in our analysis because of the availability of historical river discharge data. This is a limitation of our study to evaluate the drought indices. As a next step, the tendency of meteo-hydrological and agricultural droughts should be evaluated by using longer data periods with future projections of climate data and river discharges in the watershed.

CHAPTER 4. THE IMPACTS OF LAND-USE INPUT CONDITIONS ON FLOW AND SEDIMENT DISCHARGES IN THE DAKBLA WATERSHED, VIETNAM

4.1. Introduction

Changes in expanding hillslope cultivation, amplifying urbanization, and deforestation are some of the more notable issues in mountainous areas, particularly for countries in Southeast Asia. Areas with a transitional zone of forest and agricultural land experience the highest erosion caused by the encroachment of anthropogenic processes (Tingting et al., 2008; Nontananandh and Changnoi, 2012; Aflizar et al., 2010). Additionally, excess discharge and rainfall intensity contribute to accelerating soil erosion and increase the sediment and nutrient losses to downstream (Somura et al., 2018; Li et al., 2019).

In order to decrease erosion from the area and develop a sustainable land use plan, the watershed basis approach has been recognized as an important method. Because land-use changes are the result of choices by local citizens/farmers, companies, and governments, information, such as (1) the suitable location of development/cultivation or protection in a watershed, (2) environmental influences of land-use changes, and (3) a balancing method of human activities and water/land conservation, is crucial when considering a watershed management strategy. The information can particularly assist local land-use decision-makers. At present, many methods, including paired catchment, statistical analysis, and hydrological modeling, have been utilized to assess the impacts of environmental changes on flow and sediment in a watershed scale (Li et al., 2009; Zettam et al., 2017; Hallouz et al., 2018; and Yuan and Forshay, 2020).

The Soil and Water Assessment Tool (SWAT) has been widely applied for modeling watershed hydrology and simulating the movement of non-point-source pollution. In the existing studies on SWAT modeling, the impacts of land-use changes on runoff and sediment (Son et al., 2015; Munoth and Goyal, 2020), water balances (Makhtoumi et al., 2020), hydrological processes (Li et al., 2019), and streamflow characteristics (Marhaento et al., 2019) have already been analyzed by using a single static land use input condition in different periods, confirming its capability. However, as with other simulation models, the simulation results are significantly impacted by the temporal and spatial distributions of all the input conditions, including topographic, land use, soil, and weather data (Bieger et al., 2015). Notably, the essential factor among these variables is the land-use input condition. Thus, the condition of a watershed with frequent land use changes in a relatively short period cannot be evaluated appropriately by using a simulation model with a single land use input condition.

In another case, a delta approach is applied to analyze the impacts of land-use change in two periods using simulation results derived from different static land-use data. In such a case, the simulation results cannot comprehensively evaluate realistic land use changes, meaning that strategic land use planning would be difficult. Therefore, multi-year land use input conditions in a model simulation improve the reproducibility of water components and sediment in the watershed.

Land-use update modules via linear interpolation among time stamps have been developed in SWAT, including SWAT2009_LUC (Pai and Saraswat, 2011), LUC-R script (Tam, 2012), and SWAT-LUT (Moriassi et al., 2019). These modules are expected to provide realistic parameterization to incorporate different land use categories in watersheds (Moriassi et al., 2019). The advantages of using land-use update modules are based on the scale and intensity of land-use changes in terms of improving the spatial distribution responses and temporal predictions of the model (Pai and Saraswat, 2011). Based on these approaches, many studies have emphasized the effects of land-use changes on soil and water resources (Moriassi et al., 2019; Martinelli and Machado, 2014; Wang et al., 2017; Wagner et al., 2019), groundwater and surface runoff (Pai and Saraswat, 2011), water quality (H. Zhang et al., 2011), and water components and sediment (Son et al., 2020; Aghsaei et al., 2020).

Thus, the main objectives of this study are: (1) to create land-use maps following local statistical information in a watershed, where GIS-based information of land-use changes are infrequently updated while in the context of complicated local land-use policy changes, (2) to establish updated land-use input conditions by using the developed land-use maps, and then (3) to evaluate to what extent the updating land-use input conditions can improve the flow and sediment outputs of the model.

4.2. Materials and methods

4.2.1. Study area

The Sesan River is one of the major tributaries of the lower Mekong basin in the Southeast Asia. The DBW, a subbasin of Sesan river basin, located in the Central Highlands of Vietnam with an area of about 3,507 km² (Figure 4.1). The total length of the main river is approximately 152 km. From the foot of Ngoc Linh Mountain (Tu Mo Rong District, Kon Tum Province), Dakbla River flows through the Kon Tum and Gia Lai Provinces in a northeast–southwest direction with a high drainage density of 0.49 km/km². The river then flows to Yaly Lake in the downstream section after merging with the Poko River. The flow

rates of the river are 0.2–0.5 m/s in the dry season and 1.5–3 m/s in the rainy season (VAWR, 2012). Being a mountainous area, the topography gradually decreases in the north–south and east–west directions. There are two principal seasons due to the tropical monsoon climate, including the rainy season (May to November) and the dry season (December to April). The average annual temperature is about 23.6 °C and the average annual rainfall is approximately 2,000 mm at the Kon Tum weather station. More than half of the catchment area is covered in evergreen and mixed forests. With a proportion of 52%, clay loam is one of the most popular soil textures in the area.

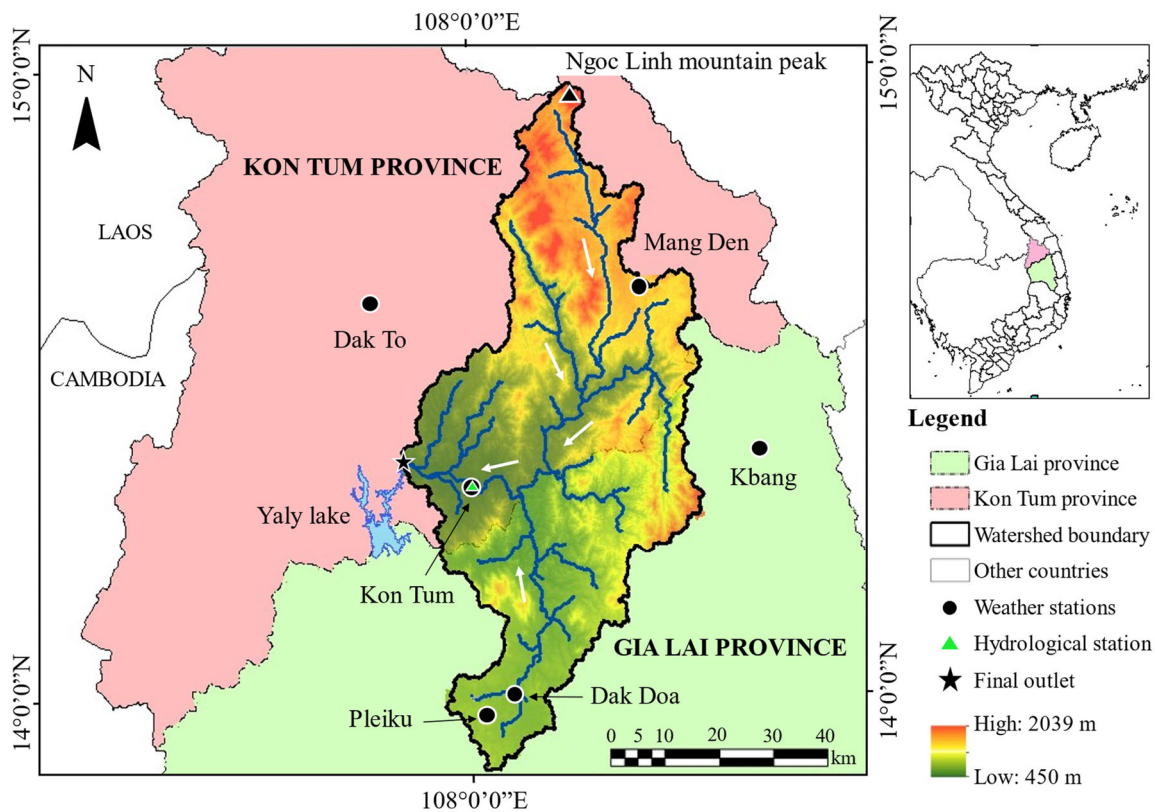


Figure 4.1. Location of the DBW. The model performance was evaluated at Kon Tum hydrological station

Rubber trees are considered to be plants that are suitable to the climatic and soil conditions in the Central Highlands of Vietnam. Since 2010, many projects have been conducted to convert mixed forests to rubber forests to create jobs and generate income for local people, especially ethnic minorities (Prime Minister, 2009); however, most of the new rubber trees have not grown in Gia Lai Province after two or three years of planting because they have been planted on dipterocarp forestland with low fertility, a thin arable soil layer, and poor organic compounds. To solve these obstacles, the conversion of inefficient rubber areas to other crops has been conducted in Gia Lai Province from 2015 onwards. As can be seen clearly in the statistical yearbooks published from the local government, the policies for land-

use categories change dramatically every year and these changes have been confirmed by the information for land-use change percentages; however, land use maps have not been developed after the rapid changes in 2005. Thus, no spatial GIS information is available for after 2005 in the study area.

4.2.2. Input data

The SWAT model requires spatial data (digital elevation model, land-use map, and soil map) and meteorological data (rainfall, maximum and minimum air temperature, relative humidity, wind speed, and solar radiation) as inputs.

The digital elevation model (DEM) was downloaded from the NASA and Japan ASTER Program (2009) with a resolution of 30 m. The range of the topographic elevation in the study area varies from 450 m to 2,039 m.

Land use data were obtained from the Department of Environment and Natural Resources for the Kon Tum and Gia Lai Provinces with a 1:50,000 scale map that was created using the information from 2005. Forestry land makes up the highest percentage with a value of 52.3%, and mixed forests occupy only 2.2%. Orchard, coffee, rubber trees, and agricultural land row crops occupy 16.6% in the total area. The remaining areas are rangelands, water areas, urban areas, and other types, in which rangeland accounts for 22.4% of the whole catchment.

Soil data were obtained from the Department of Environment and Natural Resources in Gia Lai Province and the Department of Information and Communication in Kon Tum Province with two 1:50,000 scale maps. Soil types were categorized into 6 groups based on soil textures, in which clay loam and clay were two popular soil textures with a combined proportion of 82.9%. The remaining parts account for negligible amounts, including loam, loamy sand, sand, and sandy clay.

Weather data were provided by the Central Highlands Region Hydrometeorological Centre. The Kon Tum (Kon Tum Province) and Pleiku (Gia Lai Province) are weather stations with rainfall, minimum and maximum temperature, humidity, sunshine hours, and wind speed data from 1990 to 2018. Solar radiation was calculated with the Angstrom formula by utilizing the sunshine hour data for this area (Bao and Pryor, 1997). Four other stations, including the Dak To, Dak Doa, Kbang, and Mang Den weather stations, provided daily rainfall data. Dak To weather station also provided temperature data. River discharge and total suspended sediment (TSS) concentration were recorded at Kon Tum hydrological station by the Department of Environment and Natural Resources in Kon Tum Province from 2000 to 2018.

Table 4.1. Statistical summary of the observed river flow and total suspended sediment (TSS) concentration at the Kon Tum station (2000–2018). Min/Max: minimum and maximum values; SD: standard deviation

Items	Flow (m ³ /s)	TSS (mg/L)
Min/Max	6.8/3,500	1.0/1,699.3
Median	66.3	34.1
Mean \pm SD	94.7 \pm 106.0	80.9 \pm 93.0

4.2.3. Methods

❖ Brief description of SWAT

SWAT is known as a physically based semi-distributed hydrological model that was developed by the Blackland Research and Extension Center and the Agricultural Research Service of the United States Department of Agriculture (USDA-ARS). This focused on predicting the impacts of land management practices on water and sediment in large complex watersheds over long periods of time (Arnold et al., 1998). There are many papers that have used this hydrological model to simulate water discharge and base flow (Rostamian et al., 2008; Somura et al., 2009; Tram et al., 2019), as well as sediment for specific storm events (Hussain et al., 2019). This model has also been used to show the relationships between sediment, rainfall, and simulated surface runoff (Tibebe and Bewket, 2010; Mosbahi et al., 2013). By using this model, the impacts of land use changes have also been analyzed in terms of annual hydrological components and sediment (Pai and Saraswat, 2011), as well as flow, total nitrogen, and total phosphorus loads (Wang et al., 2018). The above evidence reveals the reliability and wide applicability for the model, especially in mountainous areas.

Simulation of hydrology is based on the water balance equation, as shown in Equation (4.1):

$$SW_t = SW_0 + \sum_{i=1}^t (R_{day} - Q_{surf} - E_a - W_{seep} - Q_{gw}) \quad (4.1)$$

where SW_t : the final soil water content (mm H₂O); SW_0 : the initial soil water content (mm H₂O); t : the time (day); R_{day} : the amount of rainfall on day i (mm H₂O); Q_{surf} : the amount of surface runoff on day i (mm H₂O); E_a : the amount of evapotranspiration on day i (mm H₂O); W_{seep} : the amount of percolation and bypass flow exiting the soil profile bottom on day i (mm H₂O); Q_{gw} : the amount of return flow on day i (mm H₂O).

In addition, erosion caused by rainfall and runoff is computed with the Modified Universal Soil Loss Equation (MUSLE) in SWAT (Williams, 1975). To predict sediment loss, the peak runoff rate is used. Erosion and sediment yields are calculated for each hydrological response unit (HRU) by using Equation (4.2):

$$sed = 11.8 \times (Q_{surf} \cdot q_{peak} \cdot area_{hru})^{0.56} \times K_{USLE} \times C_{USLE} \times P_{USLE} \times LS_{USLE} \times CFRG \quad (4.2)$$

where sed: the sediment yield on a given day (metric tons); Q_{surf} : the surface-runoff volume (mm H₂O/ha); q_{peak} : the peak runoff rate (m³/s); $area_{hru}$: the area of the HRU (ha); K_{USLE} : the USLE soil erodibility factor (0.013 metric ton m² hr/(m³-metric ton cm)); C_{USLE} : the USLE cover and management factor; P_{USLE} : the USLE support practice factor; LS_{USLE} : the USLE topographic factor; CFRG: the coarse fragment factor.

❖ SWAT application

To evaluate model output accuracy, daily observed runoff and sediment data were utilized. The watershed was divided into 73 subbasins in the model. The SWAT parameter values were calibrated for 10 years from 2000 to 2009 and validated for another 9 years from 2010 to 2018. The most sensitive 13 parameters were calibrated, such as CN2 (SCS runoff curve number), SURLAG (surface-runoff lag time), SOL_AWC (available water capacity of the soil layer), SOL_K (saturated hydraulic conductivity), USLE_P (USLE support practice factor), ALPHA_BF (baseflow alpha factor), and GW_DELAY (groundwater delay), in order to improve the model performance. The calibration of the parameter values was conducted using the SUFI-2 algorithm in the calibration uncertainty program for SWAT (SWAT-CUP) (Abbaspour et al., 2007).

❖ Land-use change update module

The land-use change modules were developed for SWAT via SWAT2009_LUC (Pai and Saraswat, 2011), SWAT-LUT (Moriassi et al., 2019), or scripting with R (Tam, 2012), which is a free software package for statistical computing and graphics developed by the R Foundation for Statistical Computing (R Core Team, 2016). The software enables updated land-use changes to be considered in the SWAT model by linear interpolation at the chosen time. With many approaches, land-use changes with time stamps are simulated, while other factors remain stable (Moriassi et al., 2019).

❖ Preparation of land-use maps in 2010, 2015 and 2018 and land-use scenario settings

In the traditional SWAT applications, only a single land-use map is utilized to simulate target elements for a whole target period. In this study, a 2005 land-use map was used as the

base land-use map for the simulation; however, as many land-use policies have been implemented since 2010 by the local government, the 2005 land-use map was updated with the information from the statistical yearbook recording data, such as the area for each land-use category and the crop varieties in each province. Based on local policy decisions for land uses and the statistical information, new land-use maps were developed for 2010, 2015, and 2018 (Figure 4.2). As only statistical information was available and there was no spatial location information for the land-use changes after 2005, historical local information was employed, which mentioned that mixed forests have been converted to rubber forests in the altitude range from 600 to 800 m. This knowledge was used to update the hypothetical land-use percentages. Specifically, by using the DEM information, the mixed forest area was further divided into three categories from 400–600 m, 600–800 m, and 800–1,000 m, and mixed forest land use was updated for a 600–800 m altitude to fit the conversion percentages in the statistical yearbooks for the district data. The percentages of other land-use categories in the 2010, 2015, and 2018 land use maps were also changed to fit the statistical information from the district level without considering altitude.

In the 2010 statistical yearbook, the agricultural, forest, and urban areas increased by 8.4%, 1.8%, and 27.1%, respectively, whereas rangeland decreased by 12.4% in the watershed compared to 2005. This meant that afforestation, agricultural expansion, and urbanization were conducted until 2010, mainly in the northern, western, and northwestern areas. After 2010, crop conversion was conducted in the target area. As mixed forests in the area had been exhaustively exploited, they were no longer able to provide timber products (MARD, 2009). Moreover, there was a decreasing tendency for rubber trees from 2010 till 2014 (Gia Lai Provincial People's Council, 2015) as new rubber trees had not grown in Gia Lai Province after two or three years after planting. The combined rubber tree area for the five districts in Kon Tum Province was 4,439 ha, accounting for approximately 21.5% of the total mixed forest area (20,692 ha) (Kon Tum Provincial People's Committee, 2016), and the rubber tree area was 23.7% in Gia Lai Province (11,385 ha of rubber trees of the total 47,943 ha in the mixed forest) (Gia Lai Provincial People's Council, 2015).

In the 2015 statistical yearbook, the urban area increased continuously in the southern region with a value of 14%, while there was a decrease of forestry land by approximately 3.4% in contrast to 2010. Following the policy changes, conversion from inefficient rubber areas to other crops in Gia Lai Province was conducted. The other crops included orchard trees, agricultural crops, and industrial crops (MARD, 2018). From 2015 onwards, based on the statistical yearbooks, the orchard areas increased by 3.8% and 56.3% in the provinces of

Kon Tum and Gia Lai, respectively. At this moment, the detailed spatial areas of rubber trees converted to orchards were unknown in both provinces.

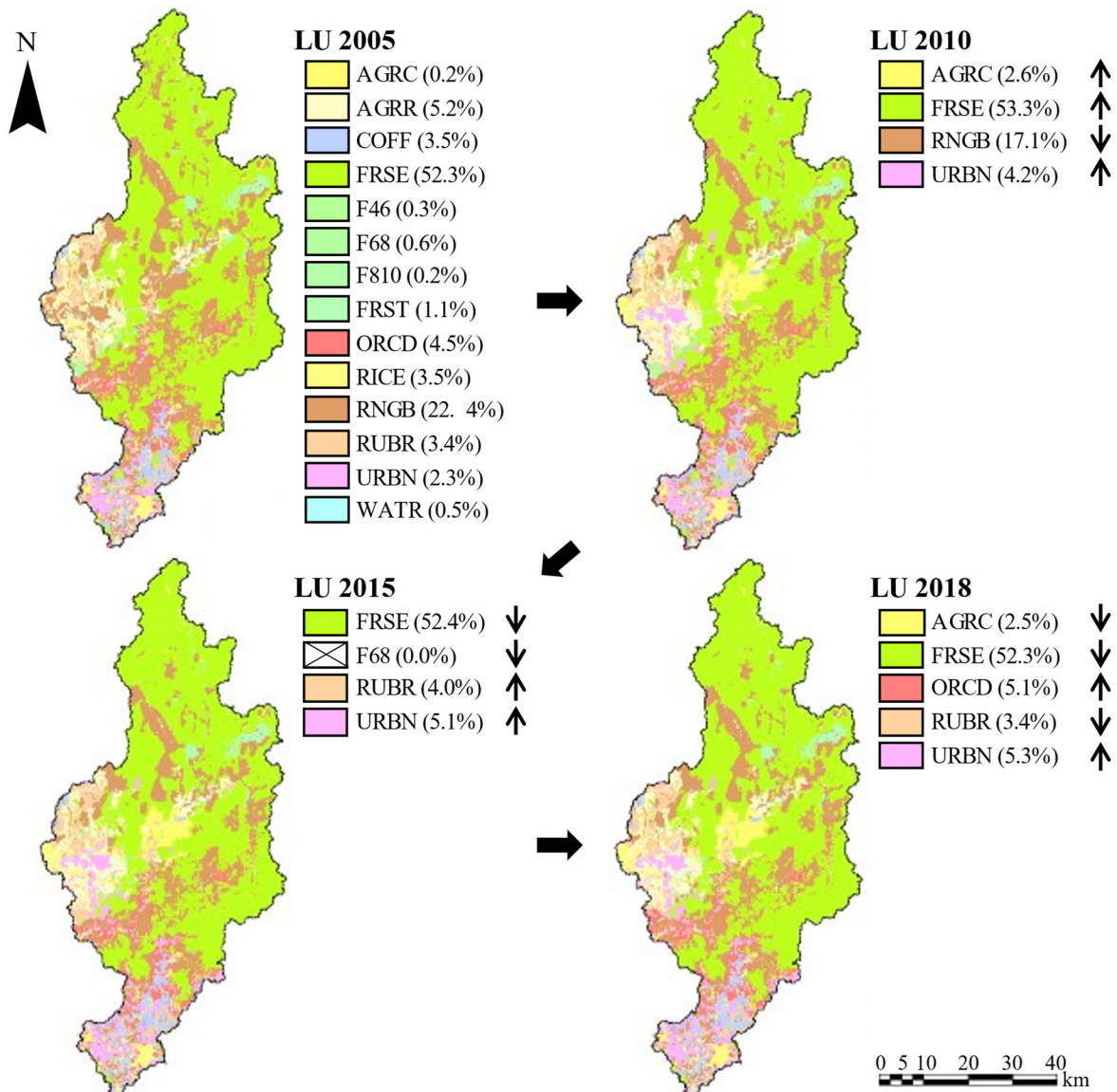


Figure 4.2. The 2005, 2010, 2015, and 2018 land-use maps in the DBW. The major changes in land use are shown in the legend for the 2010, 2015, and 2018 maps. AGRC: agricultural land, non-row crops; AGR: agricultural land row crops; COFF: coffee; FRSE: forestry land; F46: mixed forest (400–600 m); F68: mixed forest (600–800 m); F810: mixed forest (800–1,000 m); FRST: mixed forest; ORCD: orchard; RICE: rice; RNGB: rangeland; RUBR: rubber; URBN: urban; WATR: water

In the 2018 statistical yearbook, the urban area increased continuously with a value of 1.7%, while there was a decreasing tendency for agricultural land and forestland with values of approximately 0.3% and 0.6%, respectively, compared to 2015.

Four land-use scenarios were considered, including one static input condition with the 2005 land-use map (S1) and three updated input conditions (S2, S3, and S4) in the simulation (Figure 4.3). In S2, S3, and S4, the 2005 land-use map was utilized during the 2000–2004 period of simulation. In S2, the developed 2010 land-use map was used for the 2005–2018 period of simulation. For S3, the 2010 and 2015 land-use maps were utilized in the 2005–2009 and 2010–2018 simulation periods, respectively. In S4, the 2010, 2015, and 2018 land-use maps were utilized in the 2005–2009, 2010–2014, and 2015–2018 simulation periods, respectively. The weather input data between the four scenarios were the same.

	Start								End
	2000	2004	2005	2009	2010	2014	2015	2018	
S1	2005 map		→						2005 map
S2	2005 map		→ 2005 map	2010 map		→			2010 map
S3	2005 map		→ 2005 map	2010 map		→ 2015 map		→ 2015 map	
S4	2005 map		→ 2005 map	2010 map		→ 2015 map		→ 2018 map	
			: Linear interpolation period						

Figure 4.3. Land-use map input conditions in simulation scenarios 1–4. S1 represents the static input condition and S2, S3, and S4 represent the three updated input conditions

❖ Model performance evaluation

Each statistical index has the advantages and disadvantages, and it is appropriate to utilize multiple parameters to evaluate the model performance more comprehensively (Moriassi et al., 2015). In this study, to evaluate the accuracy of the SWAT model outputs, the coefficient of determination (R^2), the Nash–Sutcliffe index (NSI), and the percent bias (PBIAS) were used, as shown in Equations (4.3)–(4.5):

$$R^2 = \left[\frac{\sum_{i=1}^n (O_i - \bar{O})(P_i - \bar{P})}{\sqrt{\sum_{i=1}^n (O_i - \bar{O})^2} \sqrt{\sum_{i=1}^n (P_i - \bar{P})^2}} \right]^2 \quad (4.3)$$

$$NSI = 1 - \frac{\sum_{i=1}^n (O_i - P_i)^2}{\sum_{i=1}^n (O_i - \bar{O})^2} \quad (4.4)$$

$$PBIAS = \frac{\sum_{i=1}^n (O_i - P_i)}{\sum_{i=1}^n (O_i)} \times 100 \quad (4.5)$$

where O_i is the observed discharge, \bar{O} is the average observed discharge, P_i is the simulated discharge, \bar{P} is the average simulated discharge, and n is the number of registered data.

R^2 demonstrates the combined dispersion against the single dispersion of the observed and predicted values (Santhi et al., 2001). NSI indicates how well the plot of the observed values versus the simulated values fits the unit slope line (Nash and Sutcliffe, 1970). Values greater than 0.5 for these variables are considered acceptable. If $NSI \geq 0.65$, the simulation of model is considered extremely good (Nash and Sutcliffe, 1970; Saleh et al., 2000; Santhi et al., 2001). PBIAS represents the average trend of the simulated values to be more different than their observed counterparts. The optimal value is 0, and positive and negative values indicate a bias toward underestimation and overestimation, respectively (Gupta et al., 1999). If the PBIAS value is between -10% and 15% for monthly flow and between $\pm 10\%$ to $\pm 20\%$ for sediment, this means that the model simulation can be judged as satisfactory (Moriasi et al., 2015).

4.2.4. Uncertainty analysis method

The output uncertainty after updating the land-use change was evaluated using the relative difference (RD) indicator, which illustrates the percentage error compared to the base data.

$$RD_i = (D_i - S_i) \times 100 / S_i \quad (4.6)$$

where D_i is the model output using the updated land-use input conditions (S2, S3, or S4) and S_i is the model output while using the static land-use input condition (S1).

4.3. Results

4.3.1. Reproducibility of flow and sediment in the calibration period (2000–2009)

The flow was simulated with R^2 , NSI, and PBIAS values of 0.78, 0.70, and -8.1% , respectively (Table 4.2). Most of the values lay around the 1:1 line shown in Figure 4.4. There were some special cases with some underestimated peaks, leading to fluctuation of the statistical parameters. During this period, for example, enormous historical flooding occurred on September 29th in 2009, where the observed water discharge at Kon Tum hydrological station was $3,500 \text{ m}^3/\text{s}$ with a corresponding rainfall value of 152.4 mm at that time.

As for the sediment, the results showed that the flow simulation of the model was better than that with the sediment simulation. The reproducibility of the model was evaluated with R^2 , NSI, and PBIAS values of 0.74, 0.66, and 31.5% in the calibration period.

The simulated results for both flow and sediment were evaluated to be between “very good” and “satisfactory” in the period from 2000 to 2009, except for the PBIAS for sediment.

Table 4.2. The statistical values of R^2 , NSI, and PBIAS in the static land-use condition (S1), featuring the 2005 land-use map during entire simulation period of 2000–2018, and the updated land-use conditions (S2, S3, and S4). R^2 : coefficient of determination; NSI: Nash–Sutcliffe index; PBIAS: percent bias

	Monthly flow			Monthly sediment		
	R^2	NSI	PBIAS (%)	R^2	NSI	PBIAS (%)
Static LU condition						
Calibration (2000–2009)	0.78	0.70	–8.1	0.74	0.66	31.5
Validation (2010–2018)	0.68	0.62	–14.6	0.63	0.54	18.4
Updated LU conditions						
Calibration (2000–2009)						
S2, S3, S4	0.78	0.71	–11.2	0.75	0.67	29.2
Validation (2010–2018)						
S2	0.68	0.64	–16.3	0.63	0.55	18.6
S3	0.70	0.65	–8.0	0.67	0.62	2.1
S4	0.70	0.65	–7.4	0.67	0.62	1.1

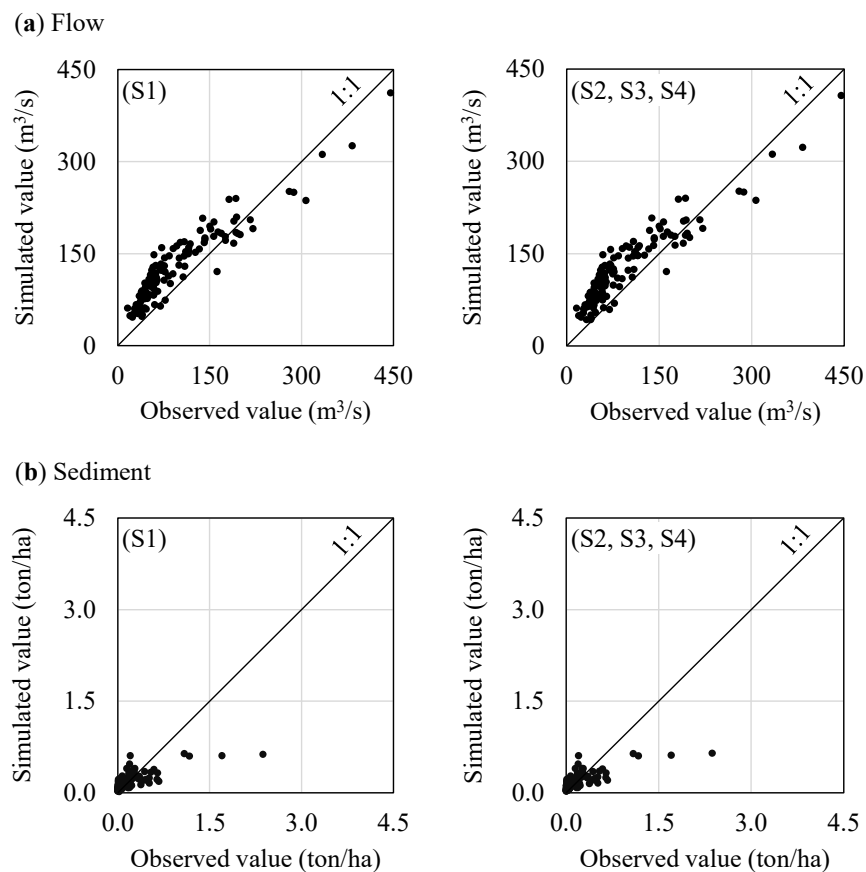


Figure 4.4. The correlation between the observed and simulated flow (a) and sediment (b) in the calibration period. S1 represents the simulation result when using the 2005 land-use map for the entire calibration period. S2, S3, and S4 represent the simulation results when

using the two land-use condition types, namely, the 2005 land-use map from 2000 to 2004, and the linearly interpolated map for the 2010 land-use condition in the calibration period

4.3.2. The influence of land-use update on flow in the validation period (2010–2018)

The validation result for the static land-use condition (S1) was lower than that with the calibration because some values were scattered around the 1:1 line (Figure 4.5). During the 2010–2018 period, there was flooding on October 19th, 2011, with flow and rainfall values of 1,000 m³/s and 57.4 mm, respectively. The reproducibility between the observed and simulated flow in S1 was evaluated as satisfactory, which was represented by $R^2 = 0.68$, NSI = 0.62, and PBIAS = -14.6%. As can be seen, the SWAT could accurately simulate flow and sediment in the target watershed. Thus, the calibrated and validated parameter values were utilized for the simulation with three updated land-use conditions.

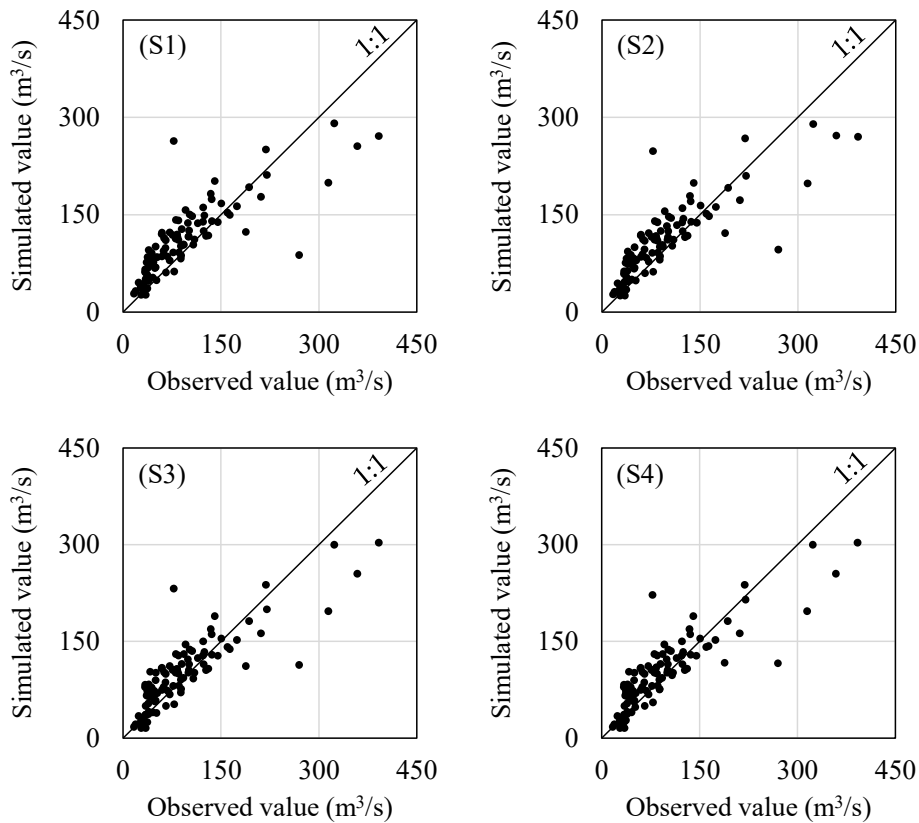


Figure 4.5. The correlation between the observed and simulated flow discharges in the validation period. S1 represents the simulation results when using the 2005 LU map for the entire validation period. S2 represents the simulation results when using the 2010 LU condition for the entire validation period. S3 represents the simulation results when using two LU condition types for 2010 and 2015, and then linearly interpolating toward 2015 after 2010, where the 2015 LU condition is employed for the 2015–2018 simulation. S4

represents the simulation results when using three LU condition types during the validation period and linearly interpolating between two LU conditions

The performance of the model when using the updated land-use scenarios was improved when compared with the S1 result for flow in the validation period. The NSI values for S2, S3, and S4 were 0.64, 0.65, and 0.65, respectively, which were slightly higher than that found with S1. The flow values tend to be closer to the 1:1 line. The R^2 values were 0.68, 0.70, and 0.70, and the PBIAS values were -16.3% , -8.0% , and -7.4% , for S2, S3, and S4, respectively. As a result, S4 had the highest accuracy of the models in terms of flow simulation.

4.3.3. The influence of land-use update on sediment in the validation period (2010–2018)

Similar to the flow simulation, the validation result for S1 found the lowest R^2 and NSI values between the four scenarios as some values were scattered around the 1:1 line (Figure 4.6). This was caused by some underestimated sediment peaks, leading to the lower accuracy of the model.

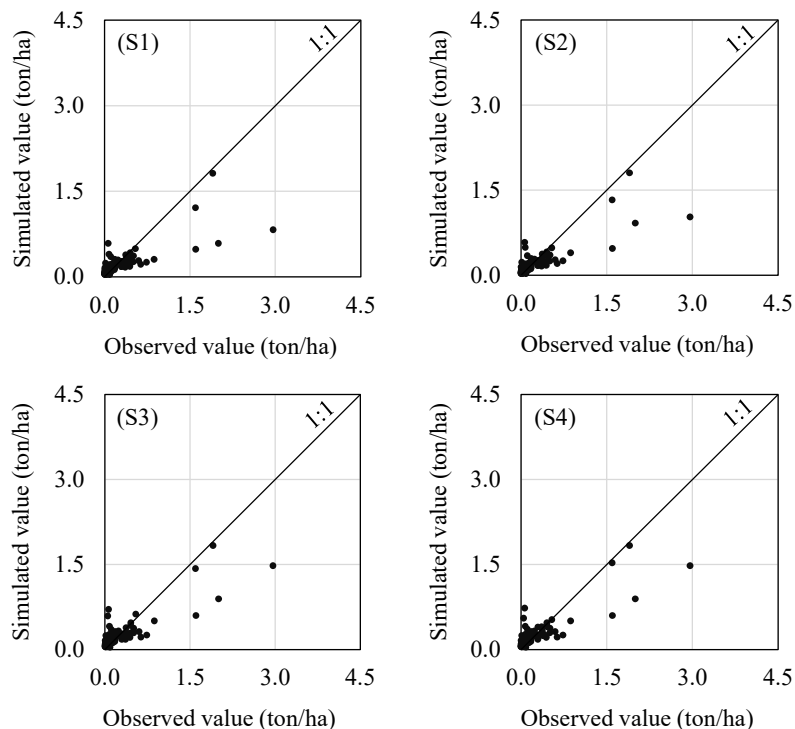


Figure 4.6. The correlation between the observed and simulated sediment discharges in the validation period. S1 represents the simulation results when using the 2005 LU map for the entire validation period. S2 represents the simulation results when using the 2010 LU condition for the entire validation period. S3 represents the simulation results when using two LU condition types for 2010 and 2015 and then linearly interpolating toward 2015 after

2010, where the 2015 LU condition is then employed during the 2015–2018 simulation. S4 represents the simulation results when using three LU condition types during the validation period and then linearly interpolating between two LU conditions

In S1, the correlation between the observed and simulated sediment values was within the satisfactory threshold with $R^2 = 0.63$, NSI = 0.54, and PBIAS = 18.4%. Focused on the three updated land-use scenarios, the NSI values were higher than S1, in which S3 and S4 both produced the highest NSI value of 0.62, and a lower value of 0.55 for S2. With S3 and S4, the PBIAS value for S4 was better than S3, although they had similar NSI values. The observed sediment data had some enormous peaks, which might be related to a limitation of the sediment measurement.

4.3.4. The responses of flow and sediment to the different land-use input conditions

For surface runoff, groundwater, water yields, and evapotranspiration, the RD values did not change much between the updated land-use scenarios and S1 (Table 4.3). There was a decrease for S2 with a value of 2.5%, whereas surface runoff in S3 and S4 increased by 5.1% and 5.2%, respectively. The RD values for groundwater did not exceed 1.5% between the different scenarios compared to S1. For water yield and evapotranspiration, the differences in S2 were higher than those in S3 and S4 when compared to S1, where there were moderate decreases with values of 1.7% and 5.3%, respectively, and these values changed slightly by only less than 2% for S3 and S4; however, the sediment yield changes were relatively large for S2 (–24.3%), S3 (25.7%), and S4 (27.1%). The highest value of sediment yield reached 8.9 tons/ha for S4 and the RD value increased dramatically by approximately 27.1%. In S2, there was a reverse tendency with a significant 24.3% RD value. The higher uncertainty of sediment was caused by the fluctuation of sediment peaks. Overall, the sediment simulation under the land-use input conditions was affected more than the other components.

On an annual basis, compared with S1, the updated land-use input scenarios slightly changed the annual flow. S2, S3, and S4 reached lower values than S1, and the RD values ranged from 0.1% to 8.9%. During the 2000–2018 period, the highest total annual flow for S1 remained the same with 1,918 m³/s in 2009, and there were decreasing trends of 2.2% for the three other scenarios in 2009. The lowest value for S1 was 1,196 m³/s in 2015 (Figure 4.7). Compared to S1, S2 had a slight decrease of 1.4%, whereas there were moderate rises of 8.6% and 9.5% for S3 and S4, respectively.

Table 4.3. Relative difference (RD) values of the target components with the updated land-use input conditions vs. static input condition

Target components	RD (S2 vs. S1)	RD (S3 vs. S1)	RD (S4 vs. S1)
Surface runoff	-2.5%	5.1%	5.2%
Groundwater	0.8%	-1.4%	-1.5%
Water yields	-1.7%	-1.0%	-1.0%
Evapotranspiration	-5.3%	1.6%	1.8%
Sediment yields	-24.3%	25.7%	27.1%

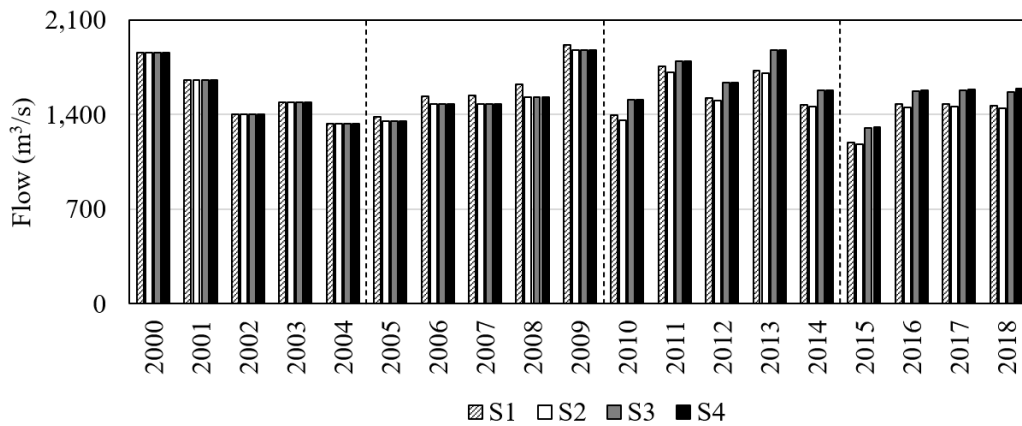


Figure 4.7. The differences of the total annual flow between the different updated land-use scenarios

The total annual sediments had larger changes than those for the flow values under different land-use input conditions, especially throughout a 2015–2018 period (Figure 4.8). In the whole simulation period, S1 reached the highest sediment values of 1,028 thousand tons in 2009, and then the value decreased by 5.8% in the others. The value in 2015 was the lowest in S1, and then the value decreased slightly by 2.0% in S2 and increased significantly in S3 and S4 by approximately 22.0% and 22.4%, respectively.

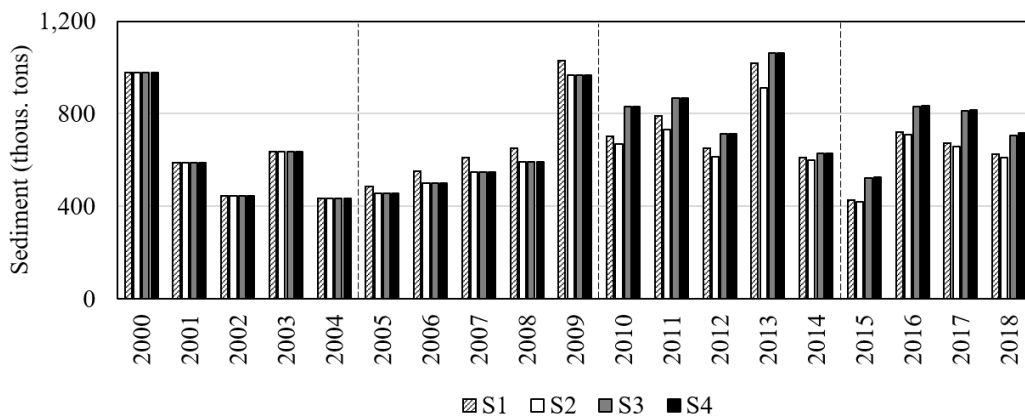


Figure 4.8. The differences of the total annual sediment between the different updated land-use conditions

On a monthly basis, the highest values for all scenarios occurred in October for runoff and November for sediment. The RD values for the monthly flow did not exceed 3.2% for S2, 6.2% for S3, and 6.3% for S4. The highest flow value in S1 was approximately 192.3 m³/s in October. S2 had a slight decrease of only 1.0%, whereas there were increasing trends with 1.0% and 1.1% for S3 and S4, respectively. Oppositely, a larger change was observed for the sediment values with the updated land-use scenarios. The RD values for monthly sediment reached 7.0% in S2, 9.4% in S3, and 9.7% in S4. The highest value in S1 was 104.6 thousand tons in November, and there were increasing tendencies of 9.2% and 9.7% for S3 and S4, while there was a decreasing tendency of an approximately 5.1% for S2 when compared with S1. The last three months, including October, November, and December, featured significant changes during the year.

As the number of loads discharging from the watershed to downstream were affected by the land-use management history, the differences in the cumulative sediment loads from 2000 to 2018 were compared between the different land-use input conditions. Significant differences were found to exist between the four scenarios at the end of the simulation (Figure 4.9). During the 2000–2004 period, where the same land-use map was used in all scenarios, the sediment loads were all 3,540 thousand tons. After 2005, where S2, S3, and S4 used the updated land-use information in the simulation, the cumulative sediment loads during 2005 to 2009 were slightly lower than those in S1, where they decreased by 232 thousand tons, corresponding 0.8 tons/ha. After 2010, S3 and S4 used updated land-use information in the simulation, where the cumulative sediment loads during 2010 to 2014 changed from 3,772 thousand tons in S1 to 3,526 thousand tons in S2; 4,105 thousand tons in S3; and 4,105 thousand tons in S4.

After 2015, where only S4 updated the land-use information via linear interpolation, the cumulative sediment loads during 2015 to 2018 changed to 2,449 thousand tons in S1; 2,397 thousand tons in S2; 2,871 thousand tons in S3; and 2,893 thousand tons in S4, respectively. During the whole simulation period from 2000 to 2018, the difference for the total cumulative sediment load between S1 and S2 was approximately 529 thousand tons, corresponding to a 1.8 tons/ha. In addition, the differences for S3 and S4 compared to S1 were approximately 524 thousand tons and 545 thousand tons, corresponding to values of 1.8 tons/ha and 1.9 tons/ha, respectively. Moreover, comparing S3 and S4 with S2, the differences became the largest with approximately 1,053 thousand tons (3.6 tons/ha) and 1,074 thousand tons (3.7 tons/ha).

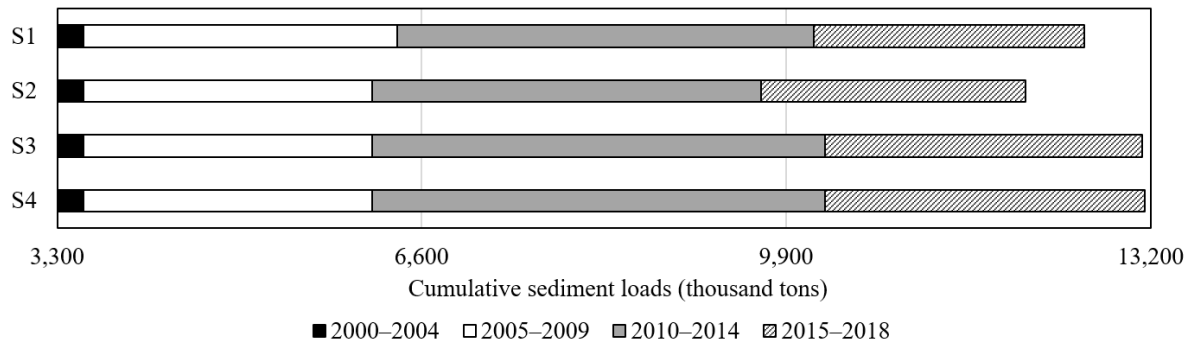


Figure 4.9. Change of cumulative sediment discharge between the scenarios (2000-2018)

4.4. Discussion

4.4.1. Importance of land-use update for improving modeling performance

SWAT simulations were conducted with 2000–2009 calibration data and 2010–2018 validation data by using the observed flow and sediment data from the Kon Tum hydrological station and the same climatic data in the watershed, along with the four different updated land use conditions (2005, 2010, 2015, and 2018). The statistical values of R^2 , NSI, and PBIAS improved from S1 (no change of land use information during the entire simulation period) to S4 (updated land-use information with linear interpolation between two land uses).

We have concluded through this research that using a single static land-use map in a region with frequent and complicated policy changes cannot illustrate the actual local conditions throughout the whole simulation period, leading to low accuracy for the model performance. This means the impact of land-use management on downstream environment would also not be appropriately evaluated if inadequate land-use information is input to the model.

In the target watershed, because of the local policy regarding land uses, rangelands have decreased because of the anthropogenic activities conducted since 2005. Mainly due to the afforestation, total sediment load discharges were simulated to decrease during the period, but the model could not capture the trend when only single static land-use information was used in the simulation. After that period, because of local policy, deforestation, urbanization, and crop conversion were again conducted, and this caused the sediment discharge to increase from 2010 to 2014. In this case, the model could not capture the influence of policy in the simulation when S1 or S2 were considered. After 2015, crop conversion was conducted continuously, and the model could not express the impact of the local policy changes in the simulation if S1 or S2 were utilized; however, S3 could be used in this case, although the accuracy was worse than that with S4.

In modeling approach, emerging land-use change categories have been updated as important inputs in a model (Moriassi et al., 2019). By using multiple land-use maps with linear interpolation (the same methodology in this research), updated time stamps have led to more realistic conditions in the modeling (Moriassi et al., 2019). After the determination of suitable land-use input conditions in a simulation, the critical subwatersheds can be appreciated in terms of their detailed internal processes, as well as further scenarios, including runoff and sediment at the watershed scale (Awotwi et al., 2019). Some researchers have already emphasized the impacts of land-use changes on flow, total nitrogen, total phosphorus (Wang et al., 2018; Moriassi et al., 2019; Wagner et al., 2019), and sediment yield (Son et al., 2020; Aghsaei et al., 2020). Apparently, the differences in the flow and sediment simulation results caused by the differences in the land-use input conditions can affect the long-term land-use planning in the DBW.

4.4.2. Influence of land-use update for flow and sediment simulation

Many researchers have already pointed out that the output of such a model is affected by the different input conditions, especially land-use changes (Stéphenne and Lambin, 2001; Zhang et al., 2011; Aghsaei et al., 2020), because land-use changes have strong effects on hydrologic processes and sediments (Tripathi et al., 2003; Munoth and Goyal, 2020). The results indicate that the reproducibility for the peak flow and sediment discharges could be improved in the simulations to improve the model accuracy, and the updated land-use conditions could then better follow the observed values. Especially, the reproducibility was better improved for the sediment simulation than the flow simulation, as the land use input data had relatively low effects in terms of the flow simulation (Wang et al., 2018). Thus, this study could show the potential of the multiple updated land-use inputs against the performance improvement of sediment simulation in a mountainous region.

In addition, the different impacts on water balance components could be expressed by the continuous land-use changes in a monthly time scale (Aghsaei et al., 2020). The seasonal responses to land-use change for flow and sediment have been emphasized due to enormous alterations, such as urbanization and agricultural expansion (Anand et al., 2018). Land-use changes have increased the risk of extreme hydrological circumstances, including flooding and drought events (Makhtoumi et al., 2020).

In the target watershed, the changes for the flow and sediment in the rainy season commonly became larger than those in the dry season, even in the different scenarios. This means that the land-use input conditions in the simulations are more significant in the rainy

season than in the dry season. The greatest influence was observed from October to December, because these months are the end of the rainy season and the beginning of dry season, and the climatic conditions will be unstable and rainfall density/intensity is higher (Dunning et al., 2018; Seth et al., 2013). Thus, updating land-use information throughout the simulation period is especially crucial for monthly and seasonal evaluations of sediment in the mountainous regions.

4.4.3. Land-use policies in the region for the future, including the DBW, and the contribution from the model simulation

Land use patterns change based on the impacts of human activities, policies, and other factors, such as climate change. Land-use changes are more prominent if the impacts on water resources, hydrological processes, and ecosystems are assessed (Li et al., 2009). Traditional cultivation methods have little effect on erosion because of the quick recolonization of vegetation. Nevertheless, land-use changes towards intensive agriculture could require a higher adoption of conservation practices in order to mitigate erosion (Yustika et al., 2019) and preserve the water quality (Aflizar et al., 2010; Somura et al., 2012). The natural flow and ecological environment is negatively affected by the increase of irrigated agriculture alongside along urban expansion. One of the negative consequences of ongoing urbanization is an increase in deforestation (Aghsaei et al., 2020). Increasing areas of urban and agricultural lands at the expense of closed and open forests results in direct impacts on surface runoff, baseflow, and water yields (Awotwi et al., 2019).

In the Central Highlands of Vietnam, some evidence has revealed that there have been dramatic land use changes during five years c. Additionally, many local policies have frequently changed to adapt and improve the current conditions, particularly crop conversion policies (Son et al., 2015; Prime Minister, 2009). Huge mixed forest areas have been converted; however, there have been no strict regulations to protect forest areas, leading to forest cover reduction (Son et al., 2020). The ongoing land-use changes pertain to converting inefficient upland fields into forests or orchards. Considering scheduled land-use condition updates, the model outputs could immediately support local governments in land-use planning and water management. Moreover, afforestation activities, especially in upstream areas of the DBW, should be encouraged to prevent soil erosion and more efficiently regulate water resources. Many projects have been conducted or planned for protecting forest areas, such as the restriction of development, afforestation, and restoration in the Central Highlands of Vietnam from 2016 to 2030 (Prime Minister, 2018). Sustainable forestry development

strategies for 2021–2030 have been proposed, with a greater vision to 2050 (MARD, 2019). Throughout 2021–2030, forest area in the region is expected to increase by approximately 2.72 million hectares (Prime Minister, 2018). Specific policies for forest areas in the region have been continuously developed towards encouraging the formation of community forest management systems. These systems are based on forest allocation to individual households, communes, and villages (MARD, 2019). Furthermore, the protection of natural forest systems in upstream areas to maintain natural forest cover is also emphasized in these policies. The main aspects pertain to strengthening the ecological environment, conserving biodiversity, providing forest environment services, alleviating poverty, and improving living standards for local residences, especially ethnic people in the region. In these policies, as expectations for the ideal conditions are involved in the area for long term adequate watershed management, the modeling can contribute to creating concrete strategies, including specific areas/locations of protection or development in order to achieve the goals in the policies via simulation with the consideration of land-use changes.

4.5. Limitation of the study

In this study, the SWAT model was used to assess the flow and sediment discharges between four land-use input conditions. However, the land-use maps in 2010, 2015, and 2018 were hypothetically developed by using the local information such as the statistical yearbook. Thus, simulation results can change and improve the accuracy if new land-use maps, GIS information, are provided by the local government in the future.

In addition, the flow discharge and sediment loads were underestimated in the extremely high-flow events. There are several possible reasons of the poor reproducibility during the situations: (1) observed data, (2) spatial distribution of weather observatories in the watershed, and (3) the SWAT model structure. Firstly, the limitation of data measurement affected the calibration and validation processes of the model (Mengistu et al., 2019). In the study area, only one hydrological station exists and records the observed data. Thus, differences in parameter values between subwatersheds may not accurately be expressed for internal hydrological processes in the watershed. Secondly, most rain gauges are located in the upper and lower parts of the watershed, and there is no weather station in the central part of the target area. During the target period of the simulation, some enormous peaks were recorded in the flood events. Thus, the uneven spatial distribution of rain gauges contributes to decreased accuracy of the simulation (Cho et al., 2009; Khoi and Suetsugi, 2014). Thirdly, the SWAT model was developed based on the empirical formulas, and simulation of flow

and erosion was limited at high flows because the upland and in-stream erosion were simulated using the oversimplified algorithms (Phomcha et al., 2011; Chandra et al., 2014). Additionally, as the SWAT model does not consider the sediment deposition remaining in the surface watershed areas, soil eroded by runoff reaches the channel directly (Oeurng et al., 2011). Thus, these influences may affect the model's performance.

4.6. Conclusions

In this study, to understand and evaluate the impacts of static and updated land-use changes on flow and sediment simulation in the DBW, the integration of land-use update modules was examined via SWAT. As land uses changed and many crop conversion projects were conducted in the DBW during the target periods in this study, these changes had significant impacts on the model performance. The important findings are summarized as follows:

- Three land-use maps were hypothetically established based on the local policy changes for land uses and the local statistic yearbook, and their effectiveness in improving the accuracy of the SWAT model outputs was confirmed.
- The impact of land-use changes on flow and sediment was expressed by the multiyear updated land-use input conditions more accurately than by the single static land-use condition at the watershed scale.
- The reproducibility of sediment simulation was more sensitive than the flow simulation.
- The updated land-use effects were higher for the rainy season than the dry season.
- S4 showed the best performance for reproducing the flow and sediment discharge trends.

The impacts of the updated land-use input conditions in terms of flow and sediment simulation are extremely important, especially in mountainous areas with frequent and complicated policy changes. The findings of this study could support decision-makers in implementing more effective land-use planning policies, soil conservation plans, and water resources management strategies for the watershed in the future. As a next step, a nutrient simulation needs to be conducted to consider a conservation plan for the downstream Yaly lake environment.

CHAPTER 5. EFFECTS OF LOCAL LAND-USE POLICIES AND ANTHROPOGENIC ACTIVITIES ON WATER QUALITY IN THE UPSTREAM SESAN RIVER BASIN, VIETNAM

5.1. Introduction

Changes in anthropogenic processes in terrestrial regions could have remarkable effects on the aquatic environment, which is represented by diverse worthwhile environmental functions. To comprehensively control and reduce the significant effects impacting water quality, policies are promulgated on the regional and local scales, especially land-use policies. In Asia, land use underwent significant changes in a relatively short-term period (Zhao et al., 2006). Even though land use occurs at the local level, land-use changes can damage economic, environmental, and ecological aspects on the local/regional/global scales if these changes occur indiscriminately (Zhao et al., 2006). These policies require detailed information on the local scale. The two most essential factors for land-use policies are spatial land use and land-use plans (Organisation for Economic Cooperation and Development: OECD, 2017). Local governments establish specific land-use planning to adjust land-use conversion under the guidance of the higher levels of government, allowing more reasonable plans for the development of an entire region/the whole nation (OECD, 2017). Policies concerning water resources and agriculture aspects should be mentioned in the water policy framework with the consideration of all pollutants and polluters at the national and river basin scales (Mateo-Sagasta et al., 2017); additionally, their long-term impacts should also be considered (Holden et al., 2015). At present, the aspect of long-term watershed management has not yet been comprehensively considered in strategies when land-use policies are updated. It is necessary to have inter-ministerial cooperation systems to ensure the coherence of policies (Mateo-Sagasta et al., 2017).

Population growth leads to deforestation, agricultural expansion, and urbanization. In recent years, these human activities have affected landscapes and downstream water quality in Southeast Asia. Agricultural land expansion towards steep-slope regions and deforestation for agricultural purposes, satisfying the food and feed demand for human beings, has led to increase vulnerability of these areas, especially intensive farming areas (Pierret et al., 2011; Fullen et al., 2011; Frohlich et al., 2013; Lin et al., 2016). Intensive farming in agriculture is one of the better ways by which to achieve growth in the agriculture sector but its impact on water quality is significant (Holden et al., 2015). Zeng et al. (2018) estimated that approximately 82 billion m² of highland regions have been developed into croplands in

Southeast Asian countries. As a result of human-induced changes on the watershed scale, impacts on river discharge (Githui et al., 2009), sediment, and nutrients (Smarzyńska and Miatkowski, 2016; Hanief and Laursen, 2017) have been observed. The nutrients cumulating from non-point sources of agricultural activities were found to be the primary factors increasing the nutrient loadings to watersheds, leading to an accelerated extent of eutrophication in the aquatic environment (Carpenter et al., 1998; Somura et al., 2012). More than 70% of the delivered nitrogen and phosphorus comes from different sources in agricultural processes to the watersheds (Yang et al., 2018). The sediment yields in agricultural watersheds were much greater than those in areas with non-anthropogenic activities, with an approximately hundredfold value in hilly terrains (Stallard, 1998). Along with a high density of rainfall, excess discharge contributes to accelerating surface erosion, thereby increasing the sediment loading and nutrient loss deposited downstream, especially during the rainy season (Sidle et al., 2006; Folliott et al., 2013; Shi et al., 2021). Controlling the pollutant discharges from point and non-point sources will reduce the nutrient loadings in the watershed without a significant impact on crop productivity (Jha et al., 2007; Alexander et al., 2008). Even though it is undeniable that anthropogenic activities have a great influence on water quality downstream, the magnitude of these impacts would be greatly increased if the crop conversion is unsuitable.

One of the challenges in mountainous areas is that the measured data and the information on pollution sources are limited to evaluating the pollution extent and the water quality monitoring network scattered on the watershed scale. Thus, modeling approaches have been utilized to address these shortcomings and to consider the impacts of local land-use policies and anthropogenic activities on water quality issues. The Soil and Water Assessment Tool (SWAT) has been widely applied around the world to assess the impacts of the river discharge, sediment discharge, and pollution loadings from the point and non-point sources that impact the water environment in large watershed scales (Huang et al., 2009; Abbaspour et al., 2015; Hanief and Laursen, 2017; Malagó et al., 2017; Keraga et al., 2019), including the Central Highlands of Vietnam (Vu et al., 2012; Khoi and Thom, 2015). The significant impacts of land-use changes on hydrology (Githui et al., 2009; Li et al., 2019), suspended sediment, and nutrient loadings (Brito et al., 2019) over a long period were also emphasized by using the single static land-use input conditions, which are normally applied to a modeling analysis. However, in the long-term evaluation of water resources in a watershed in Asian countries, this ordinary method cannot comprehensively evaluate the impacts of land-use changes occurring in a relatively short-term period following local land-use policies. Tram et al.

(2021) indicated that using multiple land-use input conditions with linear interpolation in a simulation could follow the record of land-use changes in a watershed and evaluate their impact on water resources better than utilizing the single static land-use input conditions. In addition to the multiple land-use input conditions, it is necessary to input information on detailed fertilization in agricultural cultivation. The lack of information regarding both the quantity of fertilizer and cultivation timing affects the accuracy of the model's performance (Chu et al., 2004). The impacts of land-use policies and human activities on a watershed are dissimilar despite belonging to the same river basin because of differences in climate conditions, morphological features, and physical processes within each watershed (Tobin and Bennett, 2009; Piniewski et al., 2017). This means that it is necessary to update both the historical land-use changes and detailed agricultural practices in a model to improve the accuracy of the model's performance adapted to the local situations in each period.

Thus, the main purposes of this study were (1) to evaluate the impacts of different land-use policies and agricultural practices on discharge, sediment, total nitrogen (TN), and total phosphorus (TP) at the Dakbla and Poko watersheds in different periods on the basis of temporal and spatial distributions, (2) to assess the influences of land-use policies and anthropogenic activities in each period on the aquatic environment downstream, and (3) to determine how to improve the erosion and water quality in the target river basin.

5.2. Data and methods

5.2.1. Study area

The Sesan River Basin is known as a transboundary basin of the Mekong River. The Sesan River flows through the Kon Tum and Gia Lai provinces in Vietnam. The Poko Watershed (PKW) and Dakbla Watershed (DBW) are two main subbasins of the upstream Sesan River Basin with areas of 3,210 km² in the former and 3,507 km² in the latter as shown in Figure 5.1. The lengths of the Poko and Dakbla Rivers are 121 km and 152 km, respectively. From the upstream areas, these rivers merge to a confluence before flowing to Yaly Lake downstream. Yaly Lake plays an important role in the upstream Sesan River Basin. It is mostly located in Kon Tum province, occupying 44.5 km² of the 64.5 km² total area, with an average depth of 48.2 m, a length of 38 km, and a width of 6 km at its widest point. The reservoir capacity is about 1,037 million m³. Water quality observations started in the lake in 2015. From 2015 to 2019, the water quality of Yaly Lake was deemed to be completely suitable for tourism, aquaculture, fishing, irrigation, and hydropower purposes (Kon Tum Provincial Department of Natural Resource and Environment, 2016, 2017, 2019). With the characteristics of a tropical

monsoon climate, the rainy season (May–November) and the dry season (December–April) are the two main seasons in this area. The average annual precipitation is 1,778 mm and 2,000 mm while the average annual temperature is 23.7 °C and 23.6 °C at the Dak To and Kon Tum stations, respectively. Forest areas occupy the highest proportion of the land (>52%).

In the Central Highlands, the water demand for agriculture encompassed 84% and 90% of the total water demand in Kon Tum and Gia Lai provinces, respectively, in 2015/2016 (JICA, 2018). Kon Tum had the lowest share of agriculture in 2016 among the five provinces in this region because of its poorer soil quality and lower agricultural productivity. An expansion of agricultural activities and a shift in cultivation toward the hillslope have been conducted in the target area from 2005 onwards (Tram et al., 2021). According to the 2010 statistical yearbook, there was an increasing tendency of agricultural land, urban areas, and forestry land with values of 39.9%, 56.6%, and 1.7%, respectively, compared to 2005. From 2010 onward, a crop conversion policy that encouraged a move from mixed forests to rubber forests was enacted (Tram et al., 2021). Rubber trees predominated, accounting for 61.0% (433.2 km²) of the total mixed forest area (709.6 km²) in Kon Tum province (Kon Tum Provincial People's Committee, 2016). Rubber trees occupied 23.7% (113.9 km²) of the total mixed forest area (479.4 km²) in Gia Lai province (Gia Lai Provincial People's Council, 2015). According to the 2015 statistical data, there was a continuous increase in urban areas by 2.7%, whereas the forestry land decreased by a value of 2.7% compared to 2010. Due to some areas having inefficient rubber trees, a local orchard conversion policy was enacted, leading to an increasing number of orchard areas from 2015 onward, rising by 5.4% and 19.5% in Kon Tum and Gia Lai provinces, respectively. Until 2018, agricultural land and urban areas saw an increasing trend, with increases of 28.5% and 1.5%, respectively, whereas forestland decreased continuously by approximately 4.0% in comparison to 2015.

In this study, the 2000–2018 period was categorized into four periods (2000–2004, 2005–2009, 2010–2014, and 2015–2018) on the basis of the changes in local land-use policies. The 2000–2004 period represented a base period in which no land-use policies were applied. The remaining periods illustrated the following changes in land-use policies and anthropogenic activities: 2005–2009, conducting for afforestation, agricultural expansion, and urbanization; 2010–2014, crop conversion policy involving the move from mixed forests to rubber forests; and 2015–2018, crop conversion policy involving the move from insufficient rubber forests to orchards.

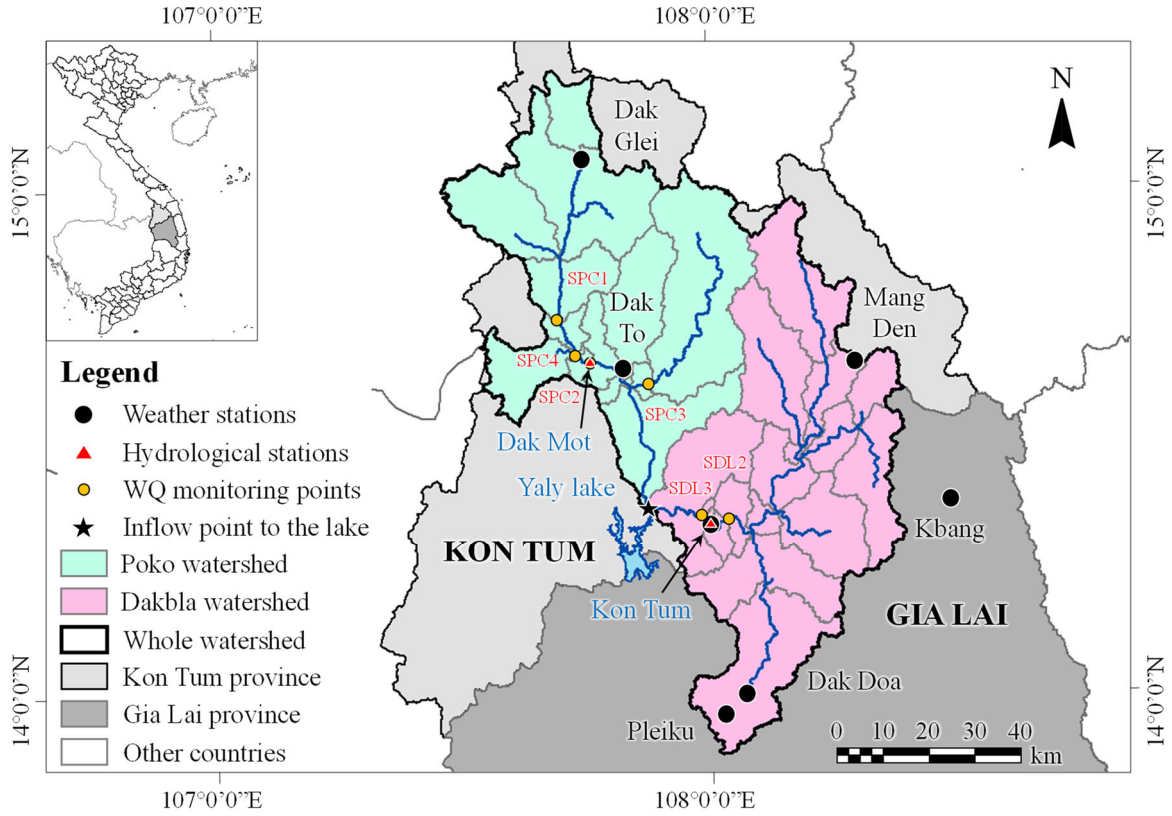


Figure 5.1. Location of the PKW and DBW. River discharges were observed at Dak Mot station in PKW and Kon Tum station in DBW. SPCs 1, 2, 3, and 4 represent the four monitoring points of water quality in the PKW, while SDLs 2 and 3 represent the two monitoring points of water quality in the DBW

5.2.2. Methods

5.2.2.1 Hydrological modeling

❖ SWAT description

SWAT is a well-known physical-hydrological model used to predict the impact of land-use changes and land management practices on river discharge (Hanief & Laursen, 2017), sediment (Shi and Huang, 2021), and nutrients (Epelde et al., 2015; Donmez et al., 2020) over long periods on the river basin scale. The hydrological cycle in SWAT is based on the water balance equation, in which surface runoff is estimated through the SCS curve number equation as follows:

$$Q_{surf} = \frac{(R_{day} - I_a)^2}{(R_{day} - I_a + S)} \quad (5.1)$$

where Q_{surf} is the accumulated runoff or rainfall excess (mmH₂O), R_{day} is the rainfall depth for the day (mmH₂O), I_a is the initial abstractions including surface storage, interception, and infiltration prior to runoff (mmH₂O), and S is the retention parameter (mmH₂O).

Sediment loadings are estimated using the Modified Universal Soil Loss Equation (MUSLE), as shown in Equation (5.2):

$$sed = 11.8 \times (Q_{surf} \times q_{peak} \times area_{hru})^{0.56} \times K_{USLE} \times C_{USLE} \times P_{USLE} \times LS_{USLE} \times CFRG \quad (5.2)$$

where sed is the sediment yield on a given day (metric tons), Q_{surf} is the surface-runoff volume (mmH₂O/ha), q_{peak} is the peak runoff rate (m³/s), $area_{hru}$ is the area of the HRU (ha), K_{USLE} is the USLE soil erodibility factor (0.013 metric ton m² hr/ (m³-metric ton cm)), C_{USLE} is the USLE cover and management factor, P_{USLE} is the USLE support practice factor, LS_{USLE} is the USLE topographic factor, and $CFRG$ is the coarse fragment factor.

For the nitrogen simulation, SWAT considers five different pools of nitrogen, with the two pools of NH₄⁺ and NO₃⁻ being the inorganic forms. The movement of nitrate occurs mainly in the organic N and nitrate forms. The amount of nitrate removed during surface runoff is estimated as follows:

$$NO_{3surf} = \beta_{NO3} \times CONC_{NO3, mobile} \times Q_{surf} \quad (5.3)$$

where NO_{3surf} is the nitrate removed during surface runoff (kg N/ha), β_{NO3} is the nitrate percolation coefficient, $CONC_{NO3, mobile}$ is the concentration of nitrate in the mobile water in the top 10 mm of soil (kg N/mmH₂O), and Q_{surf} is the surface runoff generated on a given day (mmH₂O).

For the phosphorus simulation, the model monitors six pools of phosphorus in the soil, of which three are inorganic forms. Phosphorus escapes from the soil through plant uptake and erosion. Soluble phosphorus and organic and mineral P attached to sediment during surface runoff represent the main mechanisms of phosphorus transport. The solution P transported during surface runoff is calculated as follows:

$$P_{surf} = \frac{P_{solution, surf} \times Q_{surf}}{\rho_b \times depth_{surf} \times k_{d, surf}} \quad (5.4)$$

where P_{surf} is the amount of soluble phosphorus lost in the surface runoff (kg P/ha), $P_{solution, surf}$ is the amount of phosphorus in solution in the top 10 mm (kg P/ha), Q_{surf} is the amount of surface runoff on a given day (mmH₂O), ρ_b is the bulk density of the top 10 mm (Mg/m³), $depth_{surf}$ is the depth of the surface layer, and $k_{d, surf}$ is the phosphorus soil partitioning coefficient (m³/Mg).

❖ Input data of the model and other necessary local information

Spatial data (digital elevation model, land-use map, and soil map) and meteorological data (rainfall, temperature, humidity, sunshine hours, and wind speed) are necessary as the initial inputs of the SWAT. River discharges at Kon Tum and Dak Mot stations were recorded during the 2000–2018 period by the Central Highlands Region Hydrometeorological Center. The total suspended sediment concentration at Kon Tum station was also measured by the center. Water quality data from six measuring points were collected from 2014 onward by the Kon Tum Department of Environment and Natural Resources. Furthermore, other important local information including land-use change history, crop conversion policies, and agricultural practices were collected from the department. The detailed input data information was shown in Table 5.1. For the water quality measuring points, only one measuring point, SPC2 at Dak Mot station, was used to calibrate the nutrients of the model because river discharge information was available from a nearby station to calculate loads, while the five remaining points, where concentrations were measured, were utilized to check the accuracy of the model in the different locations, mainly paying attention to average concentration.

Table 5.1. Necessary input data of the model

Data	Sources	Description
Digital elevation model	NASA and Japan ASTER Program (2009)	Topography features (30 m resolution)
Land-use map	National Institute of Agricultural Planning and Projection (2005)	Land-use classification (scale 1:50,000)
Soil map	FAO-UNESCO (2007)	Soil types (scale 1:5,000,000)
Meteorological data		Kon Tum and Pleiku stations: Daily rainfall, daily maximum and minimum temperature, daily mean humidity, daily sunshine hours, and daily mean wind speed (1990–2018) Dak Glei, Dak To, Dak Doa, Kbang, and Mang Den stations: Daily rainfall
River discharge	Central Highlands Region Hydrometeorological Center	Kon Tum station (DBW) and Dak Mot station (PKW): Daily river discharge (2000–2018)
Total suspended sediment (TSS) concentration		Kon Tum station: Daily mean TSS (2000–2018)
Water quality	Kon Tum Department of Environment and Natural Resources	Daily water quality data at SPC2 (4 times/year) • NH ₄ -N, TN, and TP (2014-2018) • NO ₃ -N (2015 and 2018)

	Six monitoring points: SDLs 2 and 3 (DBW); SPCs 1, 2, 3, and 4 (PKW). SPC2 was used to calibrate and validate the model
Land-use change information	Statistical information, land use, and crop conversion policies
Agricultural practice information	Crop types, crop calendar, and fertilizer information

❖ SWAT application

The watershed was delineated into 32 subbasins. In the PKW, the model was calibrated from 2000 to 2015 and validated from 2016 to 2018 for river discharge. The calibration and validation periods for the remaining variables (TN, TP, NO₃-N, and NH₄-N) were from 2014 to 2015 and from 2016 and 2018, respectively. In the DBW, the model was calibrated from 2000 to 2015 and validated from 2016 to 2018 for river discharge and sediment. The TN, TP, NO₃-N, and NH₄-N variables were calibrated and validated by the loads in this study. After calibration and validation of the model parameter values, the impacts on the aquatic environment downstream were evaluated. One of the initial necessary processes is to determine the length of the warm-up period so as to obtain an ‘optimal’ state in the hydrological model. The rainfall factor significantly affects the time required for the warm-up period even if it depends on the structure of the model (Kim et al., 2017). After achieving the optimal status, the response of the model is suitable for the realistic conditions leading to the higher accuracy of the model performance. The 10-year warm-up period was identified as the best choice for our study. Dak Mot station was utilized to calibrate and validate the river discharge and nutrients for the PKW, whereas Kon Tum station was used to calibrate and validate the river discharge and sediment for the DBW. A total of 28 sensitivity parameters for river discharge, sediment, and nutrients were chosen to improve the accuracy of model performance using the SUFI-2 algorithm in the SWAT-CUP program, as shown in Table 5.2.

Table 5.2. Sensitive parameters selected for the calibration of river discharge, sediment, and nutrients and their final optimal values

ID	Sensitivity parameters	Definition	Calibrated values ^(a)
<i>River discharge</i>			
1	<i>r_CN2</i>	SCS runoff curve number	-0.53
2	<i>r_SOL_K</i>	Saturated hydraulic conductivity	0.06
3	<i>r_CH_N2</i>	Manning's "n" value for the main channel	-0.27

4	<i>r_SOL_BD</i>	Moist bulk density	0.03
5	<i>r_SOL_AWC</i>	Available water capacity of the soil layer	0.15
6	<i>v_SHALLST</i>	Initial depth of water in the shallow aquifer	0.06
7	<i>v_BIOMIX</i>	Biological mixing efficiency	4.86
8	<i>r_SOL_Z</i>	Depth from soil surface to bottom of layer	-0.91
9	<i>r_GWQMN</i>	Threshold depth of water in the shallow aquifer required for return flow to occur	1.84
10	<i>r_ALPHA_BF</i>	Baseflow alpha factor	-0.02
11	<i>r_CH_N1</i>	Manning's "n" value for the tributary channels	13.00
12	<i>v_OV_N</i>	Manning's "n" value for overland flow	25.38
13	<i>v_GW_DELAY</i>	Groundwater delay	0.59
14	<i>v_RCHRG_DP</i>	Deep aquifer percolation fraction	-0.26
15	<i>v_GW_REVAP</i>	Groundwater "revap" coefficient	1.39
<i>Sediment</i>			
1	<i>r_USLE_K</i>	USLE equation soil erodibility (K) factor	-1.01
2	<i>v_LAT_SED</i>	Sediment concentration in lateral flow and groundwater flow	69.38
3	<i>v_HRU_SLP</i>	Average slope steepness	1.28
4	<i>v_ADJ_PKR</i>	Peak rate adjustment factor for sediment routing in the subbasin	2.43
5	<i>r_USLE_P</i>	USLE equation support practice factor	0.18
6	<i>v_PRF_BSN</i>	Peak rate adjustment factor for sediment routing in the main channel	5.05
<i>Nutrients</i>			
1	<i>v_ERORGN</i>	Organic N enrichment ratio	23.48
2	<i>v_NPERCO</i>	Nitrate percolation coefficient	0.02
3	<i>r_HLIFE_NGW_BSN</i>	Half-life of nitrogen in groundwater	122.75
4	<i>v_LAT_ORGN</i>	Organic N in the baseflow	6.04
5	<i>v_LAT_ORGP</i>	Organic P in the baseflow	1.78
6	<i>r_CMN</i>	Rate factor for humus mineralization of active organic nitrogen	6.53
7	<i>r_SOL_CBN</i>	Organic carbon content	0.16

*r*_: The current parameter value is multiplied by one plus a given value; *v*_: the current parameter value is to be replaced by a given value; ^(a) best fitted of the calibrated values.

5.2.2.2. Land use update module

There have been dramatic land-use changes in the Central Highlands, especially in the study area in the last five years with the expansion of urbanization and agricultural areas, along with deforestation (JICA, 2018). Model performance cannot be evaluated in depth when there is a lack of detailed land-use changes and land management information (Zettam

et al., 2017). Updating land-use change information through different approaches is important when seeking to improve the accuracy of the model’s performance (Moriassi et al., 2019; Wagner et al., 2019; and Aghsaei et al., 2020). In this study, a method confirmed by Tram et al., 2021 was used to track the frequent and complicated local land-use policies by using R script. For the analysis, multiple land-use maps were developed on the basis of local information and policies reflected by the local land-use conditions (2005, 2010, 2015, and 2018) during the simulation periods as shown in Figure 5.2. During a simulation of the 2000–2018 period, three new land-use conditions for 2010, 2015, and 2018 were updated in the model from 2005 onwards for the 2005–2009, 2010–2014, and 2015–2018 simulation periods. This R script can support updating land-use changes by the linear interpolation method at the chosen time.

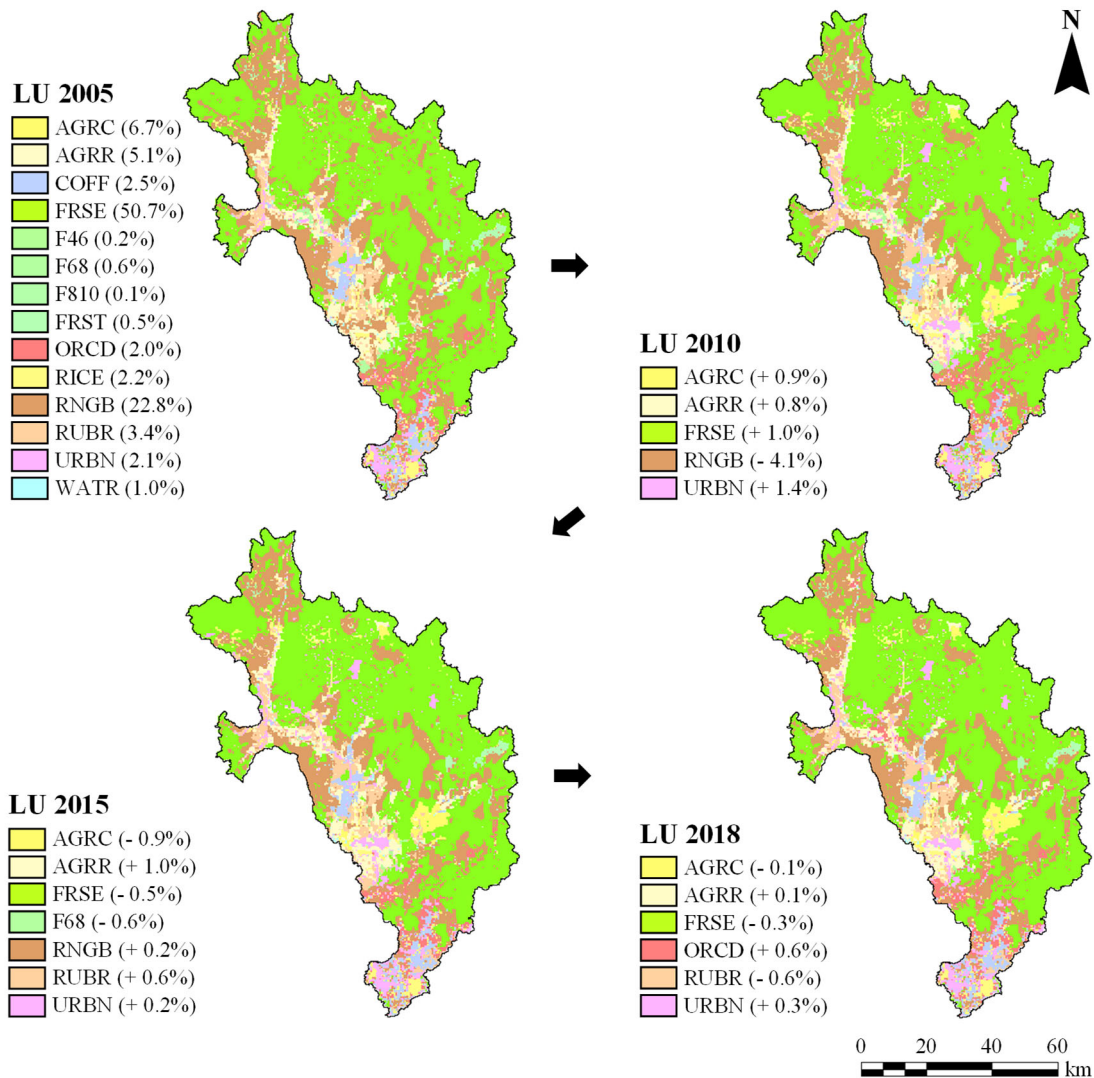


Figure 5.2. The land use maps for 2005, 2010, 2015, and 2018 in the target river basin. The main land-use types include AGRC: agricultural land, non-row crops; AGRR: agricultural land, row crops; COFF: coffee; FRSE: forestry land; F46: mixed forest (400–600 m); F68:

mixed forest (600–800 m); F810: mixed forest (800–1,000 m); FRST: mixed forest; ORCD: orchard; RICE: rice; RNGB: rangeland; RUBR: rubber; URBN: urban; and WATR: water.

The symbol “+/-” indicates the increased/decreased percentage of land use categories of that period compared to the previous period

5.2.2.3. Agricultural practices information update

Information such as the amount of fertilizer per crop and its timing should be updated in the model along with the changes in land-use policies because the significant impacts of agricultural practices on the hydrology, crop yield, and water quality processes have been emphasized (Arabi et al., 2007; Srinivasan et al., 2010; Donmez et al., 2020). The agricultural practice information for the timing of planting, fertilizing, and harvesting was collected from the local government. One of the most influential factors of agricultural practices on the environment is crop type and cultivation management, along with climate conditions and soil characteristics (Epelde et al., 2015). The three main crops in the target area are rice, coffee plants, and rubber trees. Rice is cultivated twice per year. As permanent crops, coffee beans and rubber latex are normally harvested after 4 years and 6 years of planting. The annual fertilization loads for crops range from 8.3 to 73.6 kg N/ha/year and from 4.2 to 21.2 kg P/ha/year as described in Table 5.3.

Table 5.3. Agricultural practices information

Agricultural activities	Crops			
		Rice	Coffee plants	Rubber trees
Planting period	May	December	June	May
Fertilizer period	May (46 ^a , 21.2 ^b) June (34.5, 11.5) June (34.5, 5.8)	December (46, 21.2) December (34.5, 11.5) January (34.5, 5.8)	June (27.6, 15.4); August (24.2, 13.5); October (17.3, 9.6) Year 1: June (46, 15.4); August (40.3, 13.5); Year 2: June (28.8, 9.6) Year 3: June (64.4, 15.4); August (56.4, 13.5); Year 4: June (73.6, 16.8); August (64.4, 14.7)	Year 1: June (11, 5.6); July (8.3, 4.2); September (8.3, 4.2) Year 2: June (22.1, 8.4); July (16.6, 6.3); September (16.6, 6.3) Year 3: June (27.6, 9.8); July (20.7, 7.3); September (20.7, 7.3) Year 4: June (36.8, 11.2); July (27.6, 8.4); September (27.6, 8.4)

				Year 5: June (36.8, 12.6), July (27.6, 9.4), September (27.6, 9.4)
				Year 6: June (46, 14); July (34.5, 10.5)
Harvest period	October (harvest and kill)	April (harvest and kill)	October (harvest only)	October (harvest only)

^(a) The amount of nitrogen per hectare (kg N/ha); ^(b) The amount of phosphorus per hectare (kg P/ha) (Source: Kon Tum Provincial People's Committee, 2019b)

Coffee plants and rubber trees are the priority permanent crops in the target area because these crops are strategic commodity crop groups with high economic value and great export potential. Additionally, these crops contribute to the greening of barren hills, creating jobs, reducing the poverty rate, and improving the incomes of local people, especially ethnic minorities (Phuc and Nghi, 2014; Tien et al., 2015). High-quality rubber latex in Kon Tum and Gia Lai provinces is exported to many countries. Because of the significant difference in the net income obtained from annual and perennial crops, a dramatic conversion from annual crops to perennial crops in the hillslope areas was conducted in this region (JICA, 2018).

5.2.2.4. Model performance

To assess the accuracy of the model's performance, three statistical indices, the coefficient of determination (R^2), the Nash–Sutcliffe index (NSI), and the percentage bias ($PBIAS$), were used. The performance evaluation criteria of variables in the watershed scale were described by Moriasi et al. (2015).

$$R^2 = \left[\frac{\sum_{i=1}^n (O_i - \bar{O})(P_i - \bar{P})}{\sqrt{\sum_{i=1}^n (O_i - \bar{O})^2} \sqrt{\sum_{i=1}^n (P_i - \bar{P})^2}} \right]^2 \quad (5.5)$$

$$NSI = 1 - \frac{\sum_{i=1}^n (O_i - P_i)^2}{\sum_{i=1}^n (O_i - \bar{O})^2} \quad (5.6)$$

$$PBIAS = \frac{\sum_{i=1}^n (O_i - P_i)}{\sum_{i=1}^n (O_i)} \times 100 \quad (5.7)$$

where O_i denotes the observed variables, \bar{O} denotes the average observed variables, P_i denotes the simulated variables, \bar{P} denotes the average simulated variables, and n is the number of existing variables.

Table 5.4. Criteria of performance evaluation for river discharge, sediment, nitrogen, and phosphorus on the watershed scale according to Moriasi et al. 2015

Statistical indices	Variables	Very good	Good	Satisfactory	Not satisfactory
R^2	River discharge (D)	>0.85	$0.70 \leq R^2 \leq 0.85$	$0.50 < R^2 < 0.70$	≤ 0.50
	Sediment (M)	>0.80	$0.65 \leq R^2 \leq 0.80$	$0.40 < R^2 < 0.65$	≤ 0.40
	N (M)	>0.70	$0.60 \leq R^2 \leq 0.70$	$0.30 < R^2 < 0.60$	≤ 0.30
	P (M)	>0.80	$0.65 \leq R^2 \leq 0.80$	$0.40 < R^2 < 0.65$	≤ 0.40
NSI	River discharge (D)	>0.80	$0.70 \leq NSI \leq 0.80$	$0.50 < NSI < 0.70$	≤ 0.50
	Sediment (M)	>0.80	$0.70 \leq NSI \leq 0.80$	$0.45 < NSI < 0.70$	≤ 0.45
	N (D)	>0.55	$0.40 \leq NSI \leq 0.55$	$0.25 < NSI < 0.40$	≤ 0.25
	P (M)	>0.65	$0.50 \leq NSI \leq 0.65$	$0.40 < NSI < 0.50$	≤ 0.40
$PBIAS$ (%)	River discharge (M)	$\leq \pm 3.0$	$\pm 3.0 < PBIAS < \pm 10.0$	$\pm 10.0 \leq PBIAS \leq \pm 15.0$	$> \pm 15.0$
	Sediment (M)	$\leq \pm 1.0$	$\pm 1.0 < PBIAS < \pm 10.0$	$\pm 10.0 \leq PBIAS \leq \pm 20.0$	$> \pm 20.0$
	N, P (M)	$\leq \pm 10.0$	$\pm 10.0 < PBIAS < \pm 15.0$	$\pm 15.0 \leq PBIAS \leq \pm 30.0$	$> \pm 30.0$

Note: D, Daily; M, Monthly; N, Nitrogen; P, Phosphorus.

5.2.2.5. Nutrient load calculation

The nutrient load was calculated on the basis of the concentration of water quality variables and the discharge, as described in Equation (5.8).

$$L = \sum_{t=1}^{t=T} (86.4 \times Q_t \times C_t) \quad (5.8)$$

where L is the nutrient load (kg), C_t is the daily concentration of water quality variables (mg/l), Q_t is the daily discharge (m^3/s), and t is the time (days).

5.3. Results

5.3.1. Sensitivity analysis for model simulation with updates to land-use changes and agricultural practices information

The t -stat is a sensitivity measure where larger absolute values denote greater sensitivity, while the p -value indicates the sensitivity significance where values close to zero have more significance. Among the 28 sensitivity parameters, the 6 most sensitive parameters with a larger t -stat and a smaller p -value were SCS runoff curve number ($CN2$) and saturated hydraulic conductivity (SOL_K) for river discharge, soil erodibility factor ($USLE_K$) and sediment

concentration in lateral flow and groundwater flow (*LAT_SED*) for sediment, and the organic nitrogen enrichment ratio (*ERORGN*) and nitrate percolation coefficient (*NPERCO*) for nutrient simulations. The sensitivity of *CN2* and *USLE_K* showed that the watershed features and soil characteristics had significant effects on the river discharge and soil erosion simulation. Among the different model parameters, *CN2*, *USLE_K*, and *ERORGN* were three of the most sensitive parameters influencing river discharge, sediment, and nutrients in the target river basin. For river discharge, the *CN2* is the most important parameter in the calibration of the model, and it contributes significantly to surface runoff generation (Gholami et al., 2016). The sensitivity of *CN2* represents the dramatic changes in land-use classes (Singh and Saravanan, 2020). The *CN2* parameter was extremely important due to its strong relationship with surface runoff and infiltration simulations in the watershed (Cuceoglu et al., 2021). The sensitivity parameter affecting sediment simulation was *USLE_K*. *USLE_K* is tightly related to the physical soil properties. The accurate estimation of this parameter is crucial for the implementation of soil conservation plans (Shabani et al., 2014). As for nutrients, the parameter *ERORGN* denotes the ratio of the concentration of organic nitrogen moved along with the sediment to the concentration in the soil surface layer (Neitsch et al, 2011). *ERORGN* is a crucial factor impacting the amount of nitrate loss in the watershed as indicated by Qin et al. (2018).

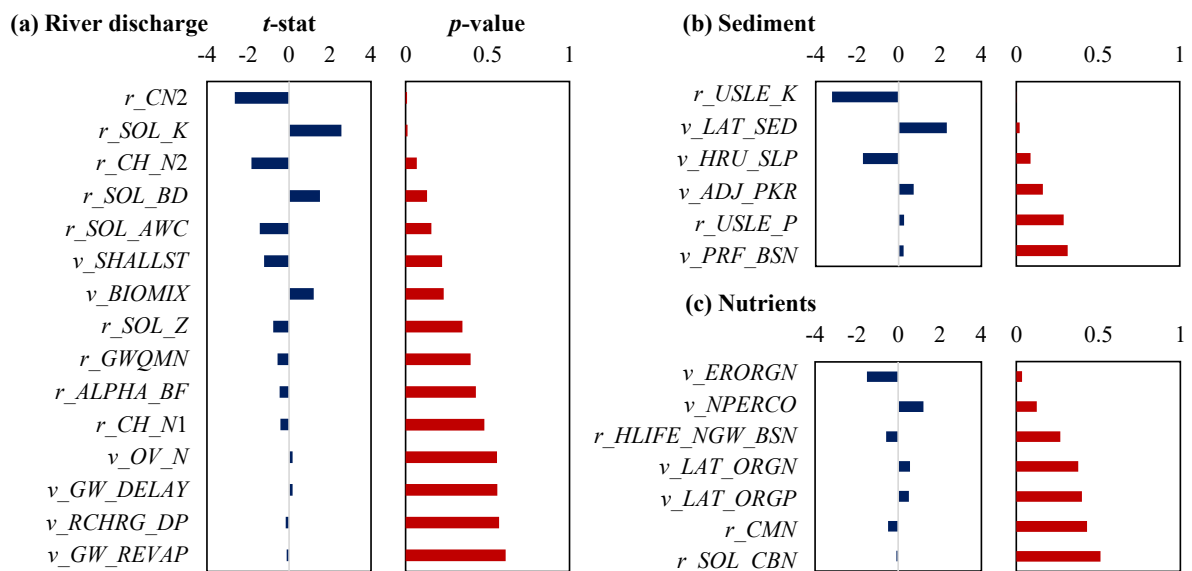


Figure 5.3. Global sensitivity analysis of river discharge, sediment, and nutrients simulations

5.3.2. Reproducibility of river discharge, sediment, and nutrient loadings during the 2000–2018 period

❖ Calibration period (river discharge and sediment: 2000–2015; nutrients: 2014–2015)

The river discharge simulation at both stations was acceptable with *NSI* indices of 0.64 at Dak Mot station in the PKW and 0.61 at Kon Tum station in the DBW. The *PBIAS* index had a good level of accuracy at Kon Tum station (5.8%) and a satisfactory level (10.9%) at Dak Mot station. With respect to sediment, the observed TSS concentration was measured only at Kon Tum station, yielding satisfactory results with *NSI* and *PBIAS* values of 0.57 and 18.5%, respectively. The main reason for simulating river discharge and sediment at Kon Tum station within a satisfactory level was due to some enormous flood peaks, and these flood events slightly reduced its total performance. Two of the highest historical flood peaks at Kon Tum station were on 29 and 30 September 2009 with river discharge values of 3,500 m³/s and 2,260 m³/s, respectively. Upon omitting these peaks, the *NSI* values increased to 0.64 instead of 0.61 for river discharge and 0.57 to 0.62 for sediment in the calibration period.

With respect to nutrients, both the TN and TP simulations were extremely good, while the *NSI* value of TP was at a good level. For the NO₃-N and NH₄-N variables, even though Moriasi et al. (2015) did not mention the performance evaluation criteria of these two parameters, the *NSI* values were also satisfactory at 0.55 and 0.62, respectively. In general, the simulation of river discharge, sediment, and nutrient variables during the calibration period ranged from “satisfactory” to “very good” thresholds. It can be seen that the simulation results for TN and TP were better than those for the remaining variables.

❖ Validation period (all variables: 2016-2018)

The river discharge simulation results for validation were better than those for calibration, with very good *NSI* values of 0.81 at Dak Mot station and 0.83 at Kon Tum station (Table 5.5). The *PBIAS* indices were good at 9.1% for the former and 7.3% for the latter. The sediment simulation in the Kon Tum station was also good with an *NSI* value of 0.72, although the *PBIAS* was satisfactory with a value of –10.5%.

Regarding TN and TP, the simulation results ranged between “good” and “very good” in terms of all three statistical parameters, except for the *PBIAS* of the TP simulation in the validation period. The *NSI* indices for NO₃-N and NH₄-N simulations in the validation period were better than those in the calibration period, especially for NO₃-N. Despite not appropriately simulating large flood peaks, the SWAT was still reasonable for mountainous areas as the target area for river discharge, sediment, and nutrients.

Table 5.5. The results of three statistical values (R^2 , NSI , and $PBIAS$) in the calibration period and validation period. The model was calibrated from 2000 to 2015 and validated from 2016 to 2018 for river discharge and sediment. The calibration and validation periods for the TN, TP, NO_3 -N, and NH_4 -N variables were from 2014 to 2015 and from 2016 to 2018. The sediment, TN, TP, NO_3 -N, and NH_4 -N variables were calibrated and validated by load

Variables	Calibration			Validation		
	R^2	NSI	$PBIAS$ (%)	R^2	NSI	$PBIAS$ (%)
<i>PKW (Dak Mot station)</i>						
River discharge	0.67 (S)	0.64 (S)	10.90 (S)	0.83 (G)	0.81 (VG)	9.10 (G)
TN	0.73 (VG)	0.62 (VG)	-4.90 (VG)	0.90 (VG)	0.88 (VG)	-5.80 (VG)
TP	0.84 (VG)	0.80 (VG)	-14.70 (G)	0.74 (G)	0.71 (VG)	-21.90 (S)
NO_3 -N	0.66	0.55	-18.70	0.85	0.82	-15.40
NH_4 -N	0.63	0.62	-5.50	0.76	0.68	-27.80
<i>DBW (Kon Tum station)</i>						
River discharge	0.65 (S)	0.61 (S)	5.80 (G)	0.86 (VG)	0.83 (VG)	7.30 (G)
Sediment	0.60 (G)	0.57 (S)	18.50 (S)	0.74 (G)	0.72 (G)	-10.50 (S)

Note: TN = total nitrogen, TP = total phosphorus, S = satisfactory, G = good, VG = very good

PKW (Dak Mot station)

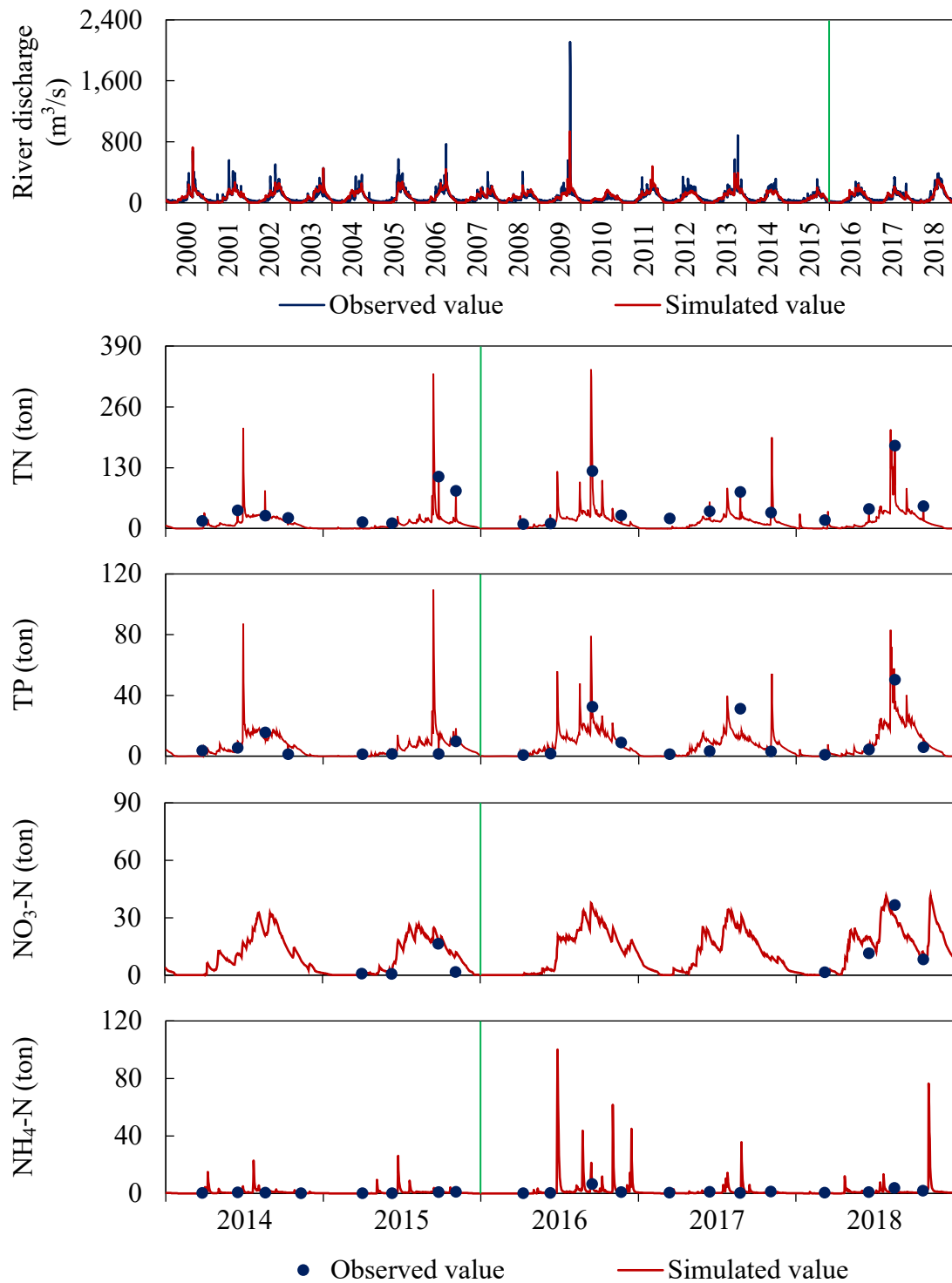


Figure 5.4. The relationship between the observed and simulated daily river discharge, TN, TP, NO₃-N, and NH₄-N loadings in the PKW. The model was calibrated from 2000 to 2015 and validated from 2016 to 2018 for river discharge. The calibration and validation periods for the remaining variables were from 2014 to 2015 and from 2016 to 2018, respectively

DBW (Kon Tum station)

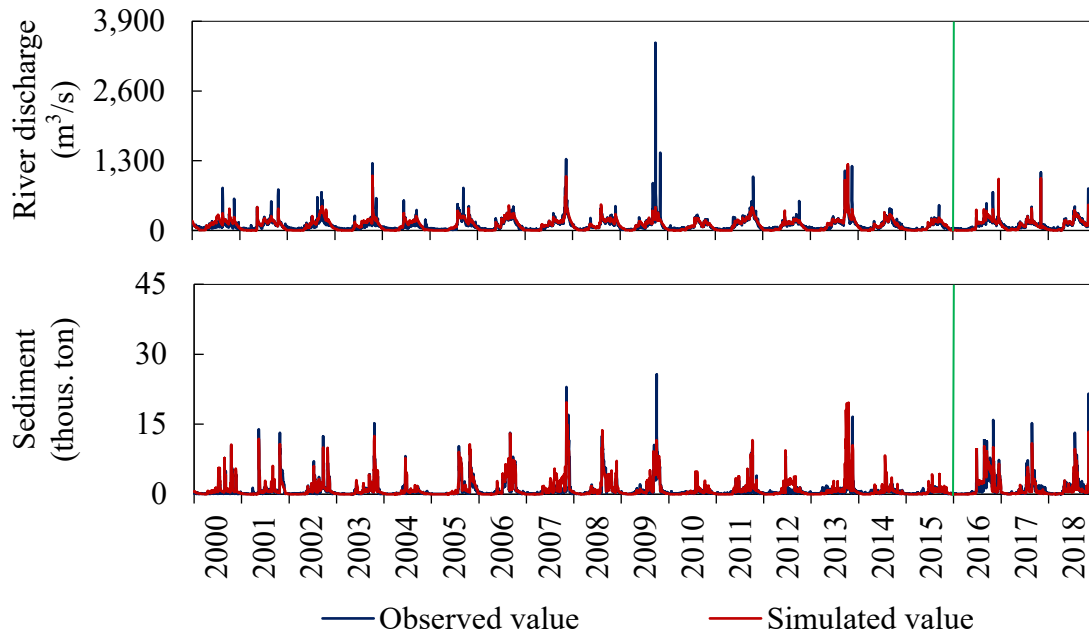


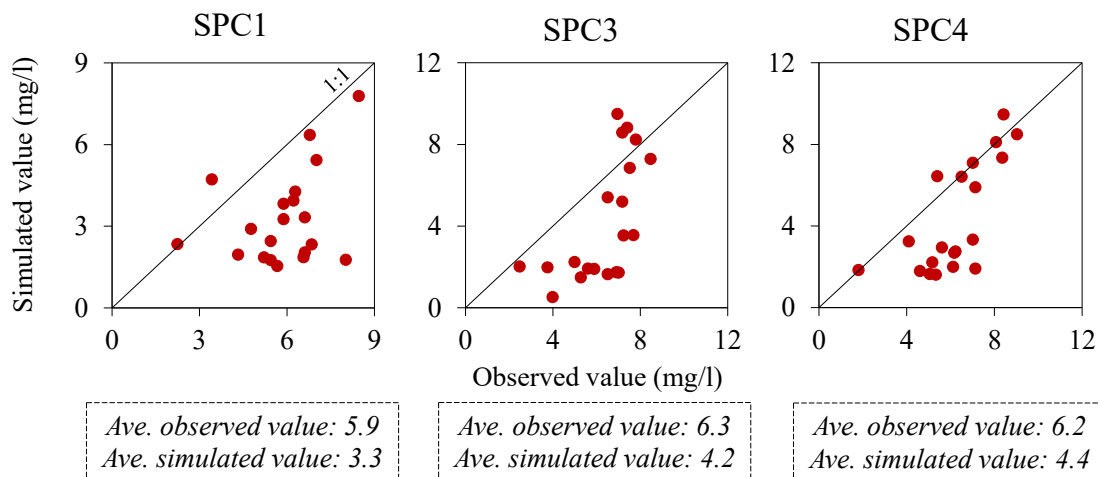
Figure 5.5. The relationship between the observed and simulated daily river discharge and sediment loading in the DBW. The model was calibrated from 2000 to 2015 and validated from 2016 to 2018 for river discharge and sediment

❖ Comparison between the observed and simulated daily TN and TP concentrations at three monitoring points in the PKW (SPC1, SPC3, and SPC4) and two monitoring points in the DBW (SDL2 and SDL3)

During the period from 2014 to 2018, the TN and TP variables at the SPC2 monitoring point were used for calibration and validation of the model by loads. On the other hand, after calibration and validation of the model, TN and TP variables at the five remaining points were used to check the accuracy of the model performance by concentrations because of the lack of river discharge information there. Mainly averaged concentrations were used for the accuracy check, and any further modifications to the parameter values were not conducted. The concentrations may change input information such as crop schedules and fertilizer information in addition to the reproducibility of the river discharges and loads at the target locations in the model. As described in the limitations of the study, the accuracy of the agricultural practices at very specific local levels are still unknown. Moreover, our aim for this study was to evaluate the impact of land-use changes and agricultural practices according to the land-use policies at monthly to annual resolutions, not at a daily resolution. Thus, the average concentrations were considered sufficient for evaluation of the accuracy at the five locations in this study. A comparison between the observed and simulated daily TN and TP

concentrations at the five points is shown in Figure 5.6 and Figure 5.7. In the PKW, the average observed TN concentrations reached 5.9 mg/l at SPC1, 6.3 mg/l at SPC3, and 6.2 mg/L at SPC4, while the average simulated values at these points were 3.3, 4.2, and 4.4 mg/l, respectively. In the DBW, the average observed concentrations were 6.3 and 7.4 mg/l at SDL2 and SDL3, respectively, while the simulated values were 4.0 mg/l at SDL2 and 4.4 mg/l at SDL3, respectively. As for TP concentration, the average observed values were 0.8, 1.0, and 0.9 mg/l at the SPC1, SPC3, and SPC4, respectively, and 1.1 and 1.2 mg/l at SDL2 and SDL3, respectively. Whereas, the average simulated values were 1.0, 1.2, and 1.2 mg/l at the SPC1, SPC3, and SPC4, respectively, and 1.0 and 1.1 mg/l at SDL2 and SDL3, respectively.

a) PKW



b) DBW

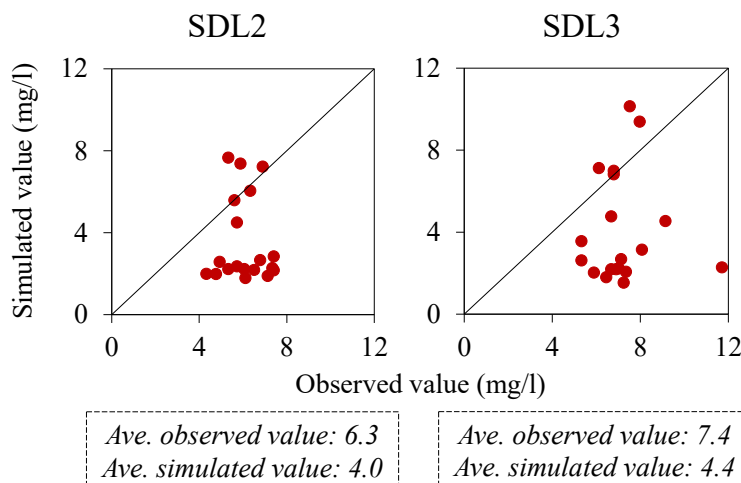
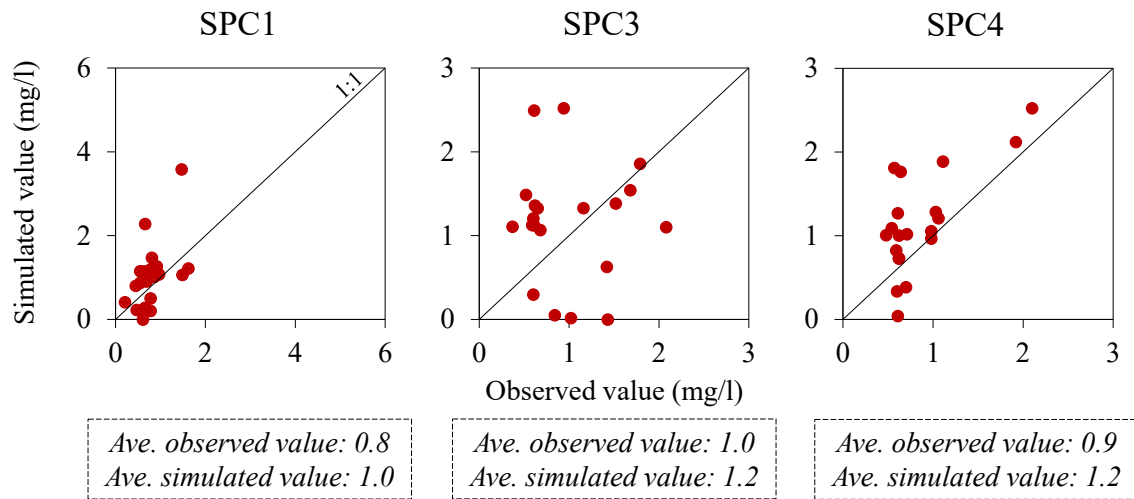


Figure 5.6. The relationship between the observed and simulated daily TN concentration at the five monitoring points in the PKW (SPC1, SPC3, and SPC4) and DBW (SDL2 and SDL3). The average observed and simulated values are described under each graph

a) PKW



b) DBW

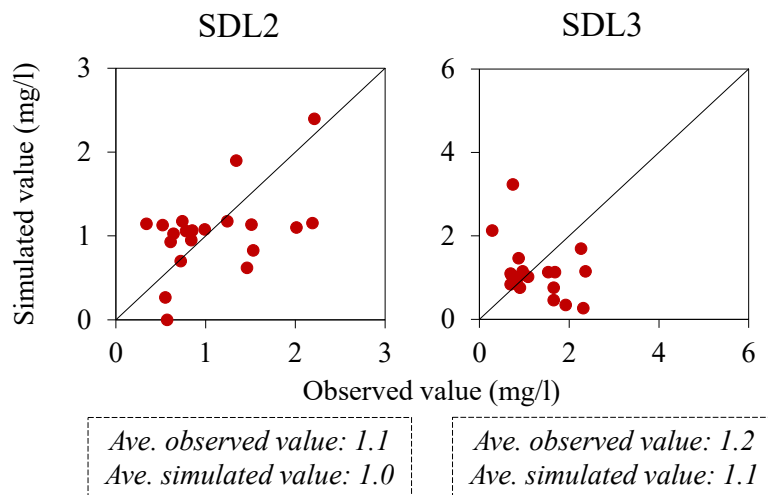


Figure 5.7. The relationship between the observed and simulated daily TP concentration at the five monitoring points in the PKW (SPC1, SPC3, and SPC4) and DBW (SDL2 and SDL3). The average observed and simulated values are described under each graph

The average simulated values of TN and TP variables were slightly lower than the observed values at the five monitoring points. There were some special cases with under/overestimated peaks of river discharge and loads affecting the accuracy of concentration simulation. The SPC4 measuring point showed a higher correlation between the observed and simulated values in the TN and TP simulations compared to the remaining points. Although the TN and TP concentrations at these monitoring points were scattered around the 1:1 line in the graphs, the simulated average concentrations were reasonably reproduced for the observed TN and TP concentrations.

5.3.3. The changes in river discharges, sediments, and nutrient loading at the outlets (Poko outlet and Dakbla outlet)

❖ Total annual river discharges, sediment, and nutrient loadings at the outlets

The total annual river discharge, sediment, TN, and TP loadings at the two outlets from 2000 to 2018 are shown in Figure 5.8. Additionally, the summary of the highest and lowest values during the simulation periods is shown in Table 5.6. The fluctuation of the total annual loadings at the two outlets was different in the four periods based on the changes in local land-use policies and anthropogenic activities. The highest total annual loadings were found in 2013 for river discharge, sediment, TN, and TP. The year 2013 belonged to the 2010–2014 period, in which a crop conversion policy involving a move from mixed forests to rubber forests was applied and agricultural activities were changed. In 2013, the total annual river discharge reached the maximum value of 2,115.6 m³/s in the PKW, which was 7.8% higher than in the DBW. Similar to the river discharge, the total annual sediment loading in the PKW reached the highest value of 692.8 thousand tons in 2013, which was 24.0% lower than in the DBW. In both watersheds, the maximum values of TN were found in 2013 with a value of 33.1 thousand tons in the PKW, which was 13.0% smaller than in the DBW. In addition, TP reached the highest value of 9.6 thousand tons in the PKW, which was 6.7% lower than in the DBW. Even though the river discharge in the PKW was slightly higher than that in the DBW in 2013, the large number of agricultural practices conducted in the DBW led to the higher annual sediment, TN, and TP loadings from this watershed in comparison to the PKW.

Table 5.6. The highest and lowest total annual river discharge, sediment, TN, and TP loadings at the outlets from 2000 to 2018.

Variables	Year	Poko watershed	Dakbla watershed	Differences (%)
River discharge (m ³ /s)	2013 (Highest value)	2,115.6	1,963.0	7.8
	2015 (Lowest value)	851.0	919.1	8.0
Sediment (thousand tons)	2013 (Highest value)	692.8	858.8	24.0
	2015 (Lowest value)	136.0	184.1	35.4
TN (thousand tons)	2013 (Highest value)	33.1	37.4	13.0
	2015 (Lowest value)	5.8	8.5	46.2
TP (thousand tons)	2013 (Highest value)	9.6	10.2	6.7
	2015 (Lowest value)	2.6	3.2	22.8

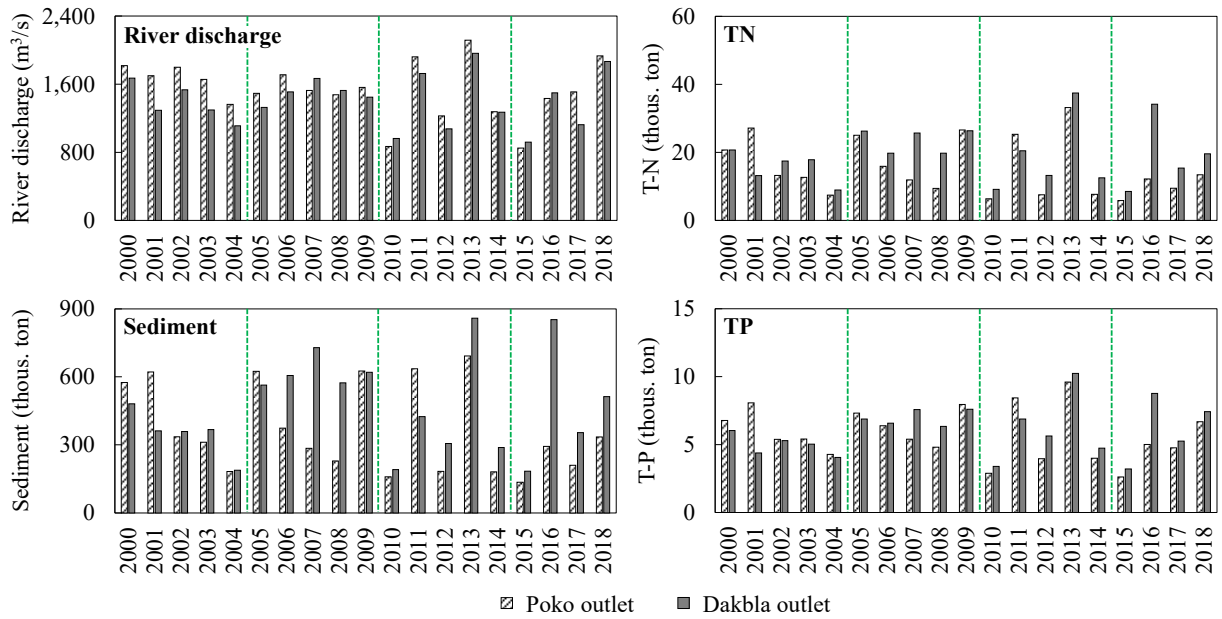


Figure 5.8. Total annual river discharge, sediment, TN, and TP loadings at the outlets from 2000 to 2018.

❖ Average monthly total river discharge, sediments, and nutrient load at the outlets

During the target period, the average monthly total river discharge and sediment loadings were the highest in September in both watersheds (Figure 5.9). The highest river discharges were 326.7 m³/s for the PKW and 256.8 m³/s for the DBW. Additionally, the highest sediment loadings were 102.8 and 94.9 thousand tons in the PKW and DBW, respectively. The river discharge and sediment values in the PKW were higher than in the DBW by 27.2% and 8.3%, respectively. The maximum TN values were reached in August at 4.7 and 4.1 thousand tons in the PKW and DBW. Similar to TN, the highest TP values of the PKW and DBW were 1.5 and 1.1 thousand tons, respectively. It is clear that the TN and TP values in the PKW were higher than those in the DBW by 14.6 % and 36.4%, respectively.

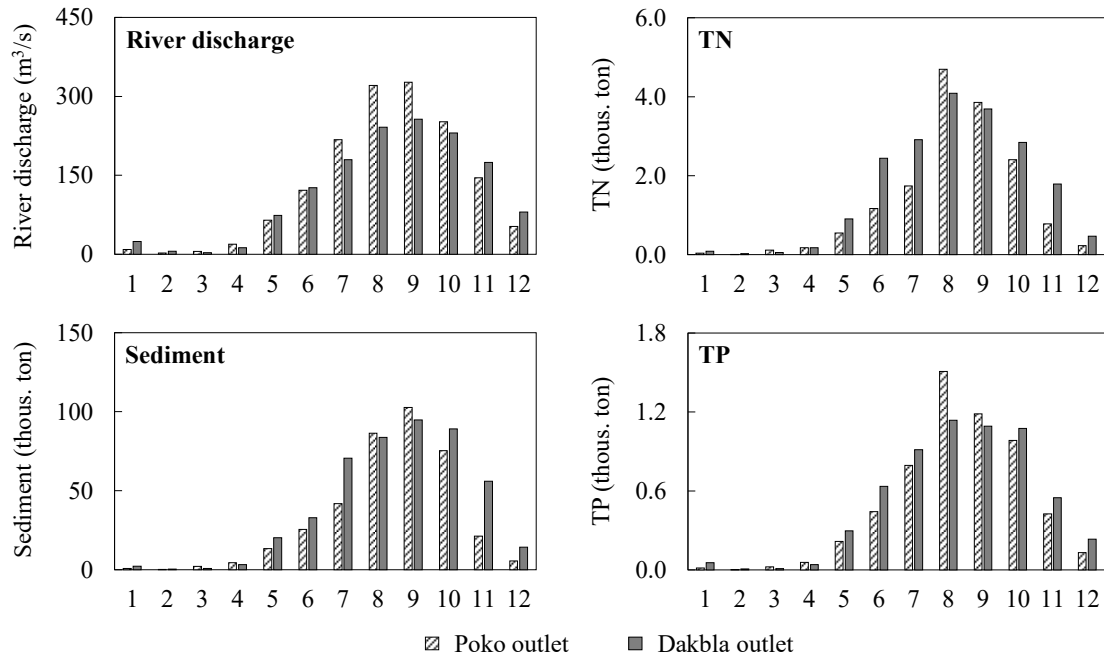


Figure 5.9. Average monthly total river discharge, sediment, and nutrient loadings at the outlets during the 2000–2018 period

❖ Total cumulative sediment, TN, and TP at the outlets

In the 2000–2004 period, many agricultural practices were conducted in the PKW instead of in the DBW. Consequently, the total cumulative values in the DBW were moderately lower than those in the PKW, by 15.3% (268.4 thousand tons) for sediment, 3.9% (3.0 thousand tons) for TN, and 20.6% (5.2 thousand tons) for TP as shown in Figure 5.10. In the 2005–2009 period, the total cumulation in the DBW increased significantly as compared to the previous period. These cumulative values in the DBW exceeded those in the PKW by 42.9% (985.7 thousand tons) for sediment, 33.3% (31.7 thousand tons) for TN, and 10.4% (3.6 thousand tons) for TP.

During the 2010–2014 period, the total cumulative values in the PKW were lower by 12.8%, 15.9%, and 7.4% for sediment, TN, and TP, respectively, as compared to those in the DBW. In the remaining period, from 2015 to 2018, the total cumulative sediment, TN, and TP values in the PKW were lower than those in the DBW by 105.0%, 97.2%, and 30.4%, respectively. Generally, the two periods (2005–2009 and 2015–2018) showed drastic differences in the two watersheds during the whole target period.

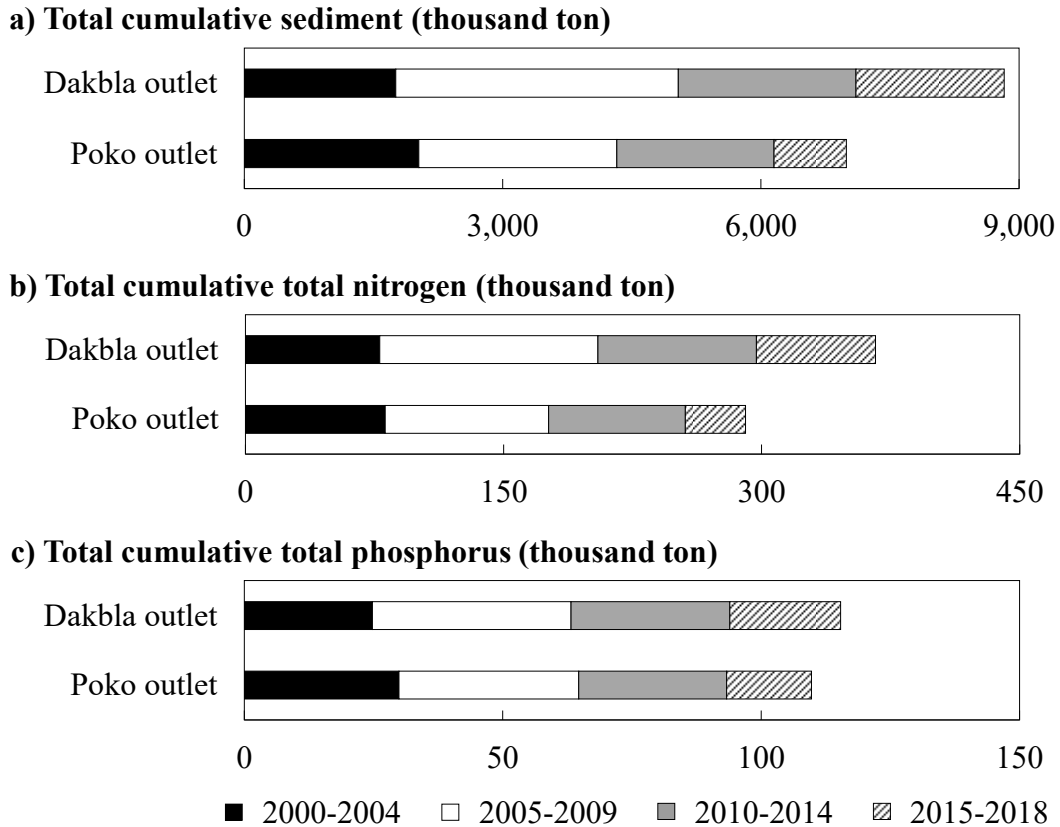


Figure 5.10. Total cumulative sediment, TN, and TP at the outlets during the whole period

5.3.4. Spatial distribution of annual sediment, TN, and TP loads in each subbasin

The spatial distribution of annual sediment, TN, and TP loadings is illustrated in Figure 5.11 to allow for a better understanding of their characteristics according to differences in land use, soil, and slope at the subbasin scale. For sediment loading, the annual value ranged from 41.4 tons/km² in subbasin 9 (2010–2014) to 666.7 tons/km² in subbasin 23 (2005–2009). In subbasin 23, arable land and permanent cropland predominated, accounting for 74.0% of the total land, and approximately 50.8% of this area had a slope greater than 15%. Compared with the 2005–2009 period, the maximum annual values in the remaining three periods were lower by 75% (2000–2004), 19.7% (2010–2014), and 4.2% (2015–2018). In the 2005–2009 period, the annual sediment loading was higher than in the eastern and southern areas. In subbasin 32, arable land and permanent cropland predominated, accounting for 50% of the total land, and approximately 45.8% of this area had a slope greater than 15%. The annual loading increased slightly in the northwestern, southwestern, and eastern directions, whereas there was a dramatic decrease in the northeastern and southern areas in the 2010–2014 period.

In the 2015–2018 period, the annual value exhibited a significant decline in the northwestern area, while there was an increasing tendency in the northeastern and southern parts.

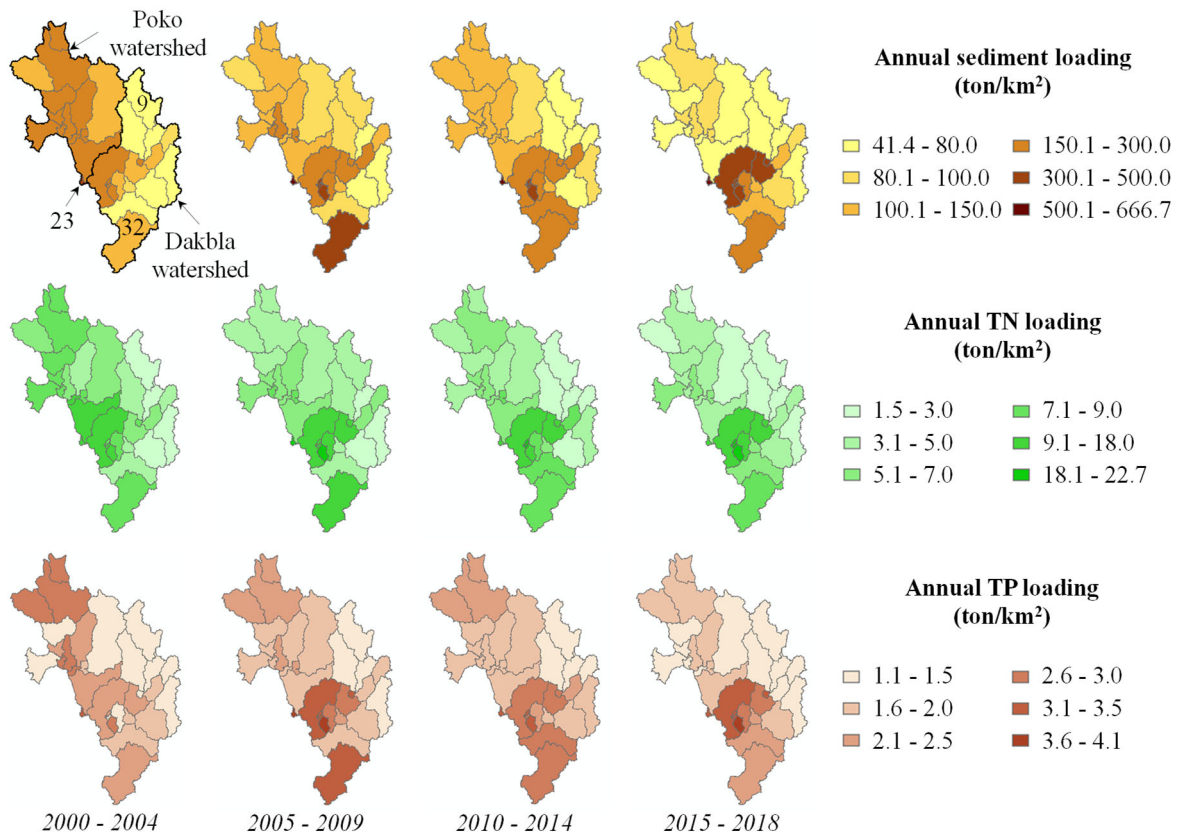


Figure 5.11. Spatial distribution of annual sediment, TN, and TP loadings in each subbasin

For the TN loading, the lowest annual value was 1.4 tons/km² in subbasin 9 in the 2010–2014 period, while the highest value was found 22.7 tons/km² in subbasin 23 in the 2005–2009 period. In the 2005–2009 period, the maximum annual TN loadings were higher than those in the 2000–2004, 2010–2014, and 2015–2018 periods by 35.5%, 14.6%, and 7.8%, respectively. Compared to that in the 2000–2004 period, the annual TN loading increased moderately in the southern and northeastern areas, whereas a dramatic decrease was seen in the northwestern and western areas in the 2005–2009 period. There was a slight increase in the northwestern, southwestern, and eastern areas, while a significant decrease was observed in the northeastern and southern areas from 2010 to 2014. Moreover, the TN loading increased in the southwestern area and slightly decreased in the northwestern area in the 2015–2018 period.

For the TP loading, the annual value ranged from 1.1 tons/km² (subbasin 9 for the 2010–2014 period) to 4.1 tons/km² (subbasin 23 for the 2005–2009 period). Compared with the 2005–2009 period, the maximum annual TP loadings were lower than in the remaining three

periods by 30.3% (2000–2004), 20.7% (2010–2014), and 7.6% (2015–2018). There was a similar tendency to sediment load during the whole period.

5.3.5. The changes in sediment, TN, and TP loadings for each land use during the four periods

Forest represented the highest percentage of land use, accounting for more than 52% of the study area across all four periods. Permanent cropland had the lowest proportion of annual sediment loading and the smallest total area, while the highest proportion of sediment loading was found in arable land, despite its area, ranging from 14.0% to 15.9% of the total during the four periods. From 2005 to 2009, extensive agricultural activities took place, as evidenced by the increase in arable land from 14.0% (2000–2004) to 15.7% (2005–2009). In this period, the sediment loading from arable land accounted for 61.3% of the total, a 7.6% increase compared to the previous period. Nevertheless, the percentage of sediment loading in forestry land decreased by 2.2% because of the increase in forest area from 52.1% to 53.1%. Considering the 2010–2014 period, the areas of arable land and permanent cropland occupied 24.3% of the total area. The sediment loading from these areas reached 67.0%, decreasing by 0.9% compared to the previous period. Between 2015 and 2018, the sediment loading tended to increase by 3.2% in the other land-use types and by 0.7% in forestry land, while there were decreasing trends of 3.4% in arable land and 0.5% in permanent cropland compared to the previous period. The 2005–2009 period had the largest percentage of sediment loading in arable land and permanent cropland.

Considering TN loading, forest had the lowest proportion of annual TN loading, while the highest percentage was recorded in arable land. The 2005–2009 period had the highest proportion of TN loading in arable land and permanent cropland at 72.3%, higher than other periods by 7.9% (2000–2004), 1.6% (2010–2014), and 3.2% (2015–2018). During the 2015–2018 period, the TN loading of forestry land also reached the highest percentage of 9.3%, increasing by 0.5%, 1.4%, and 0.3% as compared to the 2000–2004, 2005–2009, and 2010–2014 periods, respectively. For the other land-use types, the TN loadings occupied 26.8%, 19.8%, 20.3%, and 21.6% in the four periods, respectively.

Similar to sediment, permanent cropland exhibited the lowest percentage of annual TP loading, while the highest proportion was observed in arable land. Arable land and permanent cropland accounted for 65.0% in the 2005–2009 period, which is higher than the 2000–2004, 2010–2014, and 2015–2018 periods by 9.2%, 2.5%, and 5.0%, respectively. Forestry land had the highest proportion of TP loading at 15.8% in the 2015–2018 period, exhibiting 1.0%, 2.0%, and 0.7% increases as compared to the three remaining periods, respectively. The

highest percentage of other land-use types was 29.4% in the first period, followed by 24.2% (2015–2018), 22.4% (2010–2014), and 21.2% (2005–2009).

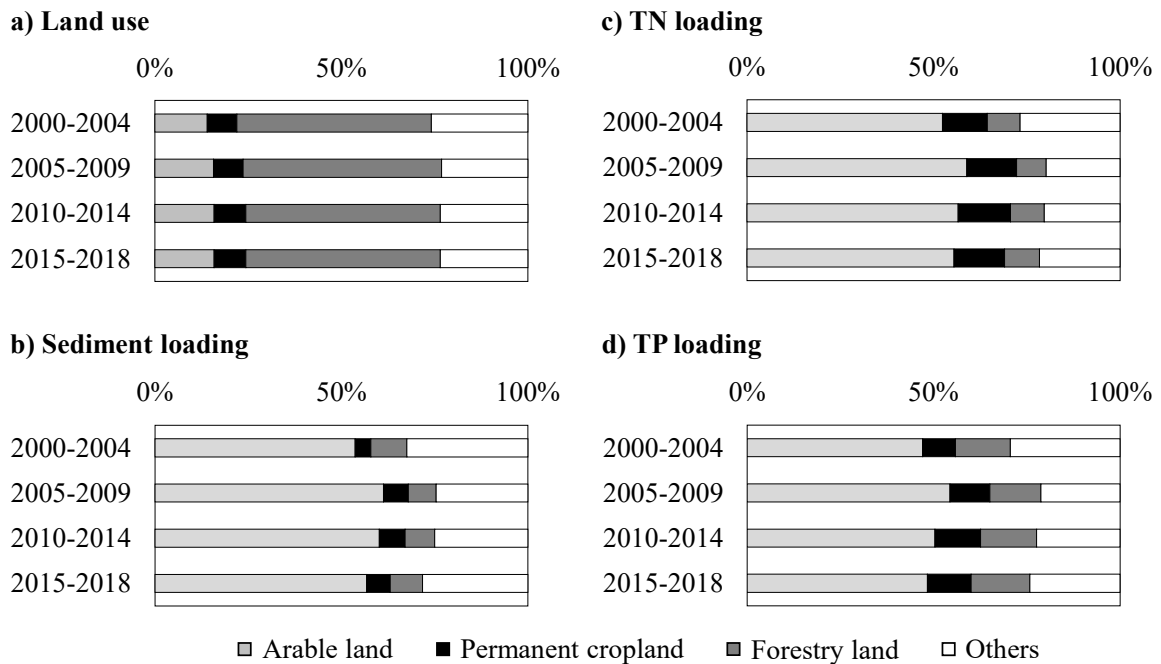


Figure 5.12. Changes of sediment, TN, and TP loadings into the reach according to land-use type during the four periods

5.3.6. The changes in total annual sediment, TN, and TP loadings at the inflow to the lake

The influence of local land-use policies and anthropogenic activities on downstream water quality was indicated by the increase in total annual sediment, TN, and TP loadings at the inflow to the lake after the enactment of land-use policies as compared to before the enactment of land-use policies. The 2000–2004 period featured no changes in land-use policies. From 2005 onward, changes in the local land-use policies and anthropogenic activities were enacted. The total annual loadings at the inflow to the lake were calculated by dividing the total annual sediment, TN, and TP for the whole target area by the total average annual rainfall of the whole target area. Changes in the total annual loadings at the inflow to the lake are illustrated in Figure 5.13.

Compared to that in the 2000–2004 period, the total average annual rainfall in the 2005–2009 period was slightly higher, by 3.2% (59.4 mm). The total annual sediment, TN, and TP loadings in the 2005–2009 period were significantly higher than those in the 2000–2004 period by 36.6%, 27.4%, and 17.1%, corresponding to 146.4, 4.6, and 1.1 thousand tons/period/ 10^3 mm, respectively.

Additionally, the total average annual rainfall in the 2010–2014 period (1,775.7 mm) was lower than that in the 2000–2004 period (1,868.7 mm) by 5.2%. However, the total annual sediment, TN, and TP loadings in the 2010–2014 period were higher than those in the 2000–2004 period by 15.1, 1.3, and 0.6 thousand tons/period/ 10^3 mm, corresponding to differences of 3.6%, 7.1%, and 9.0%, respectively.

The total average annual rainfall in the 2015–2018 period was also lower than that in the 2000–2004 period by 8.4%, corresponding to 145.2 mm. However, the total annual loadings in the 2015–2018 period were higher than those in the 2000–2004 period by 1.9% (7.6 thousand tons/period/ 10^3 mm) for sediment, 1.6% (0.3 thousand tons/period/ 10^3 mm) for TN, and 4.8% (0.3 thousand tons /period/ 10^3 mm) for TP.

As for the 2015–2018 period, the total average rainfall was lower than in the 2010–2014 period by only 3.0% (52.2 mm). The total annual sediment loading in the 2015–2018 period was lower than in the 2010–2014 period by 1.9%, equivalent to 7.6 thousand tons/period/ 10^3 mm. With a similar tendency to that of sediment, the total annual TN and TP loadings in the former period were moderately lower than those in the latter period by 6.0% (1.0 thousand tons/period/ 10^3 mm) and 4.6% (0.3 thousand tons/period/ 10^3 mm), respectively.

Additionally, the changes in rainfall in the 2000–2004 and 2010–2014 periods (93 mm) were smaller than those in the 2000–2004 and 2015–2018 periods (145.2 mm). The changes in total annual sediment loading in the 2000–2004 and 2010–2014 periods (3.6%) were slightly larger than those in the 2000–2004 and 2015–2018 periods (1.9%). The annual TN and TP loadings in the 2000–2004 and 2010–2014 periods (7.1% and 9.0%) were moderately higher than those in the 2000–2004 and 2015–2018 periods (1.6% and 4.8%).

The total annual loadings at the inflow to the lake in the 2005–2009 period were dramatically higher than those in the three remaining periods, despite rainfall in the 2005–2009 period only being slightly higher. Compared to the 2000–2004 period, there were higher total annual loadings in the 2010–2014 and 2015–2018 periods despite the rainfall in these periods being lower than that in the 2000–2004 period.

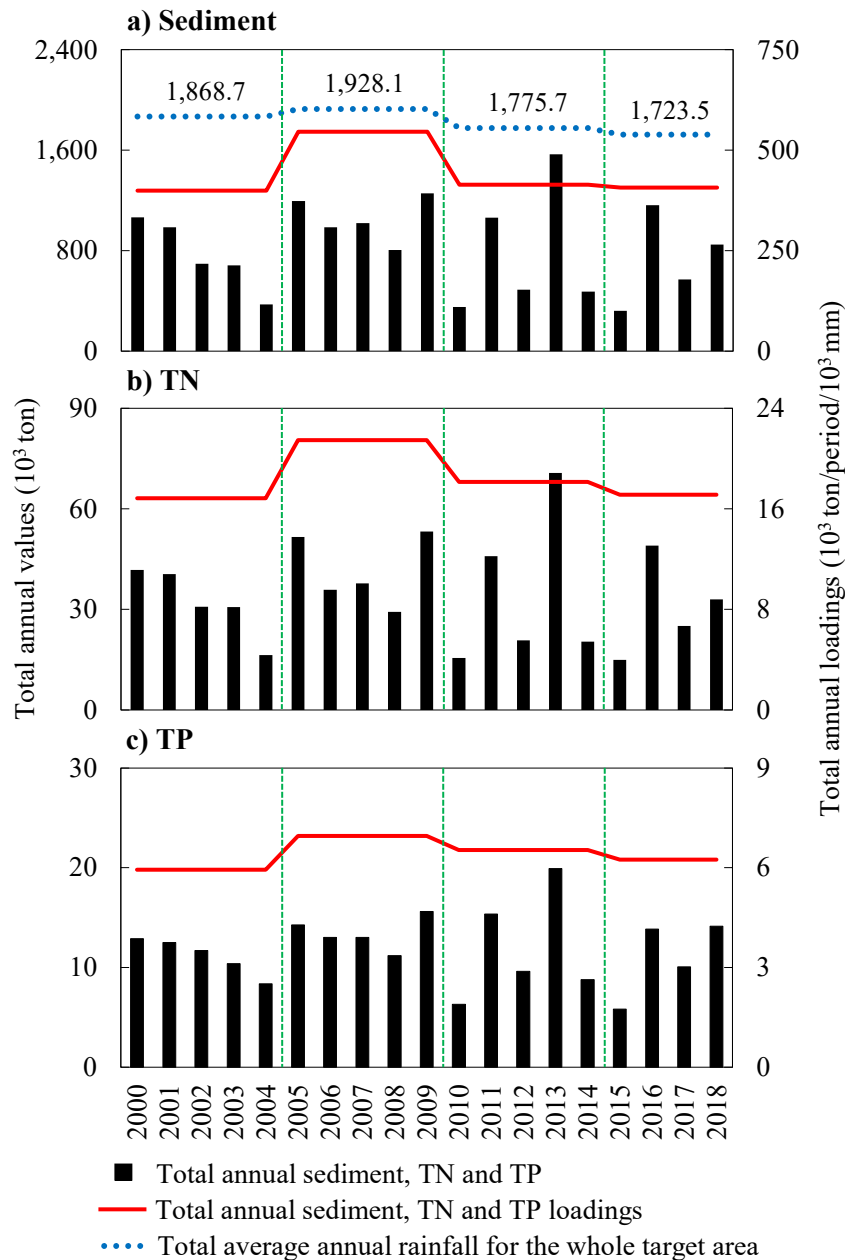


Figure 5.13. Changes in the total annual sediment, TN, and TP loadings at the inflow to the lake during the four periods. The total average annual rainfall (mm) was calculated using the Thiessen method.

Table 5.7. Comparisons of rainfall, total annual sediment, TN, and TP loadings at the inflow to the lake between pre- and post- land-use policy application, and between land-use policy period 3 and period 4. The first period, from 2000 to 2004, represents a base period without the implementation of land-use policies (period 1). The remaining periods illustrate the following changes in land-use policies: the second period (2005–2009), conducted for afforestation, agricultural expansion, and urbanization (period 2); the third period (2010–2014), crop conversion policy involving a shift from mixed forests to rubber forests (period

3); and the fourth period (2015–2018), crop conversion policy involving a shift from insufficient rubber forests to orchards (period 4). The total annual loadings during the target period per 1,000 mm of rainfall (thousand ton/period/10³mm) were calculated at the inflow to the lake for the annual sediment, TN, and TP to evaluate the influence of land-use policies.

Variables	Period 2 vs 1	Period 3 vs 1	Period 4 vs 1	Period 4 vs 3
Total average annual rainfall (mm)	↑ 3.2% (59.4)	↓ 5.2% (93)	↓ 8.4% (145.2)	↓ 3.0% (52.2)
Total annual sediment loading (thousand ton/period/10 ³ mm)	↑ 36.6% (146.4)	↑ 3.6% (15.1)	↑ 1.9% (7.6)	↓ 1.9% (7.6)
Total annual TN loading (thousand ton/period/10 ³ mm)	↑ 27.4% (4.6)	↑ 7.1% (1.3)	↑ 1.6% (0.3)	↓ 6.0% (1.0)
Total annual TP loading (thousand ton/period/10 ³ mm)	↑ 17.1 % (1.1)	↑ 9.0% (0.6)	↑ 4.8% (0.3)	↓ 4.6% (0.3)

5.4. Discussion

5.4.1. Impacts of different land-use policies and agricultural practices on river discharge, sediment, and nutrients

Before 2005, although the total area of the DBW was larger than that of the PKW by 297 km², equivalent to a difference of 9.3%, it was observed that the river discharge, sediment, and nutrient loadings in this watershed were significantly lower than those in the PKW, as shown in Figure 5.10. From 2005 onward, the total cumulative values in the DBW became higher than those in the PKW during the 2005–2009 period. This increase in the river discharge, sediment, and nutrient loadings was due to implemented land-use policies which influenced agricultural expansion and urbanization mainly in the DBW despite afforestation being conducted. The rates of agricultural expansion and urbanization were faster than the rate of afforestation. In recent years, a higher migration rate, especially in rural areas than urban areas in Kon Tum province, has led to an increase in residential and agricultural areas which slowed the afforestation rate (JICA, 2018).

From 2010 onward, crop conversion from mixed forests to rubber forests has been carried out, the majority of which took place in the DBW. Conversion to rubber forests in low-fertility areas was conducted despite these activities having the potential to destroy the biodiversity available in poorer forests (Hong et al., 2013). Rubber trees were planted instead of maintaining the mixed forests that had been exhausted and had not been able to provide timber products for a long time (Ministry of Agriculture and Rural Development: MARD, 2009). During the 2010–2014 period, the total cumulative values in both watersheds showed almost no significant differences; however, these values in the DBW were still slightly higher than those in the PKW. As can be seen, the important role of protecting natural forests and

afforesting policies in the upstream areas in the previous period enabled a reduction in the sediment and nutrient discharging downstream, especially in the DBW.

From 2015 onward, urbanization, agricultural expansion, and deforestation were conducted continuously. Along with these anthropogenic activities, crop conversion from insufficient rubber forests to orchards was conducted by the local government. The majority of these activities also took place mostly in the DBW; thus, the total cumulative sediment and nutrient loadings in this watershed were significantly higher than those in the PKW. Evidence revealed that the changes in local land-use policies and human activities during different periods significantly impacted the hydrological processes and changed the magnitude of erosion and nutrient loadings in the target area. Understanding the characteristics of each watershed can support decision makers in implementing more effective short-, middle-, and long-term land-use and water resources management strategies during different periods.

5.4.2. Spatial changes in river discharge, sediment, and nutrient loadings during the different periods

The sediment and TP loadings were higher in the northwestern PKW where range land predominated, as well as in the western and southern DBW where arable land and permanent cropland predominated. For TN loading, the downstream of both watersheds and the southern upstream of the DBW exhibited higher values because of the occurrence of agricultural activities. These locations should be considered from the agricultural perspective in policies aiming to minimize the sediment and nutrient loadings into the reaches. Despite the predominance of forestry land, there were lower annual TN and TP loadings, whereas arable land occupying a smaller area had the highest percentage of sediment loadings during all the periods, as also indicated for a mountainous watershed in Japan (Somura et al., 2012). The main sources of nitrogen and phosphorus in the target area are agricultural activities. Agricultural land receives a significantly greater amount of fertilizer than forestry land (Rodríguez-Blanco et al., 2015). Nitrate and phosphorus exhibit an increasing tendency with the expansion of the upland area (Somura et al., 2019). For arable land, the 2005–2009 and 2010–2014 periods had a higher proportion of sediment, TN, and TP loadings. Moreover, the conversion to rubber forests was represented by an increase in sediment, TN, and TP loadings in permanent cropland during the 2010–2014 period compared to the 2005–2009 period. Subsequently, the conversion from rubber forests to orchards successfully reduced the proportion of these loadings during the 2015–2018 period. Khoi et al. (2019) emphasized the

important role of spatial land-use strategies to manage local water resources management. Similar to their analysis, some areas with efficient land-use policies were found to reduce soil erosion and nutrient loadings into the reaches.

5.4.3. Impacts of different land-use policies and agricultural practices on the downstream aquatic environment, particularly Yaly lake

The impacts of applying local land-use policies and agricultural practices on the downstream area were delineated by a comparison of the four different periods (Figure 5.13). Compared to the 2000–2004 period baseline, afforestation, agricultural expansion, and urbanization along with extensive anthropogenic activities significantly contributed to increasing erosion and affected the downstream water quality despite afforestation being conducted during the 2005–2009 period. As for the 2010–2014 period, crop conversion policy involving a move from mixed forests to rubber forests and human activities had a significant influence on downstream areas compared to the 2000–2004 period. Also, the crop conversion policy involving a move from insufficient rubber forests to orchards during the 2015–2018 period was capable of minimizing the erosion and nutrient loadings to the lake despite the total annual loading during this period being higher than that in the 2000–2004 period. Comparing the 2010–2014 and 2015–2018 periods, this also reinforces the point that crop conversion from mixed forests to rubber forests and anthropogenic practices during the 2010–2014 period were some of the main practices affecting soil loss and water quality in the study area. This finding reveals that water quality was highly sensitive to local land-use policy change and anthropogenic activities, and their influence appeared on the water quality relatively in a short time.

In Yaly Lake, water quality measurements started in 2015; the water quality in the rainy season of 2016 (the second measurement in 2016) was poorer than that in the remaining years from 2015 to 2019 (KTDONRE, 2019). The $\text{NO}_3\text{-N}$ concentration was close to the A1 threshold, while the $\text{NH}_4\text{-N}$ concentration was close to the B1 and B2 levels of the national standard. Furthermore, the $\text{PO}_4\text{-P}$ concentration nearly reached the B2 level in the middle of Yaly Lake and exceeded this threshold in the eastern area of the lake. In the Vietnamese national standard QCVN 08:2008/BTNMT for surface water quality, the A1 threshold is used for domestic water supply, aquatic plants and animal conservation, and other uses as the A2, B1, and B2 criteria mentioned. The B1 threshold is used for irrigation, water transportation, and other uses as the B2 criterion mentioned. The B2 threshold is applied for water transportation and other uses with low-water-quality requirements. From 2017 onward, the

surface water quality in Kon Tum province tended to be better than that in 2016, especially in terms of TN and TP (Kon Tum Provincial People's Committee, 2018), due to the new national technical regulations on surface water quality (QCVN 08-MT:2015/BTNMT) and crop conversion policy moving from insufficient rubber forests to orchards. If the crop conversion to inefficient rubber forests during the 2010–2014 period had been continuously applied during the 2015–2018 period, the water quality would have been worse.

Water quality parameters are less sensitive to climate change than land-use changes (Khoi et al., 2019). Most of these parameters are impacted by cultivation in upland areas (Somura et al., 2019). It is difficult to reduce large nutrient loadings into the lake in a short period, especially in rural areas (Yang et al., 2016), because this requires the use of advanced technology in agricultural activities and capital investment in building infrastructure, as well as changes in residents' behaviour. Additionally, the limited data for water quality from these rivers were a noticeable issue when determining intra-seasonal changes in water quality or recognizing specific pollution sources. Thus, more frequent water quality monitoring should be conducted when considering water resources management at the regional and sub-watershed scales (Somura et al., 2018). Nevertheless, it is clear that promulgating reasonable changes in land-use policies for particular local conditions will play a crucial role in tackling the water quality issues of Yaly Lake, especially during the rainy season featuring excess discharge and high rainfall intensity.

5.4.4. Land use and crop conversion policies for the future in the Central Highlands of Vietnam, including the target watersheds

From 2006 to 2020, three strategies of forestry were implemented in Vietnam, which can be categorized into the three periods of 2006–2010, 2011–2015, and 2016–2020 (MARD, 2019). In the 2006–2010 period, the project of planting five million hectares of forest, called Program 661, was conducted (Prime Minister, 1998). Afforestation planning in this period was conducted to reduce erosion and nutrient flow downstream, especially in the northwestern and western areas of the whole watershed. In the 2011–2015 period, strategies for forest protection and development were implemented (Prime Minister, 2012). In 2014, an afforestation project was promulgated in the mountainous areas. The necessary areas for afforestation activities were 2,083 ha and 4,460 ha in Kon Tum and Gia Lai provinces, respectively (MARD, 2014). In the 2016–2020 period, the target program for sustainable forestry development (Program 886) was implemented in 2017 (Prime Minister, 2017). Additionally, strategies for sustainable forestry development in the Central Highlands for the

2021–2030 period were proposed in 2019, with priority given to the tasks that were not successfully completed in the 2016–2020 period, including forest protection and development, high-tech forestry development, community forest management, livelihood improvement, forest product development, sustainable forest management, and forest certification (Prime Minister, 2018). The role of forests in the Central Highlands is important in reducing the significant effects impacting aquatic biodiversity downstream. These strategies also depend on differences in the climate conditions, soil types, land-use types, and hydrological characteristics of each province.

In the Central Highlands, the forest area decreased by 416,994 ha from 2006 to 2019. As a result, the forest cover rate decreased from 54.6% in 2006 to 45.9% in 2019, representing the largest decrease in the country. The area of natural forest in this region decreased by 633,613 ha, whereas the planted forest area increased by 216,619 ha from 2006 to 2019. The main reasons for forest clearance in this region were urbanization, agricultural expansion, and crop conversion. Planted forests accounted for 5.11% of the total forest area in 2006 and 14.4% of the total forest area in 2019 (MARD, 2019). The forest cover rate is expected to increase to 49.2% by 2030. Protection of the natural forest system in the upstream areas will be extremely important in order to maintain the natural forest cover by encouraging co-management and community forest management systems. As can be clearly seen, the DBW and PKW belonging to the upstream Sesan River Basin play a key role in improving downstream water quality. Using these strategies, expectations for finding possible long-term solutions in the target area are necessary, especially in watershed management. The model approach, combined with consideration of local policies and agricultural practices, can contribute quantitative information for the identification of the impacts of terrestrial activities on the aquatic environment, as well as for comparisons of the different characteristics of the two watersheds, which can support local land-use planning and water resources management policies toward the sustainable development of both the terrestrial and the aquatic environments in particular areas.

5.5. Limitation of the study

The simulated results can be used to comprehensively assess the great changes in land use and anthropogenic activities in the target area. Additionally, the multiple land-use change approach should be applied to evaluate the impacts of land-use change in the future instead of using a single static land-use input condition or the delta approach, which is evaluated according to the differences in simulated outputs between two periods. Although the

improvement in the simulation results was confirmed by this study, several limitations still exist that may affect the accuracy of our results, such as: (1) the reproducibility of river discharges in the upstream of the target area; (2) the limited observation data for water quality from the rivers and Yaly lake; (3) the accuracy of the information regarding local agricultural practices; (4) the sparse distribution of rain gauges; and (5) the poor representation of the model in pollutant transport simulation. The first thing is that the river discharges were observed by the two hydrological stations located downstream of the target watersheds. This means upstream flow conditions may not be reproduced accurately, leading to the appearance of biases affecting the simulation of hydrological processes. Secondly, the amount of information on water quality from the rivers and Yaly lake was limited because water quality observation began in 2014, and these data are reported four times per year. This may not be sufficient to capture the local water quality conditions appropriately. Thirdly, the agricultural practice information was collected from the local government and used in the model. However, the local practices, such as the timing and amount of fertilizer, may be slightly different among farmers. This may affect the reproducibility of simulated outputs. Another reason is the lack of rainfall gauges in the central part of the area. The spatial distribution of rainfall can also influence the spatiotemporal uncertainty of the model in hydrology and water quality simulations (Cho et al., 2009). Finally, the simulation of pollutant transport in the river bed phase is one of the weaknesses of this model (Baffaut and Benson, 2009).

However, the calibrated outputs can be useful for different purposes, especially for controlling agricultural management practices on the watershed scale, even though there are several limitations in the observed information and the uncertainty of the model (Özcan et al., 2017).

5.6. Conclusions

The impacts of land-use policies and anthropogenic activities on river discharge, sediment, and nutrient loadings were assessed in the upstream Sesan River Basin across different periods from 2000 to 2018. The multiple land-use change conditions, along with the local agricultural practice information, were established in the original SWAT. The main findings of the study are as follows:

➤ The total cumulative river discharge, sediment, and nutrient loadings in the DBW were significantly lower than those in the PKW before 2005, despite the total area of the former being larger than the latter. From 2005 onward, these values were higher in the DBW, where the majority of anthropogenic activities occurred, especially in the 2005–2009 and

2010–2014 periods.

➤ Higher annual sediment and TP loadings were found upstream from the PKW, where range land predominated, and in southwestern and southern DBW, where arable land and permanent cropland predominated. The higher TN loadings were found upstream and downstream from the PKW as well as in southwestern and southern DBW.

➤ Arable land had the highest proportion of sediment, TN, and TP loadings across all four periods. The 2005–2009 and 2010–2014 periods exhibited higher proportions of these loadings from arable land and permanent cropland into the reaches.

➤ The important role of efficient land-use policies and afforestation in reducing erosion and improving the downstream water quality in this area has been emphasized.

➤ The crop conversion policy involving a shift from insufficient rubber forests to orchards applied in the 2015–2018 period seems to be efficient for the improvement of the water quality in the target area.

From this study, it has been proved that our methodology and results can be used to quantitatively evaluate the influences of local land-use policies on local water resources in the target river basin. By using our approach, future conditions of water resources also can be evaluated under future land-use projections in terrestrial zones on the aquatic environment downstream. The information will be useful for developing inter-ministerial cooperation systems to ensure the coherence of policies. However, to consider and execute water resources management comprehensively, several aspects need to be taken into account, such as: (1) the local water demand and changes to it, with the selection of suitable crop types and advanced technologies; (2) the available water amount and the water availability period under future climate conditions; (3) the participation of stakeholders in discussion, allowing them to share the conditions they consider to be ideal for the watershed and to prioritize necessary actions in the management of water resources; and (4) the acquisition of understanding from local residents regarding water environment protection. In addition to our results, this information and the necessary activities will assist decision makers in determining appropriate water resources management practices in the area.

CHAPTER 6. CONCLUSIONS AND RECOMMENDATION

The Dakbla and Poko watersheds play an extremely crucial role in managing water resources in the upstream Sesan river basin. The impacts from the target watersheds could affect significantly downstream where Yaly lake exists. Water resources are evaluated based on quantitative and qualitative aspects. At first, drought features were evaluated in terms of severity, duration and lag time, and frequency on the watershed scale based on a combination of a hydrological model and three drought indices including SPI, SSI, and SDI during the 2000-2018 period. Drought impacts on agriculture were emphasized because of their larger impacts on agricultural productivity over the long period. The higher drought vulnerability was found in the southwestern area, especially in agricultural drought. Rice is one of the main crops in these drought-prone agricultural areas. Also, the other agricultural crops grown in these areas are peanut, corn, soybean, pepper, cabbage, potato, cassava, sugarcane, and coffee. According to the Vietnamese National standard TCVN 8641:2011, the total water requirement for rice in the Central Highlands is normally 600-700 mm/season. For coffee, the total water requirement is about 200-265 mm/season. Corn, peanut, soybean, and cabbage require about 120-200 mm/season. Nevertheless, these crops in drought-prone areas require a higher water requirement compared to the threshold of the national standard. To solve the problem, the sowing process should be conducted earlier than in the dry years to reduce prolonged drought risk. Short-term rice varieties (< 90 days) are chosen such as HT1, VND95-20, IR56279, IR64, etc. in drought-prone areas in the downstream of Dakbla watershed. In the southern upstream of this watershed, it is recommended to use upland rice varieties with a short growing time of 100-110 days, high yield, high drought tolerance, and quick recovery from droughts such as LC93-1, LC93-4, LC227, and LC408. Moreover, conversion from barren paddy fields that could not be recovered to other short-duration crops such as cassava, peanut, sugarcane, corn, etc... should be conducted to increase production efficiency and save water for irrigation. These short-duration crops should be planted with groups of crops to easily regulate irrigation water sources. Cultivation in serious drought-risk areas for a long time should be considered carefully because of the high risks and low productivity. Focused on coffee trees, more than 25% of irrigation water will be saved by drip and sprinkler irrigation instead of traditional technique (strip irrigation). Furthermore, intercropping pepper, avocado, durian, and cashew in coffee farms to limit the evaporation, keep moist for coffee trees as well as diversify products, create more jobs, and stabilize incomes for local people. Before 2020, short-term strategies were implemented by the local

government each year to mitigate drought issues and water shortages. Many action plans are conducted such as cleaning and dredging wells; digging wells; utilizing water economically and sharing water resources per year. Nevertheless, assessing drought impacts on agriculture to how agricultural productivity can improve in the dry condition was not fully mentioned in these policies. In 2020, a drought management project for the 2021–2030 period was approved to mitigate the impacts of prolonged droughts on agriculture, which involved building a set of tools for drought management and promoting irrigation infrastructure investment. These results can evaluate and visualize drought impacts on agriculture on a watershed scale in detail and support long-term drought management strategies (2021-2030), crop conversion and irrigation system planning. Farmers can understand drought characteristics in specific drought-prone areas to choose suitable crop types, soil characteristics, and irrigation methods.

Secondly, surveying and assessing land of the whole country and regions have been evaluated once every five years in Vietnam because of the dramatic changes in the relatively short period. Previously, the impacts of land-use changes have been evaluated by using a single static land use map in different periods. In another case, the delta approach is applied to analyze the land-use change impacts in two periods by using the simulation results derived from different static land use data. Nevertheless, the frequent land-use changes in a relatively short-term period could not be assessed appropriately in the watershed by these approaches. Also, one of the most challenges to evaluate the impacts of land-use changes in a watershed is lack of the spatial location information for these LUC policies leading to insufficient long-term land use planning and watershed management strategies. In this study, the impacts of land-use input conditions on flow and sediment discharge were assessed by updating the different land-use conditions in the hydrological model. The scenario updating multiyear land use input conditions had the best performance for reproducing the flow and sediment discharge trends. It means updating different land use input conditions had led to more realistic conditions in the modeling instead of using a single static land use map. Differences in flow and sediment simulation will affect the long-term land use plan in the target area. And then, the effects of local land-use policies and anthropogenic activities on water quality were evaluated in the upstream Sesan river basin. The annual sediment, TN and TP loads were higher than in the northwestern area where the range land predominated, and in the southwestern area where arable land and permanent cropland predominated. If the changes in the 2005-2009 period do not apply, the huge amount of sediment, TN, and TP in the southwestern area will not estimate leading to significant impacts on the local land use

strategies. Similarly, if the changes in the 2010-2014 period continuously apply for the 2015-2018 period, the large amount of sediment, TN, and TP in the northwestern and southwestern areas will consider leading to the inaccuracy assessment of water quality downstream. Applying the different local land-use change policies had significant effects on the aquatic environment downstream. Compared to before applying land use policies (2000-2004), the total annual sediment, TN, and TP loading at the inflow to the lake increased by 36.6%, 27.4%, and 17.1% in the 2005-2009 period with applying local policies. Similarly, these values increased by 3.6%, 7.1%, and 9.0% for sediment, TN, and TP loading, respectively in the 2010-2014 period with applying inappropriate local policies and anthropogenic activities. Also, these values increased by 1.9% for sediment, 1.6% for TN, and 4.8% for TP in the 2015-2018 period with applying appropriate local policies and anthropogenic activities.

Generally, an image of popular issues concerning water resources and agriculture aspects was shown based on the spatio-temporal analysis on the watershed scale. The specific areas occurring the different issues such as drought, erosion, and nutrient losses were described in this dissertation. Understanding the watershed characteristics along with the combination of spatial land use, local land-use policies, and agricultural practices will could support decision policy-makers in implementing more effective local land-use policies, soil conservation, and water resources management strategies for the watershed in the future. As for local farmers, this knowledge can support them in establishing an appropriate crop calendars, stabilizing cultivation, improving crop production, and minimizing the drought risks in the drought-prone areas in the dry season as well as reducing erosion and excessive fertilizers downstream in the rainy season. Based on the above results, the future directions are recommended as follows:

- The lack of data on agriculture is also one of the obstacles in the target area. Besides meteo-hydrological data, the local crop yield and evapotranspiration information should be recorded in the long-term period to evaluate drought impacts on agriculture and predict drought tendency in detail. And then, assessing socio-economic drought will be conducted to evaluate the vulnerability of droughts to human livelihood.

- The tendency of meteo-hydrological and agricultural droughts should be predicted by using longer data periods (more than 30 years) of future projections in the target watersheds. Global weather data can be used to predict droughts in the future with supporting of the downscaling model.

➤ Establishing local land-use change input conditions in the next specific short periods is necessary for the study area where GIS-based information of local land-use changes is infrequently updated.

➤ Improvement of the accuracy of TSS measurement is required in the target area, especially in flood events because the impact of land-use changes on the sediment simulation was more sensitive than with the flow simulation.

➤ Interviewing local farmers in terms of the impacts of drought and inappropriate land use policies on human livelihood will be conducted.

➤ Understanding the dynamic carbon flux from burning activities in agriculture is es

APPENDIX

A1. Brief description of SWAT model

The SWAT model is known as a physically-based semi-distributed hydrological model developed by the Black land Research and Extension Center and the United States Department of Agriculture- Agricultural Research Service (USDA-ARS). The model is applied to simulate the impact of environmental changes on water, sediment, and nutrients in the watershed scale during the long-term period (Neitsch et al., 2011). As for watershed delineation, watersheds are delineated into subbasins connected by a stream network. Hydrologic response units (HRUs), the fundamental spatial units, were then divided from each subbasin due to the combination of unique land use, soil, and slope characteristics. The wide range SWAT applications indicated its advantages for evaluating several environmental processes to support policy-makers in watershed management more comprehensively. Simulating the hydrology of a watershed included the land phase and the water or routing phase of the hydrologic cycle. The land phase is utilized to estimate flow, sediment, and nutrient loadings to the main channel in each subbasin. The remaining phase is used to evaluate the movement of flow and sediment discharge through the channel to the outlet of the watershed.

Mentioned to the nitrogen cycle in the soil, there were three main forms of nitrogen in mineral soils including organic nitrogen associated with humus, mineral forms of nitrogen held by soil colloids and solution. Nitrogen is released from the soil through processes such as plant uptake, leaching, volatilization, denitrification, and erosion. In the SWAT model, five different pools of nitrogen in the soil were monitored, in which NH_4^+ and NO_3^- are two pools of inorganic forms and three remaining pools are organic forms. While fresh organic nitrogen is combined with crop residue and microbial biomass, the active and stable forms of organic nitrogen are combined with the soil humus.

As for the phosphorus cycle in the soil, there were three main forms of phosphorus in mineral soils including organic phosphorus associated with humus, insoluble forms of the mineral phosphorus, and plant-available phosphorus in soil solution. Phosphorus is released from the soil through processes such as plant uptake and erosion. In the SWAT model, six different pools of phosphorus in the soil were monitored, of which three pools are inorganic forms and three remaining pools are organic forms. While fresh organic phosphorus is combined with crop residue and microbial biomass, the active and stable forms of organic

phosphorus are combined with the soil humus. The solution, active and stable pools belong to inorganic phosphorus.

A2. Input data of SWAT model

Digital Elevation Model (DEM) was downloaded from the NASA and Japan ASTER program (2009) with a 30-meter resolution. The range of the topographic elevation of the study area varies from 45 m to 2,604 m. DEM data was re-projected to UTM coordinates WGS_1984_48N which can be represented as a raster.

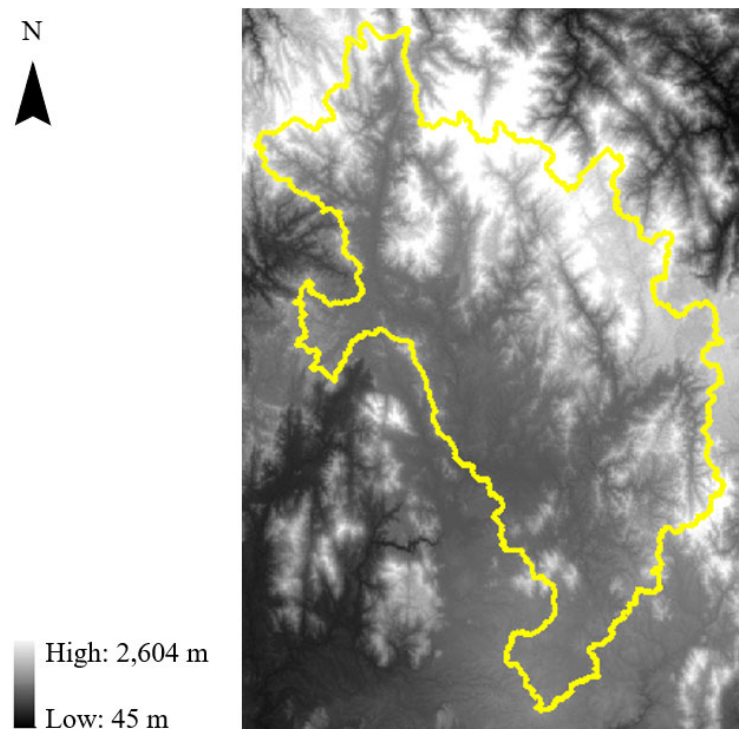


Figure A1. Digital Elevation Model of the target area

Land use data in 2005 were collected from the National Institute of Agricultural Planning and projection for the Kon Tum and Gia Lai provinces with a 1:50,000 scale map. The land use types were converted to SWAT code from Vietnamese code. The categories specified in the land use map area reclassified into fourteen types after processing including AGRC: agricultural land, non-row crops; AGRR: agricultural land row crops; COFF: coffee; FRSE: forestry land; F46: mixed forest (400–600 m); F68: mixed forest (600–800 m); F810: mixed forest (800–1,000 m); FRST: mixed forest; ORCD: orchard; RICE: rice; RNGB: rangeland; RUBR: rubber; URBN: urban; WATR: water. Forestry land predominated by 53.4% in the study area.

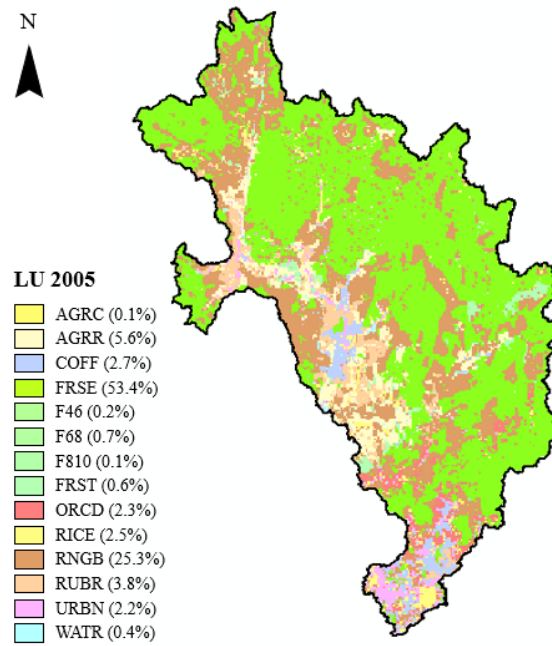


Figure A2. Land use map in 2005

Soil data were obtained from the Food and Agriculture Organization – United Nations Educational, Scientific and Cultural Organization (FAO-UNESCO) with a 1:5,000,000 scale map. Soil types were identified based on the soil texture classes (SICL: Silty clay, CL: Clay, SC: sandy clay, SCL: Sandy clay loam, SIC: Silty clay; SIL: Silt loam), in which Clay class occupied the highest proportion with 56.8%.

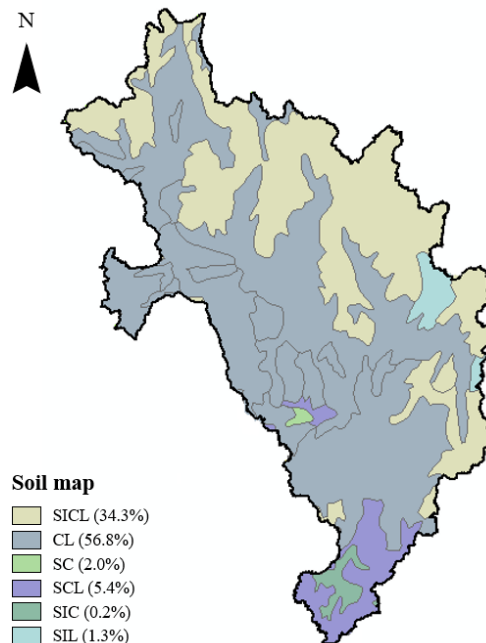


Figure A3. Soil texture classes in the target area

Weather data were collected from the Central Highlands Region Hydrometeorological Centre. Weather data including daily rainfall, daily maximum and minimum temperature,

daily mean humidity, daily sunshine hours, and daily mean wind speed at Kon Tum and Pleiku stations were recorded in the 2000-2018 period. Daily rainfall at Dak Glei, Dak To, Dak Doa, Kbang, and Mang Den stations was also measured by the Centre.

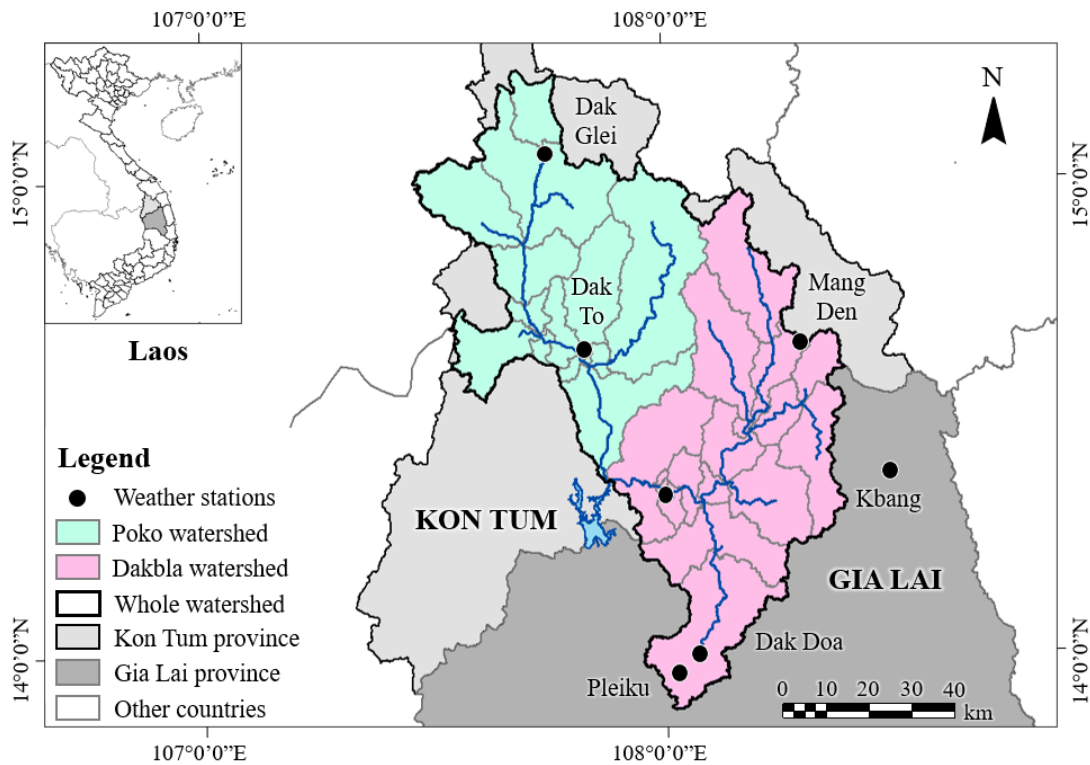


Figure A4. Location of weather stations in the target area

A3. Updating land use changes in the model

The land-use change module was written in the R script by Tam, 2012.

Step 1. Opening the “TxtInOut” and “.mdb” files in the ArcSWAT project for each land use scenario.

- The HRUs information in these files was used to create input files for the R script. This HRUs information related to a diversity of features within the HRU includes subbasins, HRU, land use, soil, HRU fraction, slope, and so on.

Step 2. Preparing the input files with the HRUs information of each land use scenario for the R script.

- The private input files were created with the name “hru_lu_2005.txt”, “hru_lu_2010.txt”, “hru_lu_2015.txt”, and “hru_lu_2018.txt”.

- The first line is the title line with the capitalized letters and the second line is the data in free format as shown in Figure A1.

OID	SUBBASIN	HRU	LANDUSE	SOIL	SLOPE_CD	HRU_FR
1	1	1	AGRR	CL	5-10	0.0067
2	1	2	AGRR	CL	15-9999	0.0133
3	1	3	AGRR	CL	0-5	0.0031
4	1	4	AGRR	CL	10-15	0.0069
5	1	5	AGRR	SICL	15-9999	0.0030

Figure A5. Input files for the R script

Step 3. Creating the general HRU output file for all land use scenarios by using the R script.

- Modifying the name of private input files in the R script.

- After running the R script, a general HRU output file named “hru_lu_all.txt” contains the information on the land use changes among scenarios.

```

1 *****
2 # USER DEFINE PARAMETER - PLEASE CHANGE ONLY WITHIN THIS PART
3
4 hru_landuse <- c()
5 hru_landuse[1] <- "E:/3.Nutrients/LUC_13.9/05/hru_lu_2005.txt"
6 hru_landuse[2] <- "E:/3.Nutrients/LUC_13.9/10/hru_lu_2010.txt"
7 hru_landuse[3] <- "E:/3.Nutrients/LUC_13.9/15/hru_lu_2015.txt"
8 hru_landuse[4] <- "E:/3.Nutrients/LUC_13.9/18/hru_lu_2018.txt"
9 ouput_file <- "E:/3.Nutrients/LUC_13.9/hru_lu_all.txt"

```

Figure A6. The interface of R script to add the HRUs information of all land use scenarios.

Step 4. Creating the “newTxtInOut” folder for all land use scenarios for simulating land use changes.

```

12 Lu[1] <- "E:/LUC_1/05/Scenarios/05/TxtInOut"
13 Lu[2] <- "E:/LUC_1/10/Scenarios/10/TxtInOut"
14 Lu[3] <- "E:/LUC_1/15/Scenarios/15/TxtInOut"
15 Lu[4] <- "E:/LUC_1/18/Scenarios/18/TxtInOut"
16 # add Lu[4] or remove Lu[3] if needed
17
18 date <- c( "01012005", "01012010", "01012015", "01012018" )
19 inter_date[[1]] <- c( "01012006", "01012007", "01012008", "01012009")
20 inter_date[[2]] <- c( "01012011", "01012012", "01012013", "01012014")
21 inter_date[[3]] <- c( "01012016", "01012017")
22
23 ofolder <- "E:/LUC_1/newTxtInOut"
24 hru_lu_all <- "E:/LUC_1/hru_lu_all.txt"

```

Figure A7. Creating the “new TxtInOut” folder for the ArcSWAT project.

- An general output file named “newTxtInOut” contains the information on the land use changes among scenarios.

- The first part from Line 12 to Line 15 is the information of each TxtInOut folder of each land use scenario.

- The second part from Line 18 to Line 21 is the date of land use scenarios and which years the author interpolates land use.
- The final part from Line 23 to Line 24 is the necessary output files to update land use changes in the ArcSWAT project.

Step 5. Updating the “newTxtInOut” folder into the ArcSWAT project

- After updating the “newTxtInOut” folder into the ArcSWAT project, the “lup.dat” file was checked for the land use changes for each specific year.

1	1	1	2006	01012006.dat
2	1	1	2007	01012007.dat
3	1	1	2008	01012008.dat
4	1	1	2009	01012009.dat
5	1	1	2010	01012010.dat
6	1	1	2011	01012011.dat
7	1	1	2012	01012012.dat
8	1	1	2013	01012013.dat
9	1	1	2014	01012014.dat
10	1	1	2015	01012015.dat
11	1	1	2016	01012016.dat
12	1	1	2017	01012017.dat
13	1	1	2018	01012018.dat

Figure A8. The “lup.dat” file after updating land use changes.

REFERENCES

CHAPTER 1

- Affessa, G.M., Belew, A.Z., Tenagashaw, D.Y., Tamirat, D.M., 2022. Land use/cover change impacts on hydrology using swat model on Borkena watershed, Ethiopia. *Water Conservation Science and Engineering* 7(1), 55–63. <https://doi.org/10.1007/s41101-022-00128-1>.
- Alexander, R.B., Smith, R.A., Schwarz, G.E., Boyer, E.W., Nolan, J.V., Brakebill, J.W., 2008. Differences in phosphorus and nitrogen delivery to the Gulf of Mexico from the Mississippi River Basin. *Environmental Science and Technology* 42(3), 822–830. <https://doi.org/10.1021/es0716103>.
- Altdorff, D., Galagedara, L., Unc, A., 2017. Impact of projected land conversion on water balance of boreal soils in western newfoundland. *Journal of Water and Climate Change* 8(4), 613–626. <https://doi.org/10.2166/wcc.2017.016>.
- Cung, N., Truong, Q., Khoi, D.N., Nguyen, H.Q., Kondoh, A., 2022. Impact of forest conversion to agriculture on hydrologic regime in the large basin in Vietnam. *Water (Switzerland)* 2022, 14, 854. <https://doi.org/10.3390/w14060854>.
- CGIAR Research Program on Climate Change, Agriculture and Food Security - Southeast Asia (CCAFS-SEA), 2016. Assessment Report: The drought crisis in the Central Highlands of Vietnam. CGIAR Research Program on Climate Change, Agriculture and Food Security (CCAFS), Hanoi, Vietnam.
- Directorate of Water Resources (WRD), 2016. Drought in the Central Highlands of Vietnam. Assessment report, Hanoi City, Vietnam.
- Folliott, P., Brooks, K., Neary, D., Roberto, T., Chevesich, P., 2013. Soil erosion and sediment production on watershed landscapes: Processes and control. The United Nations Educational, Scientific and Cultural Organizations (UNESCO). <https://www.fs.usda.gov/treesearch/pubs/46794>.
- Frohlich, H.L., Schreinemachers, P., Stahr, K., Clemens, G., 2013. Sustainable land use and rural development in Southeast Asia: Innovations and policies for mountainous areas. Springer Environmental Science and Engineering. <https://doi.org/10.1007/978-3-642-33377-4>.
- Gia Lai provincial Department of Agriculture and Rural Development (GLDARD), 2019. The drought situation in Gia Lai province. Assessment report, Gia Lai, Vietnam, 4 pages.
- Holden, J., Haygarth, P., MacDonald, J., Jenkins, A., Spaiets, A., Orr, H., Dunn, N., Harris,

- B., Pearson, P., McGonigle, D., Humble, A., Ross, M., Harris, J., Meacham, T., Benton, T., Staines, A., Noble, A., 2015. Farming and water 1: Agriculture's impacts on water quality. *Global Food Security*.
- Kon Tum People's Committee, 2019. Drought plan in the dry season of the 2019-2020 year in Kon Tum province. Decision number 3297/KH-UBND, Kon Tum, Vietnam, 7 pages.
- Kon Tum People's Committee, 2020. Project on drought management in Kon Tum province during a 2021 – 2030 period. Decision number 1167/QĐ-UBND, Kon Tum, Vietnam, 2 pages.
- Kon Tum provincial Department of Agriculture and Rural Development (KTDARD), 2018. Report on dam and reservoir safety in Kon Tum province. Assessment report, Kon Tum, Vietnam, 4 pages.
- Li, Y., Chang, J., Luo, L., Wang, Y., Guo, A., Ma, F., Fan, J., 2019. Spatiotemporal impacts of land use land cover changes on hydrology from the mechanism perspective using SWAT model with time-varying parameters. *Hydrology Research* 50(1), 244–261. <https://doi.org/10.2166/nh.2018.006>.
- Makhtoumi, Y., Li, S., Ibeanusi, V., Chen, G., 2020. Evaluating water balance variables under land use and climate projections in the upper Choctawhatchee river watershed, in Southeast US. *Water (Switzerland)* 12, 2205. <https://doi.org/10.3390/w12082205>.
- Munoth, P., Goyal, R., 2020. Impacts of land use land cover change on runoff and sediment yield of Upper Tapi River Sub-Basin, India. *International Journal of River Basin Management* 18(2), 177–189. <https://doi.org/10.1080/15715124.2019.1613413>.
- National Assembly of Vietnam, 2013. Land law. Hanoi City, Vietnam, 124 pages.
- Pierret, A., De Rouw, A., Chaplot, V., Valentin, C., Noble, A., Suhardiman, D., Drechsel, P., 2011. Reshaping upland farming policies to support nature and livelihoods: Lesson from soil erosion in Southeast Asia with emphasis on Lao PDR. Institut de Recherche pour le Développement (IRD), Marseille, France and International Water Management Institute (IWMI), Colombo, Sri Lanka. <https://doi.org/10.5337/2011.213>.
- Prime Minister, 2009. The rubber development planning up to 2015 and vision to 2020. Hanoi City, Vietnam, 6 pages (in Vietnamese).
- Shi, Z.H., Fang, N.F., Wu, F.Z., Wang, L., Yue, B.J., Wu, G.L., 2012. Soil erosion processes and sediment sorting associated with transport mechanisms on steep slopes. *Journal of Hydrology* 454–455, 123–130. <https://doi.org/10.1016/j.jhydrol.2012.06.004>.
- Son, N.T., Binh, N.D., Shrestha, R.P., 2015. Effect of land use change on runoff and sediment yield in Da river basin of Hoa Binh province, Northwest Vietnam. *Journal of Mountain*

Science 12, 1051–1064. <https://doi.org/10.1007/s1162-013-2925-9>.

The Economic and Social Commission for Asia and the Pacific and The Association of Southeast Asian Nations (ESCAP and ASEAN), 2020. Ready for the dry years: Building resilience to drought in South-east Asia. In United Nations. <https://doi.org/10.18356/adcafl1d0-en>.

Vietnam Academy for Water Resources (VAWR), 2012. Irrigation planning Kon Tum during a period from 2011 to 2020 and orientation to 2025. Hanoi, Vietnam.

World Bank. (2017). Water resources management. <https://www.worldbank.org/en/topic/waterresourcesmanagement#1> (accessed 6 March, 2022).

World Health Organization (WHO), 2010. Drinking water quality in the Southeast Asia region. WHO Regional Office for South-East Asia. <https://apps.who.int/iris/handle/10665/204999>.

World Meteorological Organization and Global Water Partnership (WMO and GWP), 2016. Handbook of drought indicators and indices. Integrated Drought Management Programme (IDMP). WMO, Geneva, Switzerland and GWP, Stockholm, Sweden.

Zhao, S., Peng, C., Jiang, H., Tian, D., Lei, X., Zhou, X., 2006. Land use change in Asia and the ecological consequences. *Ecological Research* 21(6), 890–896. <https://doi.org/10.1007/s11284-006-0048-2>.

CHAPTER 2

Abbaspour, K.C., Rouholahnejad, E., Vaghefi, S., Srinivasan, R., Yang, H., Kløve, B., 2015. A continental-scale hydrology and water quality model for Europe: Calibration and uncertainty of a high-resolution large-scale SWAT model. *Journal of Hydrology* 524, 733–752. <https://doi.org/10.1016/j.jhydrol.2015.03.027>.

Aflizar, Saidi, A., Husnain, Indra, R., Darmawan, Harmailis, Somura, H., Wakatsuki, T., Masunaga, T., 2010. Soil erosion characterization in an agricultural watershed in West Sumatra, Indonesia. *Tropics* 19(1), 29–42. <https://doi.org/10.3759/tropics.19.29>.

Aghsaei, H., Dinan, N.M., Moridi, A., Asadolahi, Z., Delavar, M., Fohrer, N., Wagner, P.D., 2020. Effects of dynamic land use/land cover change on water resources and sediment yield in the Anzali wetland catchment, Gilan, Iran. *Science of the Total Environment* 712, 1–11. <https://doi.org/10.1016/j.scitotenv.2019.136449>.

Alexander, R.B., Smith, R.A., Schwarz, G.E., Boyer, E.W., Nolan, J.V., Brakebill, J.W., 2008. Differences in phosphorus and nitrogen delivery to the Gulf of Mexico from the

- Mississippi River Basin. *Environmental Science and Technology* 42(3), 822–830. <https://doi.org/10.1021/es0716103>.
- An, P.H.H., Sylvain, H., Henry des Tureaux, T., Orange, D., Jouquet, P., Valentin, C., De Rouw, A., Toan, T. D., 2012. Impact of fodder cover on runoff and soil erosion at plot scale in a cultivated catchment of North Vietnam. *Geoderma* 177–178, 8–17. <https://doi.org/10.1016/j.geoderma.2012.01.031>.
- Bisht, D.S., Sridhar, V., Mishra, A., Chatterjee, C., Raghuwanshi, N.S., 2019. Drought characterization over India under projected climate scenario. *International Journal of Climatology* 39(4), 1889–1911. <https://doi.org/10.1002/joc.5922>.
- Carpenter, S.R., Bolgrien, D., Lathrop, R.C., Stow, C.A., Reed, T., Wilson, M.A., 1998. Ecological and economic analysis of lake eutrophication by nonpoint pollution. *Australian Journal of Ecology* 23, 68–79. <https://doi.org/10.1111/j.1442-9993.1998.tb00706.x>.
- CGIAR Research Program on Climate Change, Agriculture and Food Security - Southeast Asia (CCAFS-SEA), 2016. Assessment Report: The drought crisis in the Central Highlands of Vietnam. CGIAR Research Program on Climate Change, Agriculture and Food Security (CCAFS), Hanoi, Vietnam.
- Cung, N., Truong, Q., Khoi, D.N., Nguyen, H.Q., Kondoh, A., 2022. Impact of forest conversion to agriculture on hydrologic regime in the large basin in Vietnam. *Water (Switzerland)* 2022, 14, 854. <https://doi.org/10.3390/w14060854>.
- Cuong, H.V., Nam, D.H., Toan, T.Q., 2019. Assessment of hydro-climatological drought conditions for Hong-Thai Binh river watershed in Vietnam using high-resolution model simulation. *Vietnam Journal of Science, Technology and Engineering* 61(2), 90–96. [https://doi.org/10.31276/vjste.61\(2\).90-96](https://doi.org/10.31276/vjste.61(2).90-96).
- Daniel, T., Ardakanian, R., 2015. Regional Workshop on Capacity Development to Support National Drought Management Policies for Asia-Pacific Countries. UN-Water Decade Programme on Capacity Development (UNW-DPC).
- Directorate of Water Resources (WRD), 2016. Drought in the Central Highlands of Vietnam. Assessment report, Hanoi City, Vietnam.
- Dung, N.V, Vien, T.D., Lam, N.T., Tuong, T.M., Cadisch, G., 2008. Analysis of the sustainability within the composite swidden agroecosystem in northern Vietnam: 1. Partial nutrient balances and recovery times of upland fields. *Agriculture, Ecosystems and Environment* 128(1–2), 37–51. <https://doi.org/10.1016/j.agee.2008.05.004>.
- FAO, 2022. Statistical Database of the Food and Agricultural Organization of the United

- Nations. <https://www.fao.org/statistics/en/>. (accessed 6 March, 2022).
- Folliott, P., Brooks, K., Neary, D., Roberto, T., Chevesich, P., 2013. Soil erosion and sediment production on watershed landscapes: Processes and control. The United Nations Educational, Scientific and Cultural Organizations (UNESCO). <https://www.fs.usda.gov/treearch/pubs/46794>.
- Guse, B., Pfannerstill, M., Fohrer, N., 2015. Dynamic Modelling of Land Use Change Impacts on Nitrate Loads in Rivers. *Environmental Processes* 2(4), 575–592. <https://doi.org/10.1007/s40710-015-0099-x>.
- Ha, M., Wu, M., (2017). Land management strategies for improving water quality in biomass production under changing climate. *Environmental Research Letters* 12(3). <https://doi.org/10.1088/1748-9326/aa5f32>.
- Hang, V.T., Thanh, N.D., Tan, P.V., 2014. Evolution of meteorological drought characteristics in Vietnam during the 1961–2007 period. *Theoretical and Applied Climatology* 118(3), 367–375. <https://doi.org/10.1007/s00704-013-1073-z>.
- Hanief, A., Laursen, A.E., 2017. SWAT modeling of hydrology, sediment and nutrients from the grand river, Ontario. *Water Quality Research Journal* 52(4), 243–257. <https://doi.org/10.2166/wqrj.2017.014>.
- Hao, Z., AghaKouchak, A., 2013. Multivariate Standardized Drought Index: A parametric multi-index model. *Advances in Water Resources* 57, 12–18. <https://doi.org/10.1016/j.advwatres.2013.03.009>.
- Holden, J., Haygarth, P., MacDonald, J., Jenkins, A., Spaiets, A., Orr, H., Dunn, N., Harris, B., Pearson, P., McGonigle, D., Humble, A., Ross, M., Harris, J., Meacham, T., Benton, T., Staines, A., Noble, A., 2015. Farming and water 1: Agriculture’s impacts on water quality. *Global Food Security*.
- Huang, Z., Xue, B., Pang, Y., 2009. Simulation on stream flow and nutrient loadings in Gucheng Lake, Low Yangtze river basin, based on SWAT model. *Quaternary International* 208(1–2), 109–115. <https://doi.org/10.1016/j.quaint.2008.12.018>.
- Hung, L.M., Kim, H., Moon, H., Zhang, R., Lakshmi, V., Bang, N. L., 2020. Assessment of drought conditions over Vietnam using standardized precipitation evapotranspiration index, MERRA-2 re-analysis, and dynamic land cover. *Journal of Hydrology: Regional Studies* 32, 100767. <https://doi.org/10.1016/j.ejrh.2020.100767>.
- Huyen, N.T., Tu, L.H., Tram, V.N.Q., Minh, D.N., Liem, N.D., Loi, N.K., 2017. Assessing the impacts of climate change on water resources in the Srepok watershed, Central Highland of Vietnam. *Journal of Water and Climate Change* 8(3), 524–534.

- <https://doi.org/10.2166/wcc.2017.135>.
- Jha, M.K., Gassman, P.W., Arnold, J.G., 2007. Water quality modeling for the Raccoon river watershed using SWAT. *Transactions of the American Society of Agricultural and Biological Engineers* 50(2), 479–493. <https://doi.org/10.13031/2013.22660>.
- Kamali, B., Kouchi, D.H., Yang, H., Abbaspour, K.C., 2017. Multilevel drought hazard assessment under climate change scenarios in semi-arid regions-a case study of the karkheh river basin in Iran. *Water (Switzerland)* 9(4). <https://doi.org/10.3390/w9040241>.
- Keraga, A.S., Kiflie, Z., Engida, A.N., 2019. Evaluation of SWAT performance in modeling nutrients of Awash river basin, Ethiopia. *Modeling Earth Systems and Environment* 5(1), 275–289. <https://doi.org/10.1007/s40808-018-0533-y>.
- Khoi, D.N., Nguyen, V.T., Sam, T.T., Nhi, P.T.T., 2019. Evaluation on effects of climate and land-use changes on streamflow and water quality in the La Buong river basin, Southern Vietnam. *Sustainability (Switzerland)* 11(24). <https://doi.org/10.3390/SU11247221>.
- Khoi, D.N., Sam, T.T., Loi, P.T., Hung, B.V., Nguyen, V.T., 2021. Impact of climate change on hydro-meteorological drought over the Be river basin, Vietnam. *Journal of Water and Climate Change* 12(7), 3159–3169. <https://doi.org/10.2166/wcc.2021.137>.
- Khoi, D.N., Suetsugi, T., 2014. The responses of hydrological processes and sediment yield to land-use and climate change in the Be River Catchment, Vietnam. *Hydrological Processes* 28(3), 640–652. <https://doi.org/10.1002/hyp.9620>.
- Khoi, D.N., Thom, V.T., 2015. Impacts of climate variability and land-use change on hydrology in the period 1981-2009 in the Central Highlands of Vietnam. *Global Nest Journal* 17(4), 870–881. <https://doi.org/10.30955/gnj.001706>.
- Łabędzki, L., 2007. Estimation of local drought frequency in central Poland using the standardized precipitation index SPI. *Irrigation and Drainage* 56(1), 67–77. <https://doi.org/10.1002/ird.285>.
- Le, M.H., Perez, G.C., Solomatine, D., Nguyen, L.B., 2016. meteorological drought forecasting based on climate signals using artificial neural network - A case study in Khanh hoa province, Vietnam. *Procedia Engineering* 154, 1169–1175. <https://doi.org/10.1016/j.proeng.2016.07.528>.
- Le, T., Sun, C., Choy, S., Kuleshov, Y., 2021. Regional drought risk assessment in the Central Highlands and the South of Vietnam. *Geomatics, Natural Hazards and Risk* 12(1), 3140–3159. <https://doi.org/10.1080/19475705.2021.1998232>.
- Lee, D., Han, J.H., Park, M.J., Engel, B.A., Kim, J., Lim, K.J., Jang, W.S., 2019. Development of advanced web-based SWAT LUC system considering yearly land use

- changes and recession curve characteristics. *Ecological Engineering* 128, 39–47. <https://doi.org/10.1016/j.ecoleng.2019.01.001>.
- Li, X., Zipp, K.Y., 2019. Dynamics and uncertainty in land use conversion for perennial energy crop production: Exploring effects of payments for ecosystem services policies. *Agricultural and Resource Economics Review* 48(2), 328–358. <https://doi.org/10.1017/age.2019.3>.
- Li, Y., Chang, J., Luo, L., Wang, Y., Guo, A., Ma, F., Fan, J., 2019. Spatiotemporal impacts of land use land cover changes on hydrology from the mechanism perspective using SWAT model with time-varying parameters. *Hydrology Research* 50(1), 244–261. <https://doi.org/https://doi.org/10.2166/nh.2018.006>.
- Li, Z., Liu, W.Z., Zhang, X.Z., Zheng, F.L., 2009. Impacts of land use change and climate variability on hydrology in an agricultural catchment on the Loess Plateau of China. *Journal of Hydrology* 377(1–2), 35–42. <https://doi.org/10.1016/j.jhydrol.2009.08.007>.
- Loi, N.K., Huyen, N.T., Tu, L.H., Tram, V.N.Q., Liem, N.D., Dat, N.L.T, Nhat, T.T., Minh, D.N., 2016. Sustainable land use and watershed management in response to climate change impacts: Case study in Srepok watershed, Central Highland of Vietnam. *Environmental Sustainability and Climate Change Adaptation Strategies*, 255–295. <https://doi.org/10.4018/978-1-5225-1607-1.ch010>.
- Lu, H., Wu, Y., Li, Y., Liu, Y., 2017. Effects of meteorological droughts on agricultural water resources in southern China. *Journal of Hydrology* 548, 419–435. <https://doi.org/10.1016/j.jhydrol.2017.03.021>.
- Lweendo, M.K., Lu, B., Wang, M., Zhang, H., Xu, W. (2017). Characterization of droughts in humid subtropical region, upper Kafue river basin (Southern Africa). *Water (Switzerland)* 9(4), 242. <https://doi.org/10.3390/w9040242>.
- Malagó, A., Bouraoui, F., Vigiak, O., Grizzetti, B., Pastori, M., 2017. Modelling water and nutrient fluxes in the Danube river basin with SWAT. *Science of the Total Environment* 603–604, 196–218. <https://doi.org/10.1016/j.scitotenv.2017.05.242>.
- Martinelli, M., Machado, E.H., 2014. Static and dynamic maps, developed from an analytical or synthesis reasoning, in school geographic atlas: The methodological feasibility. *Revista Brasileira de Cartografi* 66(7), 899–920.
- Mateo-Sagasta, J., Marjani, S., Turrall, H., Burke, J., 2017. Water pollution from agriculture: a global review. FAO and IWMI.
- Momm, H.G., Porter, W.S., Yasarer, L.M., ElKadiri, R., Bingner, R.L., Aber, J.W., 2019. Crop conversion impacts on runoff and sediment loads in the Upper Sunflower river

- watershed. *Agricultural Water Management* 217, 399–412. <https://doi.org/10.1016/j.agwat.2019.03.012>.
- Morgan, R.P.C., 2005. *Soil erosion and conservation (Third Edition)*. Blackwell Publishing Ltd, United Kingdom.
- Moriassi, D.N., Pai, N., Steiner, J.L., Gowda, P.H., Winchell, M., Rathjens, H., Starks, P. J., Verser, J.A., 2019. SWAT-LUT: A desktop graphical user interface for updating land use in SWAT. *Journal of the American Water Resources Association* 55(5), 1102–1115. <https://doi.org/https://doi.org/10.1111/1752-1688.12789>.
- Munoth, P., Goyal, R., 2020. Impacts of land use land cover change on runoff and sediment yield of Upper Tapi River Sub-Basin, India. *International Journal of River Basin Management* 18(2), 177–189. <https://doi.org/10.1080/15715124.2019.1613413>.
- Narasimhan, B., Srinivasan, R., 2005. Development and evaluation of Soil Moisture Deficit Index (SMDI) and Evapotranspiration Deficit Index (ETDI) for agricultural drought monitoring. *Agricultural and Forest Meteorology* 133(1–4), 69–88. <https://doi.org/10.1016/j.agrformet.2005.07.012>.
- Nauditt, A., Firoz, A.B.M., Trinh, V.Q., Fink, M., Stolpe, H., Ribbe, L., 2017. Hydrological Drought Risk Assessment in an Anthropogenically Impacted Tropical Catchment, Central Vietnam. *Water Resources Development and Management* 223–239. https://doi.org/10.1007/978-981-10-2624-9_14.
- Nga, L.T.T., Giang, N.T., Dung, B.Q., 2019. Investigation of selecting drought index for agricultural drought rezoning in Gia Lai province. *Vietnam Journal of Hydrometeorology* 2019(2–1), 29–36. [https://doi.org/10.36335/vnjhm.2019\(2-1\).29-36](https://doi.org/10.36335/vnjhm.2019(2-1).29-36).
- Nguyen, L.B., Li, Q.F., Ngoc, T.A., Hiramatsu, K., 2015. Drought assessment in Cai River basin, Vietnam: A comparison with regard to SPI, SPEI, SSI, and SIDI. *Journal of the Faculty of Agriculture, Kyushu University* 60(2), 417–425. <https://doi.org/10.5109/1543404>.
- Nguyen, T.D., 2007. *Coping with drought in the Central Highlands – Vietnam*. Institute of Environment and Resources, Technical University of Denmark.
- Pai, N., Saraswat, D., 2011. SWAT2009_LUC: A tool to activate the land use change module in SWAT 2009. *Transactions of the American Society of Agricultural and Biological Engineers* 54(5), 1649–1658.
- Phong, L.V.V., Tan, P.V., Khiem, M.V., Duc, T.Q., 2019. Space–time variability of drought over Vietnam. *International Journal of Climatology* 39, 5437–5451. <https://doi.org/10.1002/joc.6164>.

- Quang, C.N.X., Hoa, H.V., Giang, N.N.H., Hoa, N.T., 2021. Assessment of meteorological drought in the Vietnamese Mekong delta in period 1985-2018. *IOP Conference Series: Earth and Environmental Science* 652(1). <https://doi.org/10.1088/1755-1315/652/1/012020>.
- Quyen, N.T.N., Liem, N.D., Loi, N.K., 2014. Effect of land use change on water discharge in Srepok watershed, Central Highland, Viet Nam. *International Soil and Water Conservation Research* 2(3), 74–86. [https://doi.org/10.1016/S2095-6339\(15\)30025-3](https://doi.org/10.1016/S2095-6339(15)30025-3).
- Sam, T.T., Khoi, D.N., Thao, N.T.T., Nhi, P.T.T., Quan, N.T., Hoan, N.X., Tinh, N.V., 2019. Impact of climate change on meteorological, hydrological and agricultural droughts in the Lower Mekong River Basin: A case study of the Srepok Basin, Vietnam. 33, 547–559. *Water and Environment Journal*. <https://doi.org/10.1111/wej.12424>.
- Sehgal, V., Sridhar, V., 2019. Watershed-scale retrospective drought analysis and seasonal forecasting using multi-layer, high-resolution simulated soil moisture for Southeastern U.S. *Weather and Climate Extremes* 23, 100191. <https://doi.org/10.1016/j.wace.2018.100191>.
- Shukla, S., Wood, A.W., 2008. Use of a standardized runoff index for characterizing hydrologic drought. *Geophysical Research Letters* 35(2), 1–7. <https://doi.org/10.1029/2007GL032487>.
- Sidle, R.C., Ziegler, A.D., Negishi, J.N., Nik, A.R., Siew, R., Turkelboom, F., 2006. Erosion processes in steep terrain - Truths, myths, and uncertainties related to forest management in Southeast Asia. *Forest Ecology and Management* 224(1–2), 199–225. <https://doi.org/10.1016/j.foreco.2005.12.019>.
- Somura, H., Takeda, I., Arnold, J.G., Mori, Y., Jeong, J., Kannan, N., Hoffman, D., 2012. Impact of suspended sediment and nutrient loading from land uses against water quality in the Hii River basin, Japan. *Journal of Hydrology* 450–451, 25–35. <https://doi.org/10.1016/j.jhydrol.2012.05.032>.
- Son, N.T., Binh, N.D., Shrestha, R.P., 2015. Effect of land use change on runoff and sediment yield in Da river basin of Hoa Binh province, Northwest Vietnam. *Journal of Mountain Science* 12, 1051–1064. <https://doi.org/10.1007/s1162-013-2925-9>.
- Son, N.T., Huong, H.L., Loc, N.D., Phuong, T.T., 2022. Application of SWAT model to assess land use change and climate variability impacts on hydrology of Nam Rom Catchment in Northwestern Vietnam. *Environment, Development and Sustainability* 24(3), 3091–3109. <https://doi.org/10.1007/s10668-021-01295-2>.
- Son, N.T., Huong, H.L., Phuong, T.T., Loc, N.D., 2020. Application of SWAT model to

- Assess Land Use and Climate Changes Impacts on Hydrology of Nam Rom River Basin in Vietnam. Preprints, 1–17. <https://doi.org/10.20944/preprints202001.0362.v1>.
- Stallard, R.F., 1998. Terrestrial sedimentation and the carbon cycle: Coupling weathering and erosion to carbon burial. *Global Biogeochemical Cycles* 12(2), 231–257. <https://doi.org/10.1029/98GB00741>.
- Stojanovic, M., Liberato, M. L. R., Sorí, R., Vázquez, M., Tan, P. V., Hieu, D. V., Tin, H. C., Phuong, N. N. B., Nieto, R., and Gimeno, L. (2020). Trends and Extremes of Drought Episodes in Vietnam Sub-Regions during 1980–2017 at Different Timescales. *Water (Switzerland)* 12, 813. <https://doi.org/10.3390/w12030813>.
- Stott, T., Mount, N., 2004. Plantation forestry impacts on sediment yields and downstream channel dynamics in the UK: A review. *Progress in Physical Geography* 2(28), 197–240. <https://doi.org/https://doi.org/10.1191/0309133304pp410ra>.
- Sun, F., Mejia, A., Zeng, P., Che, Y., 2019. Projecting meteorological, hydrological and agricultural droughts for the Yangtze River basin. *Science of the Total Environment* 696, 134076. <https://doi.org/10.1016/j.scitotenv.2019.134076>.
- Thang, N.V., Khiem, M.V., Mau, N.D., 2014. Determining the drought criteria for the South Central region. *Vietnam Journal of Hydrometeorology* 639, 49–55.
- Tingting, L.V., Xiaoyu, S., Dandan, Z., Zhenshan, X., Jianming, G., 2008. Assessment of soil erosion risk in Northern Thailand. *International Archives of the Photogrammetry, Remote Sensing and Spatial Information Sciences XXXVII*, 703–708.
- Tran, V.B., Ishidaira, H., Nakamura, T., Do, T.N., Nishida, K., 2017. Estimation of nitrogen load with multi-pollution sources using the SWAT model: A case study in the Cau river basin in Northern Vietnam. *Journal of Water and Environment Technology* 15(3), 106–119. <https://doi.org/10.2965/jwet.16-052>.
- Trenberth, K.E., Dai, A., Van Der Schrier, G., Jones, P.D., Barichivich, J., Briffa, K.R., Sheffield, J., 2014. Global warming and changes in drought. *Nature Climate Change* 4(1), 17–22. <https://doi.org/10.1038/nclimate2067>
- Tri, D.Q., Dat, T.T., Truong, D.D., 2019. Application of meteorological and hydrological drought indices to establish drought classification maps of the Ba river basin in Vietnam. *Hydrology* 6(49), 20. <https://doi.org/10.3390/hydrology6020049>.
- Tripathi, M.P., Panda, R.K., Raghuvanshi, N.S., 2003. Identification and prioritisation of critical sub-watersheds for soil conservation management using the SWAT model. *Biosystems Engineering* 85(3), 365–379.
- Tuan, N.H., Canh, T.T., 2021. Analysis of trends in drought with the non-parametric

- approach in Vietnam: A case study in Ninh Thuan province. *American Journal of Climate Change* 10(01), 51–84. <https://doi.org/10.4236/ajcc.2021.101004>.
- Vietnam Academy for Water Resources (VAWR), 2012. Irrigation planning Kon Tum during a period from 2011 to 2020 and orientation to 2025. Hanoi, Vietnam.
- Vezina, K., Bonn, F., Cu, P.V., 2006. Agricultural land-use patterns and soil erosion vulnerability of watershed units in Vietnam's northern highlands. *Landscape Ecology* 21(8), 1311–1325. <https://doi.org/10.1007/s10980-006-0023-x>.
- Vu, M.T., Raghavan, S.V., Pham, D.M., Liong, S.Y., 2015a. Investigating drought over the Central Highland, Vietnam, using regional climate models. *Journal of Hydrology* 526, 265–273. <https://doi.org/10.1016/j.jhydrol.2014.11.006>.
- Vu, M.T., Raghavan, V.S., Liong, S.Y., 2015b. Ensemble Climate Projection for Hydro-Meteorological Drought over a river basin in Central Highland, Vietnam. *KSCE Journal of Civil Engineering* 19(2), 427–433. <https://doi.org/10.1007/s12205-015-0506-x>.
- Vu, M.T., Vo, N.D., Gourbesville, P., Raghavan, S.V., Liong, S.Y., 2017. Hydro-meteorological drought assessment under climate change impact over the Vu Gia–Thu Bon river basin, Vietnam. *Hydrological Sciences Journal* 62(10), 1654–1668. <https://doi.org/10.1080/02626667.2017.1346374>.
- Wagner, P.D., Bhallamudi, S.M., Narasimhan, B., Kumar, S., Fohrer, N., Fiener, P., 2019. Comparing the effects of dynamic versus static representations of land use change in hydrologic impact assessments. *Environmental Modelling and Software* 122, 1–9. <https://doi.org/10.1016/j.envsoft.2017.06.023>.
- Wang, Q., Liu, R., Jiao, L., Li, L., Wang, Y., Cao, L., 2022. Significance of using dynamic land-use data and its threshold in hydrology and water quality simulation models. *Environmental Monitoring and Assessment* 194(2). <https://doi.org/10.1007/s10661-022-09761-8>.
- Wang, Q., Liu, R., Men, C., Guo, L., Miao, Y., 2018. Effects of dynamic land use inputs on improvement of SWAT model performance and uncertainty analysis of outputs. *Journal of Hydrology* 563, 874–886. <https://doi.org/10.1016/j.jhydrol.2018.06.063>.
- World Meteorological Organization and Global Water Partnership (WMO and GWP), 2016. Handbook of drought indicators and indices. Integrated Drought Management Programme (IDMP). WMO, Geneva, Switzerland and GWP, Stockholm, Sweden.
- Yang, Q., Almendinger, J.E., Zhang, X., Huang, M., Chen, X., Leng, G., Zhou, Y., Zhao, K., Asrar, G.R., Srinivasan, R., Li, X., 2018. Enhancing SWAT simulation of forest ecosystems for water resource assessment: A case study in the St. Croix River basin.

- Ecological Engineering 120, 422–431. <https://doi.org/10.1016/j.ecoleng.2018.06.020>.
- Yonaba, R., Biaou, A.C., Koïta, M., Tazen, F., Mounirou, L.A., Zouré, C.O., Queloz, P., Karambiri, H., Yacouba, H., 2020. A dynamic land use/land cover input helps in picturing the Sahelian paradox: assessing variability and attribution of changes in surface runoff in a Sahelian watershed. *Science of The Total Environment* 143792. <https://doi.org/10.1016/j.scitotenv.2020.143792>.
- Zhang, Z., Sheng, L., Yang, J., Chen, X.A., Kong, L., Wagan, B., 2015. Effects of land use and slope gradient on soil erosion in a red soil hilly watershed of southern China. *Sustainability (Switzerland)* 7(10), 14309–14325. <https://doi.org/10.3390/su71014309>.
- Zhao, S., Peng, C., Jiang, H., Tian, D., Lei, X., Zhou, X., 2006. Land use change in Asia and the ecological consequences. *Ecological Research* 21(6), 890–896. <https://doi.org/10.1007/s11284-006-0048-2>.

CHAPTER 3

- Barbosa, P., Masante, D., Arias, M.C., Cammalleri, C., de Jager, A., Magni, D., Mazzeschi, M., McCormick, N., Naumann, G., Spinoni, J., Vogt, J., 2020. Drought in mainland Southeast Asia. JRC Global Drought Observatory (GDO) and ERCC Analytical Team. Analytical report, 10 pages.
- Brouziyne, Y., Abouabdillah, A., Chehbouni, A., Hanich, L., Bergaoui, K., McDonnell, R., Benaabidate, L., 2020. Assessing hydrological vulnerability to future droughts in a Mediterranean watershed: Combined indices-based and distributed modeling approaches. *Water (Switzerland)* 12(9). <https://doi.org/10.3390/W12092333>.
- CGIAR Research Program on Climate Change, Agriculture and Food Security - Southeast Asia (CCAFS-SEA), 2016. Assessment Report: The drought crisis in the Central Highlands of Vietnam. CGIAR Research Program on Climate Change, Agriculture and Food Security (CCAFS), Hanoi, Vietnam.
- Directorate of Water Resources (WRD), 2016. Drought in the Central Highlands of Vietnam. Assessment report, Hanoi City, Vietnam.
- Food and Agriculture Organization (FAO), 2014. Understanding the drought impact agricultural areas: on the global of El Niño: An assessment using FAO's Agricultural Stress Index (ASI). FAO, Rome, Italy, 52 pages.
- General Statistics Office of Vietnam (GSO), 2021. Rice productivity in Kon Tum province. <https://www.gso.gov.vn/en/agriculture-forestry-and-fishery/> (accessed March 1, 2021)
- Gia Lai provincial Department of Agriculture and Rural Development (GLDARD), 2016.

- The drought situation in Gia Lai province. Assessment report, Gia Lai, Vietnam, 4 pages.
- Gia Lai provincial Department of Agriculture and Rural Development (GLDARD), 2019. Management and exploitation of irrigation systems in Gia Lai provinces. Assessment report, Gia Lai, Vietnam, 3 pages.
- Grosjean, G., Monteils, F., Hamilton, S.D., Blaustein-Rejto, D., Gatto, M., Talsma, T., Bourgoin, C., Sebastian, L.S., Catacutan, D., Mulia, R., Bui, Y., Tran, D.N., Nguyen, K.G., Pham, M.T., Lan, L.N., Läderach, P., 2016. Increasing resilience to droughts in Viet Nam: The role of forests, agroforestry, and climate smart agriculture. CCAFS-CIAT-UN-REDD Position Paper, Hanoi, Vietnam, 10 pages.
- Hao, Z., AghaKouchak, A., 2013. Multivariate Standardized Drought Index: A parametric multi-index model. *Advances in Water Resources* 57, 12–18. <https://doi.org/10.1016/j.advwatres.2013.03.009>.
- Kamali, B., Kouchi, D.H., Yang, H., Abbaspour, K.C., 2017. Multilevel drought hazard assessment under climate change scenarios in semi-arid regions-a case study of the karkheh river basin in Iran. *Water (Switzerland)* 9(4). <https://doi.org/10.3390/w9040241>
- Kon Tum provincial Department of Agriculture and Rural Development (KTDARD), 2018. Report on dam and reservoir safety in Kon Tum province. Assessment report, Kon Tum, Vietnam, 4 pages.
- Kon Tum General Statistics Office (KTGSO), 2016. Socio-economic situation of Kon Tum province in 2016. Assessment report, Kon Tum, Vietnam, 23 pages.
- Kon Tum People's Committee, 2019. Drought plan in the dry season of the 2019-2020 year in Kon Tum province. Decision number 3297/KH-UBND, Kon Tum, Vietnam, 7 pages.
- Kon Tum People's Committee, 2020. Project on drought management in Kon Tum province during a 2021 – 2030 period. Decision number 1167/QĐ-UBND, Kon Tum, Vietnam, 2 pages.
- Li, Z., Liu, W.Z., Zhang, X.Z., Zheng, F.L., 2009. Impacts of land use change and climate variability on hydrology in an agricultural catchment on the Loess Plateau of China. *Journal of Hydrology* 377(1–2), 35–42. <https://doi.org/10.1016/j.jhydrol.2009.08.007>.
- Lweendo, M.K., Lu, B., Wang, M., Zhang, H., Xu, W., 2017. Characterization of droughts in humid subtropical region, Upper Kafue river basin (Southern Africa). *Water (Switzerland)* 9(4), 242. <https://doi.org/10.3390/w9040242>.
- McKee, T.B., Doesken, N.J., Kleist, J., 1993. The relationship of drought frequency and duration to time scales. *Proceedings of Eighth Conference on Applied Climatology* January 17-22. Anaheim, California, 179-184.

- Moriasi, D.N., Gitau, M.W., Pai, N., Daggupati, P., 2015. Hydrologic and water quality models: Performance measures and evaluation criteria. *Transactions of the American Society of Agricultural and Biological Engineers* 58(6), 1763–1785. <https://doi.org/10.13031/trans.58.10715>.
- Nalbantis, I., Tsakiris, G., 2009. Assessment of hydrological drought revisited. *Water Resources Management* 23(5), 881–897. <https://doi.org/10.1007/s11269-008-9305-1>.
- NASA and Japan ASTER Program, 2009. ASTER Global Digital Elevation Model (GDEM). <https://asterweb.jpl.nasa.gov/gdem.asp> (accessed June 10, 2020)
- Nash, J.E., Sutcliffe, J.V., 1970. River flow forecasting through conceptual models. Part I - A discussion of principles. *Journal of Hydrology* 10(3), 282–290.
- Nga, L.T.T., Giang, N.T., Dung, B.Q., 2019. investigation of selecting drought index for agricultural drought rezoning in Gia Lai province. *Vietnam Journal of Hydrometeorology* 2019(2–1), 29–36. [https://doi.org/10.36335/vnjhm.2019\(2-1\).29-36](https://doi.org/10.36335/vnjhm.2019(2-1).29-36).
- Phong, N.B., Chinh, D.K., 2017. A study on the influence of ENSO upon tropical cyclones action over East Sea of Vietnam for period of 2000-2015. *Vietnam Journal of Hydrometeorology*, 8, 41–49.
- Saeid, E., Faezeh, E., 2017. *Handbook of drought and water scarcity: Principles of drought and water scarcity*. Saeid, E., Faezeh, E. (eds). CRC Press, New York, US.
- Sam, T.T., Khoi, D.N., Thao, N.T.T., Nhi, P.T.T., Quan, N.T., Hoan, N.X., Tinh, N.V., 2019. Impact of climate change on meteorological, hydrological and agricultural droughts in the Lower Mekong River Basin: A case study of the Srepok Basin, Vietnam. 33, 547–559. *Water and Environment Journal*. <https://doi.org/10.1111/wej.12424>.
- Santhi, C., Arnold, J.G., Williams, J.R., Dugas, W.A., Srinivasan, R., Hauck, L.M., 2001. Validation of the SWAT model on a large river basin with point and nonpoint sources. *Journal of the American Water Resources Association* 37(5), 1169–1188.
- Sehgal, V., Sridhar, V., 2019. Watershed-scale retrospective drought analysis and seasonal forecasting using multi-layer, high-resolution simulated soil moisture for Southeastern U.S. *Weather and Climate Extremes* 23, 100191. <https://doi.org/10.1016/j.wace.2018.100191>.
- Shukla, S., Wood, A.W., 2008. Use of a standardized runoff index for characterizing hydrologic drought. *Geophysical Research Letters* 35(2), 1–7. <https://doi.org/10.1029/2007GL032487>.

- Somura, H., Arnold, J., Hoffman, D., Takeda, I., Mori, Y., Di Luzio, M., 2009. Impact of climate change on the Hii River basin and salinity in Lake Shinji: A case study using the SWAT model and a regression curve. *Hydrological Processes*, 23, 1887–1900. <https://doi.org/10.1002/hyp>.
- The Economic and Social Commission for Asia and the Pacific and The Association of Southeast Asian Nations (ESCAP and ASEAN), 2020. Ready for the dry years: Building resilience to drought in South-east Asia. In United Nations. <https://doi.org/10.18356/adcafl1d0-en>.
- Thom, H.S.C., 1958. A note on the Gamma distribution. *Monthly Weather Review* 86(4), 117–122. <https://doi.org/10.1126/science.12.306.731-a>.
- Vietnam Academy for Water Resources (VAWR), 2012. Irrigation planning Kon Tum during a period from 2011 to 2020 and orientation to 2025. Hanoi, Vietnam.
- Veettil, A.V., Mishra, A.K., 2020. Multiscale hydrological drought analysis: Role of climate, catchment and morphological variables and associated thresholds. *Journal of Hydrology* 582, 124533. <https://doi.org/10.1016/j.jhydrol.2019.124533>.
- Vu, M.T., Raghavan, S.V., Pham, D.M., Liong, S.Y., 2015a. Investigating drought over the Central Highland, Vietnam, using regional climate models. *Journal of Hydrology* 526, 265–273. <https://doi.org/10.1016/j.jhydrol.2014.11.006>.
- Vu, M.T., Raghavan, V.S., Liong, S.Y., 2015b. Ensemble Climate Projection for Hydro-Meteorological Drought over a river basin in Central Highland, Vietnam. *KSCE Journal of Civil Engineering* 19(2), 427–433. <https://doi.org/10.1007/s12205-015-0506-x>.
- Williams, R.S., Jitendra, P.S., Mark, R., James, T., Leocardio, S., 2019. Striking a Balance: Managing El Niño and La Niña in Vietnam’s Agriculture. World Bank, Report number 132068, Washington, DC. <https://doi.org/10.1016/j.prrro.2015.02.016>.
- World Meteorological Organization (WMO), Global Water Partnership (GWP), 2016. Handbook of drought indicators and indices. Integrated Drought Management Programme (IDMP). WMO, Geneva, Switzerland and GWP, Stockholm, Sweden.
- Zhao, L., Lyu, A., Wu, J., Hayes, M., Tang, Z., He, B., Liu, J., Liu, M., 2014. Impact of meteorological drought on streamflow drought in Jinghe River Basin of China. *Chinese Geographical Science* 24(6), 694–705. <https://doi.org/10.1007/s11769-014-0726-x>.

CHAPTER 4

Abbaspour, K.C., Yang, J., Maximov, I., Siber, R., Bogner, K., Mieleitner, J., Zobrist, J.,

- Srinivasan, R., 2007. Modelling hydrology and water quality in the pre-alpine/alpine Thur watershed using SWAT. *Journal of Hydrology* 333(2–4), 413–430. <https://doi.org/10.1016/j.jhydrol.2006.09.014>.
- Aflizar, Saidi, A., Husnain, Indra, R., Darmawan, Harmailis, Somura, H., Wakatsuki, T., Masunaga, T., 2010. Soil erosion characterization in an agricultural watershed in West Sumatra, Indonesia. *Tropics* 19(1), 29–42. <https://doi.org/10.3759/tropics.19.29>.
- Aghsaei, H., Dinan, N.M., Moridi, A., Asadolahi, Z., Delavar, M., Fohrer, N., Wagner, P.D., 2020. Effects of dynamic land use/land cover change on water resources and sediment yield in the Anzali wetland catchment, Gilan, Iran. *Science of the Total Environment* 712, 1–11. <https://doi.org/10.1016/j.scitotenv.2019.136449>.
- Anand, J., Gosain, A.K., Khosa, R., 2018. Prediction of land use changes based on Land Change Modeler and attribution of changes in the water balance of Ganga basin to land use change using the SWAT model. *Science of the Total Environment* 644, 503–519. <https://doi.org/10.1016/j.scitotenv.2018.07.017>.
- Arnold, J.G., Srinivasan, R., Muttiah, R.S., Williams, J.R., 1998. Large area hydrologic modeling and assessment. Part I: Model development. *Journal of the American Water Resources Association* 34(1), 73–89.
- Awotwi, A., Anornu, G.K., Quaye-Ballard, J.A., Annor, T., Forkuo, E.K., Harris, E., Agyekum, J., Terlabie, J.L., 2019. Water balance responses to land-use/land-cover changes in the Pra River Basin of Ghana, 1986–2025. *Catena* 182, 104129. <https://doi.org/10.1016/j.catena.2019.104129>.
- Bao, N.T., Pryor, T.L., 1997. The relationship between global solar radiation and sunshine duration in Vietnam. *Renewable Energy* 11(1), 47–60.
- Bieger, K., Hörmann, G., Fohrer, N., 2015. Detailed spatial analysis of SWAT-simulated surface runoff and sediment yield in a mountainous watershed in China. *Hydrological Sciences Journal* 60(5), 784–800. <https://doi.org/10.1080/02626667.2014.965172>.
- Chandra, P., Patel, P.L., Porey, P.D., Gupta, I.D., 2014. Estimation of sediment yield using SWAT model for Upper Tapi basin. *ISH Journal of Hydraulic Engineering* 20(3), 291–300. <https://doi.org/10.1080/09715010.2014.902170>.
- Cho, J., Bosch, D., Lowrance, R., Strickland, T., Vellidis, G., 2009. Effect of spatial distribution of rainfall on temporal and spatial uncertainty of SWAT output. *Transactions of the American Society of Agricultural and Biological Engineers* 52(5), 1545–1555. <https://doi.org/10.13031/2013.29143>.
- Dunning, C.M., Black, E., Allan, R.P., 2018. Later wet seasons with more intense rainfall

- over Africa under future climate change. *Journal of Climate* 31(23), 9719–9738. <https://doi.org/10.1175/JCLI-D-18-0102.1>
- Gia Lai provincial People's Council, 2015. Rubber trees development under the rubber development project in Gia Lai province from 2008 to present. Assessment report, Gia Lai province, Vietnam, 9 pages (in Vietnamese).
- Gupta, H.V., Sorooshian, S., Yapo, P.O., 1999. Status of automatic calibration for hydrologic models: Comparison with multilevel expert calibration. *Journal of Hydrologic and Engineering* 4(2), 135–143.
- Hallouz, F., Meddi, M., Mahé, G., Alirahmani, S., Keddar, A., 2018. Modeling of discharge and sediment transport through the SWAT model in the basin of Harraza (Northwest of Algeria). *Water Science* 32(1), 79–88. <https://doi.org/10.1016/j.wsj.2017.12.004>.
- Hussain, F., Nabi, G., Wu, R.S., Hussain, B., Abbas, T., 2019. Parameter evaluation for soil erosion estimation on small watersheds using SWAT model. *International Journal of Agricultural and Biological Engineering* 12(1), 96–108. <https://doi.org/10.25165/j.ijabe.20191201.3769>
- Khoi, D.N., Suetsugi, T., 2014. The responses of hydrological processes and sediment yield to land-use and climate change in the Be River Catchment, Vietnam. *Hydrological Processes* 28(3), 640–652. <https://doi.org/10.1002/hyp.9620>.
- Kon Tum provincial People's Committee, 2016. The status of forest in Kon Tum province. Decision number 637/QĐ-UBND, Kon Tum province, Vietnam, 9 pages (in Vietnamese).
- Li, M., Shi, X., Shen, Z., Yang, E., Bao, H., Ni, Y., 2019. Effect of hillslope aspect on landform characteristics and erosion rates. *Environmental Monitoring and Assessment* 191, 598. <https://doi.org/10.1007/s10661-019-7760-1>
- Li, Y., Chang, J., Luo, L., Wang, Y., Guo, A., Ma, F., Fan, J., 2019. Spatiotemporal impacts of land use land cover changes on hydrology from the mechanism perspective using SWAT model with time-varying parameters. *Hydrology Research* 50(1), 244–261. <https://doi.org/10.2166/nh.2018.006>.
- Li, Z., Liu, W.Z., Zhang, X.Z., Zheng, F.L., 2009. Impacts of land use change and climate variability on hydrology in an agricultural catchment on the Loess Plateau of China. *Journal of Hydrology* 377(1–2), 35–42. <https://doi.org/10.1016/j.jhydrol.2009.08.007>.
- Makhtoumi, Y., Li, S., Ibeanusi, V., Chen, G., 2020. Evaluating water balance variables under land use and climate projections in the upper Choctawhatchee river watershed, in Southeast US. *Water (Switzerland)* 12, 2205. <https://doi.org/10.3390/w12082205>.

- Marhaento, H., Booij, M.J., Rientjes, T.H.M., Hoekstra, A.Y., 2019. Sensitivity of streamflow characteristics to different spatial land-use configurations in tropical catchment. *Journal of Water Resources Planning and Management* 145(12), 04019054. [https://doi.org/10.1061/\(ASCE\)WR.1943-5452.0001122](https://doi.org/10.1061/(ASCE)WR.1943-5452.0001122).
- Martinelli, M., Machado, E.H., 2014. Static and dynamic maps, developed from an analytical or synthesis reasoning, in school geographic atlas: The methodological feasibility. *Revista Brasileira de Cartografi* 66(7), 899–920.
- Mengistu, A.G., van Rensburg, L.D., Woyessa, Y.E., 2019. Techniques for calibration and validation of SWAT model in data scarce arid and semi-arid catchments in South Africa. *Journal of Hydrology: Regional Studies*, 25, 100621. <https://doi.org/10.1016/j.ejrh.2019.100621>.
- Ministry of Agriculture and Rural Development (MARD), 2009. The criteria for the identification and classification of forests. Circular number 34/2009/TT-BNNPTNT, Hanoi city, Vietnam, 5 pages (in Vietnamese).
- Ministry of Agriculture and Rural Development (MARD), 2018. Crop conversion for the inefficient rubber areas. Decision number 5683/VPCP-NN, Hanoi City, Vietnam (in Vietnamese).
- Ministry of Agriculture and Rural Development (MARD), 2019. The sustainable forestry development strategies for the period 2021-2030, and a vision to 2050. Assessment report, Hanoi city, Vietnam, 149 pages (in Vietnamese).
- Moriasi, D.N., Gitau, M.W., Pai, N., Daggupati, P., 2015. Hydrologic and water quality models: Performance measures and evaluation criteria. *Transactions of the American Society of Agricultural and Biological Engineers* 58(6), 1763–1785. <https://doi.org/10.13031/trans.58.10715>.
- Moriasi, D.N., Pai, N., Steiner, J.L., Gowda, P.H., Winchell, M., Rathjens, H., Starks, P. J., Verser, J.A., 2019. SWAT-LUT: A desktop graphical user interface for updating land use in SWAT. *Journal of the American Water Resources Association* 55(5), 1102–1115. <https://doi.org/10.1111/1752-1688.12789>.
- Mosbahi, M., Benabdallah, S., Boussema, M.R., 2013. Assessment of soil erosion risk using SWAT model. *Arabian Journal of Geosciences* 6(10), 4011–4019. <https://doi.org/10.1007/s12517-012-0658-7>
- Munoth, P., Goyal, R., 2020. Impacts of land use land cover change on runoff and sediment yield of Upper Tapi River Sub-Basin, India. *International Journal of River Basin*

- Management 18(2), 177–189. <https://doi.org/10.1080/15715124.2019.1613413>.
- NASA and Japan ASTER Program, 2009. ASTER Global Digital Elevation Model (GDEM). <https://asterweb.jpl.nasa.gov/gdem.asp> (accessed June 10, 2020)
- Nash, J.E., Sutcliffe, J.V., 1970. River flow forecasting through conceptual models. Part I - A discussion of principles. *Journal of Hydrology* 10(3), 282–290.
- National Assembly of Vietnam, 2013. Land law. Hanoi City, Vietnam, 124 pages.
- Nontananandh, S., Changnoi, B., 2012. Internet GIS, based on USLE modeling, for assessment of soil erosion in Songkhram watershed, Northeastern of Thailand. *Kasetsart Journal - Natural Science* 46(2), 272–282.
- Oeurng, C., Sauvage, S., Sánchez-Pérez, J.M., 2011. Assessment of hydrology, sediment and particulate organic carbon yield in a large agricultural catchment using the SWAT model. *Journal of Hydrology* 401(3–4), 145–153. <https://doi.org/10.1016/j.jhydrol.2011.02.017>.
- Pai, N., Saraswat, D., 2011. SWAT2009_LUC: A tool to activate the land use change module in SWAT 2009. *Transactions of the American Society of Agricultural and Biological Engineers* 54(5), 1649–1658.
- Phomcha, P., Wirojanagud, P., Vangpaisal, T., Thaveevouthti, T., 2011. Predicting sediment discharge in an agricultural watershed: A case study of the Lam Sonthi watershed, Thailand. *ScienceAsia* 37(1), 43–50. <https://doi.org/10.2306/scienceasia1513-1874.2011.37.043>.
- Prime Minister, 2009. The rubber development planning up to 2015 and vision to 2020. Hanoi City, Vietnam, 6 pages (in Vietnamese).
- Prime Minister, 2018. Project for forest protection, restoration and sustainable development in the Central Highlands from 2016 to 2030. Decision number 297/QĐ-TTg, Hanoi city, Vietnam, 6 pages (in Vietnamese).
- R Core Team, 2016. R: A language and environment for statistical computing. R Foundation for Statistical Computing. Vienna, Austria.
- Rostamian, R., Jaleh, A., Afyuni, M., Mousavi, S.F., Heidarpour, M., Jalalian, A., Abbaspour, K.C., 2008. Application of a SWAT model for estimating runoff and sediment in two mountainous basins in Central Iran. *Hydrological Sciences Journal* 53(5), 977–988. <http://dx.doi.org/10.1623/hysj.53.5.977>.
- Saleh, A., Arnold, J.G., Gassman, P.W., Hauck, L.M., Rosenthal, W.D., Williams, J.R., McFarland, A.M.S., 2000. Application of SWAT for the Upper North Bosque River Watershed. *Transactions of the American Society of Agricultural and Biological Engineers* 43(5), 1077–1087. <https://doi.org/10.13031/2013.3000>

- Santhi, C., Arnold, J.G., Williams, J.R., Dugas, W.A., Srinivasan, R., Hauck, L.M., 2001. Validation of the SWAT model on a large river basin with point and nonpoint sources. *Journal of the American Water Resources Association* 37(5), 1169–1188.
- Seth, A., Rauscher, S.A., Biasutti, M., Giannini, A., Camargo, S.J., Rojas, M., 2013. CMIP5 projected changes in the annual cycle of precipitation in monsoon regions. *Journal of Climate* 26(19), 7328–7351. <https://doi.org/10.1175/JCLI-D-12-00726.1>.
- Somura, H., Arnold, J., Hoffman, D., Takeda, I., Mori, Y., Di Luzio, M., 2009. Impact of climate change on the Hii River basin and salinity in Lake Shinji: A case study using the SWAT model and a regression curve. *Hydrological Processes*, 23, 1887–1900. <https://doi.org/10.1002/hyp>.
- Somura, H., Kunii, H., Yone, Y., Takeda, I., Sato, H., 2018. Importance of considering nutrient loadings from small watersheds to a lake – A case study of the Lake Shinji watershed, Shimane Prefecture, Japan. *International Journal of Agricultural and Biological Engineering* 11(5), 124–130. <https://doi.org/10.25165/j.ijabe.20181105.4351>.
- Somura, H., Takeda, I., Arnold, J.G., Mori, Y., Jeong, J., Kannan, N., Hoffman, D., 2012. Impact of suspended sediment and nutrient loading from land uses against water quality in the Hii river basin, Japan. *Journal of Hydrology*, 450–451, 25–35. <https://doi.org/10.1016/j.jhydrol.2012.05.032>.
- Son, N.T., Binh, N.D., Shrestha, R.P., 2015. Effect of land use change on runoff and sediment yield in Da river basin of Hoa Binh province, Northwest Vietnam. *Journal of Mountain Science* 12, 1051–1064. <https://doi.org/10.1007/s1162-013-2925-9>.
- Son, N.T., Huong, H.L., Phuong, T.T., Loc, N.D., 2020. Application of SWAT model to Assess Land Use and Climate Changes Impacts on Hydrology of Nam Rom River Basin in Vietnam. *Preprints*, 1–17. <https://doi.org/10.20944/preprints202001.0362.v1>.
- Stéphanne, N., Lambin, E.F., 2001. A dynamic simulation model of land-use changes in Sudano-sahelian countries of Africa (SALU). *Agriculture, Ecosystems and Environment*, 85, 145–161. [https://doi.org/10.1016/S0167-8809\(01\)00181-5](https://doi.org/10.1016/S0167-8809(01)00181-5).
- Tam, N.V., 2012. A Simple tool for creating txtinout files for simulating land use change with SWAT. https://github.com/tamnva/SWAT_LUC (accessed June 20 2020).
- Tibebe, D., Bewket, W., 2010. Surface runoff and soil erosion estimation using the SWAT model in the Keleta Watershed, Ethiopia. *Land Degradation and Development* 22, 551–564. <https://doi.org/10.1002/dr.1034>.
- Tingting, L.V., Xiaoyu, S., Dandan, Z., Zhenshan, X., Jianming, G., 2008. Assessment of soil erosion risk in Northern Thailand. *International Archives of the Photogrammetry*,

- Remote Sensing and Spatial Information Sciences XXXVII, 703–708.
- Tram, V.N. , Liem, N.D., Loi, N.K., 2019. Simulating surface flow and baseflow in Poko catchment, Kon Tum province, Vietnam. *Journal of Water and Climate Change* 10(3), 494–503. <https://doi.org/10.2166/wcc.2018.185>.
- Tripathi, M.P., Panda, R.K., Raghuvanshi, N.S., 2003. Identification and prioritisation of critical sub-watersheds for soil conservation management using the SWAT model. *Biosystems Engineering* 85(3), 365–379.
- Vietnam Academy for Water Resources (VAWR), 2012. Irrigation planning Kon Tum during a period from 2011 to 2020 and orientation to 2025. Hanoi, Vietnam.
- Wagner, P.D., Bhallamudi, S.M., Narasimhan, B., Kumar, S., Fohrer, N., Fiener, P., 2019. Comparing the effects of dynamic versus static representations of land use change in hydrologic impact assessments. *Environmental Modelling and Software* 122, 1–9. <https://doi.org/10.1016/j.envsoft.2017.06.023>.
- Wang, Q., Liu, R., Men, C., Guo, L., Miao, Y., 2018. Effects of dynamic land use inputs on improvement of SWAT model performance and uncertainty analysis of outputs. *Journal of Hydrology* 563, 874–886. <https://doi.org/10.1016/j.jhydrol.2018.06.063>.
- Wang, Y., Chen, X., Chen, Y., Liu, M., Gao, L., 2017. Flood/drought event identification using an effective indicator based on the correlations between multiple time scales of the Standardized Precipitation Index and river discharge. *Theoretical and Applied Climatology* 128(1–2), 159–168. <https://doi.org/10.1007/s00704-015-1699-0>.
- Williams, J.R., 1975. Sediment routing for agricultural watersheds. *JAWRA Journal of the American Water Resources Association* 11(5), 965–974. <https://doi.org/10.1111/j.1752-1688.1975.tb01817.x>.
- Yuan, L., Forshay, K.J., 2020. Using SWAT to evaluate streamflow and lake sediment loading in the Xinjiang river basin with limited data. *Water (Switzerland)* 12(1). <https://doi.org/10.3390/w12010039>
- Yustika, R.D., Somura, H., Yuwono, S.B., Arisin, B., Ismono, H., Masunaga, T., 2019. Assessment of soil erosion in social forest-dominated watersheds in Lampung, Indonesia. *Environmental Monitoring and Assessment* 191, 726. <https://doi.org/10.1007/s10661-019-7890-5>.
- Zettam, A., Taleb, A., Sauvage, S., Boithias, L., Belaidi, N., Sánchez-Pérez, J.M., 2017. Modelling hydrology and sediment transport in a semi-arid and anthropized catchment using the SWAT model: The case of the Tafna River (Northwest Algeria). *Water (Switzerland)* 9(3), 216. <https://doi.org/10.3390/w9030216>.

Zhang, H., Li, H., Chen, Z., 2011. Analysis of land use dynamic change and its impact on the water environment in Yunnan plateau lake area - A case study of the Dianchi Lake drainage area. *Procedia Environmental Sciences* 10, 2709–2717. <https://doi.org/10.1016/j.proenv.2011.09.421>

CHAPTER 5

Abbaspour, K.C., Rouholahnejad, E., Vaghefi, S., Srinivasan, R., Yang, H., Kløve, B., 2015. A continental-scale hydrology and water quality model for Europe: Calibration and uncertainty of a high-resolution large-scale SWAT model. *Journal of Hydrology* 524, 733–752. <https://doi.org/10.1016/j.jhydrol.2015.03.027>.

Aghsaei, H., Dinan, N.M., Moridi, A., Asadolahi, Z., Delavar, M., Fohrer, N., Wagner, P.D., 2020. Effects of dynamic land use/land cover change on water resources and sediment yield in the Anzali wetland catchment, Gilan, Iran. *Science of the Total Environment* 712, 1–11. <https://doi.org/10.1016/j.scitotenv.2019.136449>.

Alexander, R.B., Smith, R.A., Schwarz, G.E., Boyer, E.W., Nolan, J.V., Brakebill, J.W., 2008. Differences in phosphorus and nitrogen delivery to the Gulf of Mexico from the Mississippi River Basin. *Environmental Science and Technology* 42(3), 822–830. <https://doi.org/10.1021/es0716103>.

Arabi, M., Frankenberger, J.R., Engel, B.A., Arnold, J.G., 2007. Representation of agricultural conservation practices with SWAT. *Hydrological Processes* 22, 3042–3055. <https://doi.org/10.1002/hyp.6890>.

Baffaut, C., Benson, V.W., 2009. Modeling Flow and Pollutant Transport in a Karst Watershed with SWAT. *Transactions of the American Society of Agricultural and Biological Engineers* 52(2), 469–479. <https://doi.org/10.13031/2013.26840>.

Brito, D., Neves, R., Branco, M.A., Prazeres, Â., Rodrigues, S., Gonçalves, M.C., Ramos, T.B., 2019. Assessing water and nutrient long-term dynamics and loads in the Enxoé temporary river basin (Southeast Portugal). *Water (Switzerland)* 11(2), 354. <https://doi.org/10.3390/w11020354>.

Carpenter, S.R., Bolgrien, D., Lathrop, R.C., Stow, C.A., Reed, T., Wilson, M.A., 1998. Ecological and economic analysis of lake eutrophication by nonpoint pollution. *Australian Journal of Ecology* 23(1), 68–79. <https://doi.org/10.1111/j.1442-9993.1998.tb00706.x>.

Cho, J., Bosch, D., Lowrance, R., Strickland, T., Vellidis, G., 2009. Effect of spatial distribution of rainfall on temporal and spatial uncertainty of SWAT output. *Transactions*

- of the American Society of Agricultural and Biological Engineers 52(5), 1545–1555. <https://doi.org/10.13031/2013.29143>.
- Chu, T.W., Shirmohammadi, A., Montas, H., Sadeghi, A., 2004. Evaluation of the SWAT model's sediment and nutrient components in the piedmont physiographic region of Maryland. *Transactions of the American Society of Agricultural Engineers* 47(5), 1523–1538. <https://doi.org/10.13031/2013.17632>.
- Cuceoglu, G., Seker, D.Z., Tanik, A., Ozturk, I., 2021. Analyzing effects of two different land use datasets on hydrological simulations by using SWAT model. *International Journal of Environment and Geoinformatics* 8(2), 172–185.
- Donmez, C., Sari, O., Berberoglu, S., Cilek, A., Satir, O., Volk, M., 2020. Improving the applicability of the swat model to simulate flow and nitrate dynamics in a flat data-scarce agricultural region in the Mediterranean. *Water (Switzerland)* 12(12), 3479. <https://doi.org/10.3390/w12123479>.
- Epelde, A.M., Cerro, I., Sánchez-Pérez, J.M., Sauvage, S., Srinivasan, R., Antigüedad, I., 2015. Application of the SWAT model to assess the impact of changes in agricultural management practices on water quality. *Hydrological Sciences Journal* 60(5), 825–843. <https://doi.org/10.1080/02626667.2014.967692>.
- Folliott, P., Brooks, K., Neary, D., Roberto, T., Chevesich, P., 2013. Soil erosion and sediment production on watershed landscapes: Processes and control. UNESCO Special Technical Publication No. 32. Montevideo, Uruguay: UNESCO, International Hydrological Programme, Regional Office for Science for Latin American and the Caribbean.
- Food and Agriculture Organization - United Nations Educational, Scientific and Cultural Organization (FAO-UNESCO). 2007. Digital Soil Map of the World. <http://www.fao.org/soils-portal/data-hub/soil-maps-and-databases/en/> (accessed 10 June 2020).
- Frohlich, H.L., Schreinemachers, P., Stahr, K., Clemens, G., 2013. Sustainable Land Use and Rural Development in Southeast Asia: Innovations and Policies for Mountainous Areas. Springer Environmental Science and Engineering. Springer Berlin, Heidelberg. <https://doi.org/10.1007/978-3-642-33377-4>.
- Fullen, M.A., Booth, C.A., Panomtaranichagul, M., Subedi, M., Mei, Y.L., 2011. Agro-environmental lessons from the “Sustainable highland agriculture in South-east Asia” (SHASEA) project. *Journal of Environmental Engineering and Landscape Management* 19(1), 101–113. <https://doi.org/10.3846/16486897.2011.557476>.

- Gholami, A., Habibnejad Roshan, M., Shahedi, K., Vafakhah, M., and Solaymani, K., 2016. Hydrological stream flow modeling in the Talar catchment (central section of the Alborz Mountains, north of Iran): Parameterization and uncertainty analysis using SWAT-CUP. *Journal of Water and Land Development* 30(1), 57–69. <https://doi.org/10.1515/jwld-2016-0022>.
- Gia Lai Provincial People’s Council, 2015. Rubber trees development under the rubber development project in Gia Lai province from 2008 to present. Assessment report, Gia Lai province, Vietnam, 9 pages (in Vietnamese).
- Githui, F., Mutua, F., Bauwens, W., 2009. Estimating the impacts of land-cover change on runoff using the soil and water assessment tool (SWAT): Case study of Nzoia catchment, Kenya. *Hydrological Sciences Journal* 54(5), 899–908. <https://doi.org/10.1623/hysj.54.5.899>.
- Hanief, A., Laursen, A.E., 2017. SWAT modeling of hydrology, sediment and nutrients from the grand river, Ontario. *Water Quality Research Journal* 52(4), 243–257. <https://doi.org/10.2166/wqrj.2017.014>.
- Holden, J., Haygarth, P., MacDonald, J., Jenkins, A., Spaiets, A., Orr, H., Dunn, N., Harris, B., Pearson, P., McGonigle, D., Humble, A., Ross, M., Harris, J., Meacham, T., Benton, T., Staines, A., Noble, A., 2015. Farming and water 1: Agriculture’s impacts on water quality. *Global Food Security*.
- Hong, T., Hue, T.T.M., Tri, P.C., Phuc, V.N., Ngoc, N.Q., Uyen, D.T.L., 2013. Basin profile of the upper Sesan River in Vietnam. Project report: Challenge Program on Water & Food Mekong project MK3 “Optimizing the management of a cascade of reservoirs at the catchment level”. ICEM – International Centre for Environmental Management, Hanoi, Vietnam.
- Huang, Z., Xue, B., Pang, Y., 2009. Simulation on stream flow and nutrient loadings in Gucheng lake, Low Yangtze river basin, based on SWAT model. *Quaternary International* 208, 109–115. <https://doi.org/10.1016/j.quaint.2008.12.018>.
- Jha, M.K., Gassman, P.W., Arnold, J.G., 2007. Water quality modeling for the Raccoon river watershed using SWAT. *Transactions of the American Society of Agricultural Engineers* 50(2), 479–493. <https://doi.org/10.13031/2013.22660>.
- JICA, 2018. Final report: Data collection survey on water resources management in Central Highlands. Japan International Cooperation Agency, Nippon Koei Co., Ltd.

- Keraga, A.S., Kiflie, Z., Engida, A.N., 2019. Evaluation of SWAT performance in modeling nutrients of Awash River basin, Ethiopia. *Modeling Earth Systems and Environment* 5(1), 275–289. <https://doi.org/10.1007/s40808-018-0533-y>.
- Khoi, D.N., Nguyen, V.T., Sam, T.T., Nhi, P.T.T., 2019. Evaluation on effects of climate and land-use changes on streamflow and water quality in the La Buong river basin, Southern Vietnam. *Sustainability (Switzerland)* 11(24). <https://doi.org/10.3390/SU11247221>.
- Khoi, D.N., Thom, V.T., 2015. Impacts of climate variability and land-use change on hydrology in the period 1981-2009 in the Central Highlands of Vietnam. *Global Nest Journal* 17(4), 870–881. <https://doi.org/10.30955/gnj.001706>
- Kim, K.B., Kwon, H-H., Han, D., 2017. Exploration of warm-up period in conceptual hydrological modelling. *Journal of Hydrology* 556, 194–210. <https://doi.org/10.1016/j.jhydrol.2017.11.015>.
- Kon Tum Provincial Department of Natural Resource and Environment (KTDONRE), 2016. Report of environmental monitoring results in 2016. Assessment report, Kon Tum province, Vietnam, 130 pages (in Vietnamese).
- Kon Tum Provincial Department of Natural Resource and Environment (KTDONRE), 2017. Report of environmental monitoring results in 2017. Assessment report, Kon Tum province, Vietnam, 166 pages (in Vietnamese).
- Kon Tum Provincial Department of Natural Resource and Environment (KTDONRE), 2019. Report of environmental monitoring results in 2019. Assessment report, Kon Tum province, Vietnam, 156 pages (in Vietnamese).
- Kon Tum Provincial People’s Committee, 2016. The status of forest in Kon Tum province. Decision number 637/QĐ-UBND, Kon Tum province, Vietnam, 9 pages (in Vietnamese).
- Kon Tum Provincial People’s Committee, 2018. Report on environmental protection in 2018. Assessment report number 239/BC-UBND, Kon Tum province, Vietnam, 40 pages (in Vietnamese).
- Kon Tum Provincial People’s Committee, 2019. Technical and economic norms of plant and livestock in Kon Tum province. Decision number 31/2019/QĐ-UBND, Kon Tum province, Vietnam, 139 pages (in Vietnamese).
- Li, Y., Chang, J., Luo, L., Wang, Y., Guo, A., Ma, F., Fan, J., 2019. Spatiotemporal impacts of land use land cover changes on hydrology from the mechanism perspective using SWAT model with time-varying parameters. *Hydrology Research* 50(1), 244–261. <https://doi.org/10.2166/nh.2018.006>.

- Lin, C., Ma, R., He, B., 2016. Identifying watershed regions sensitive to soil erosion and contributing to lake eutrophication — A case study in the Taihu lake basin (China). *International Journal of Environmental Research and Public Health*, 13(1), 77. <https://doi.org/10.3390/ijerph13010077>.
- Malagó, A., Bouraoui, F., Vigiak, O., Grizzetti, B., Pastori, M., 2017. Modelling water and nutrient fluxes in the Danube river basin with SWAT. *Science of the Total Environment* 603–604, 196–218. <https://doi.org/10.1016/j.scitotenv.2017.05.242>.
- Mateo-Sagasta, J., Marjani, S., Turrall, H., Burke, J., 2017. Water pollution from agriculture: a global review - Executive summary. Food and Agriculture Organization of the United Nations (FAO), Rome, Italy; International Water Management Institute (IWMI), Colombo, Sri Lanka.
- Ministry of Agriculture and Rural Development (MARD), 2009. The criteria for the identification and classification of forests. Circular number 34/2009/TT-BNNPTNT, Hanoi city, Vietnam, 5 pages (in Vietnamese).
- Ministry of Agriculture and Rural Development (MARD), 2014. Project on afforestation when changing the forest use purpose to other purposes. Decision number 829/QĐ-BNN-TCLN, Hanoi city, Vietnam, 7 pages (in Vietnamese).
- Ministry of Agriculture and Rural Development (MARD), 2019. The sustainable forestry development strategies for the period 2021-2030, and a vision to 2050. Assessment report, Hanoi city, Vietnam, 149 pages (in Vietnamese).
- Moriasi, D.N., Gitau, M.W., Pai, N., Daggupati, P., 2015. Hydrologic and water quality models: Performance measures and evaluation criteria. *Transactions of the American Society of Agricultural and Biological Engineers* 58(6), 1763–1785. <https://doi.org/10.13031/trans.58.10715>.
- Moriasi, D.N., Pai, N., Steiner, J.L., Gowda, P.H., Winchell, M., Rathjens, H., Starks, P.J., Verser, J.A., 2019. SWAT-LUT: A desktop graphical user interface for updating land use in SWAT. *Journal of the American Water Resources Association*, 55(5), 1102–1115. <https://doi.org/10.1111/1752-1688.12789>.
- NASA and Japan ASTER Program, 2009. ASTER Global Digital Elevation Model (GDEM). <https://asterweb.jpl.nasa.gov/gdem.asp> (accessed 10 June 2020).
- National Institute of Agricultural Planning and Projection. 2005. Land use maps of Vietnam. <http://www.niapp.org.vn/info/vi/dt/ban-do-dat-cac-tinh-tren-toan-quoc/54434> (accessed 10 June 2020).

- Neitsch, S.L., Arnold, J.G., Kiniry, J.R., Williams, J.R., 2011. Soil & Water Assessment Tool theoretical documentation, version 2009. Texas Water Resources Institute, USA. <https://doi.org/10.1016/j.scitotenv.2015.11.063>.
- Organisation for Economic Cooperation and Development (OECD), 2017. The governance of land use: Policy highlights. OECD, France. <https://doi.org/10.4324/9781315438689-25>.
- Özcan, Z., Başkan, O., Düzgün, H.Ş., Kentel, E., Alp, E., 2017. A pollution fate and transport model application in a semi-arid region: Is some number better than no number? *Science of the Total Environment* 595, 425–440. <https://doi.org/10.1016/j.scitotenv.2017.03.240>.
- Phuc, T.X., Nghi, T.H., 2014. Rubber expansion and forest protection in Vietnam rubber expansion and forest protection in Vietnam. Tropenbos International Vietnam, Hue city, Vietnam, 55 pages.
- Pierret, A., de Rouw, A., Chaplot, V., Valentin, C., Noble, A., Suhardiman, D., Drechsel, P., 2011. Reshaping upland farming policies to support nature and livelihoods: Lesson from soil erosion in Southeast Asia with emphasis on Lao PDR. In Marseille, France: Institut de Recherche pour le Développement (IRD); Colombo, Sri Lanka: International Water Management Institute (IWMI). <https://doi.org/10.5337/2011.213>
- Piniewski, M., Szcześniak, M., Kardel, I., Berezowski, T., Okruszko, T., Srinivasan, R., Schuler, D.V., Kundzewicz, Z.W., 2017. Hydrological modelling of the Vistula and Odra river basins using SWAT. *Hydrological Sciences Journal* 62(8), 1266–1289. <https://doi.org/10.1080/02626667.2017.1321842>.
- Prime Minister, 1998. Project of planting new five million hectares of forest. Decision number 661/QĐ-TTg, Hanoi city, Vietnam, 9 pages (in Vietnamese).
- Prime Minister, 2012. Plan for forest protection and development in the 2011-2020 period. Decision number 57/QĐ-TTg, Hanoi city, Vietnam, 12 pages (in Vietnamese).
- Prime Minister, 2017. Target program for sustainable forestry development. Decision number 886/QĐ-TTg, Hanoi city, Vietnam, 12 pages (in Vietnamese).
- Prime Minister, 2018. Project for forest protection, restoration and sustainable development in the Central Highlands from 2016 to 2030. Decision number 297/QĐ-TTg, Hanoi city, Vietnam, 6 pages (in Vietnamese).
- Qin, G., Liu, J., Wang, T., Xu, S., Su, G., 2018. An integrated methodology to analyze the total nitrogen accumulation in a drinkingwater reservoir based on the SWAT model driven by CMADS: A case study of the Biliuhe reservoir in Northeast China. *Water (Switzerland)* 10(11). <https://doi.org/10.3390/w10111535>.

- Rodríguez-Blanco, M.L., Taboada-Castro, M.M., Taboada-Castro, M.T., Oropeza-Mota, J.L., 2015. Relating nitrogen export patterns from a mixed land use catchment in NW Spain with rainfall and streamflow. *Hydrological Processes* 29(12), 2720–2730. <https://doi.org/10.1002/hyp.10388>.
- Shabani, F., Kumar, L., Esmaeili, A., 2014. Improvement to the prediction of the USLE K factor. *Geomorphology* 204, 229–234. <https://doi.org/10.1016/j.geomorph.2013.08.008>.
- Shi, W., Huang, M., 2021. Predictions of soil and nutrient losses using a modified SWAT model in a large hilly-gully watershed of the Chinese Loess Plateau. *International Soil and Water Conservation Research* 9(2), 291–304. <https://doi.org/10.1016/j.iswcr.2020.12.002>.
- Sidle, R.C., Ziegler, A.D., Negishi, J.N., Nik, A.R., Siew, R., Turkelboom, F., 2006. Erosion processes in steep terrain - Truths, myths, and uncertainties related to forest management in Southeast Asia. *Forest Ecology and Management* 224(1–2), 199–225. <https://doi.org/10.1016/j.foreco.2005.12.019>.
- Singh, L., Saravanan, S., 2020. Simulation of monthly streamflow using the SWAT model of the Ib River watershed, India. *HydroResearch* 3, 95–105. <https://doi.org/10.1016/j.hydres.2020.09.001>.
- Smarzyńska, K., Miatkowski, Z., 2016. Calibration and validation of SWAT model for estimating water balance and nitrogen losses in a small agricultural watershed in central Poland. *Journal of Water and Land Development* 29, 31–47. <https://doi.org/10.1515/jwld-2016-0010>.
- Somura, H., Kunii, H., Yone, Y., Takeda, I., Sato, H., 2018. Importance of considering nutrient loadings from small watersheds to a lake – A case study of the Lake Shinji watershed, Shimane Prefecture, Japan. *International Journal of Agricultural and Biological Engineering*, 11(5), 124–130. <https://doi.org/10.25165/j.ijabe.20181105.4351>.
- Somura, H., Takeda, I., Arnold, J.G., Mori, Y., Jeong, J., Kannan, N., Hoffman, D., 2012. Impact of suspended sediment and nutrient loading from land uses against water quality in the Hii river basin, Japan. *Journal of Hydrology* 450–451, 25–35. <https://doi.org/10.1016/j.jhydrol.2012.05.032>.
- Somura, H., Yuwono, S.B., Ismono, H., Arifin, B., Fitriani, F., Kada, R., 2019. Relationship between water quality variations and land use in the Batutege Dam watershed, Sekampung, Indonesia. *Lakes and Reservoirs: Research and Management* 24, 93–101. <https://doi.org/10.1111/lre.12221>.
- Srinivasan, R., Zhang, X., Arnold, J., 2010. SWAT ungauged: Hydrological budget and crop yield predictions in the upper Mississippi river basin. *Transactions of the American*

- Society of Agricultural and Biological Engineers 53(5), 1533–1546.
<https://doi.org/10.13031/2013.34903>.
- Stallard, R.F., 1998. Terrestrial sedimentation and the carbon cycle: Coupling weathering and erosion to carbon burial. *Global Biogeochemical Cycles* 12(2), 231–257.
<https://doi.org/10.1029/98GB00741>.
- Tien, T.M., Truc, H.C., Bo, N.V., 2015. Research Findings: Potassium Application and Uptake in Coffee (*Coffea robusta*) plantations in Vietnam. *Electronic International Fertilizer Correspondent* 42, 3–9.
- Tobin, K.J., Bennett, M.E., 2009. Using SWAT to model streamflow in two river basins with ground and satellite precipitation data. *Journal of the American Water Resources Association* 45(1), 253–271. <https://doi.org/10.1111/j.1752-1688.2008.00276.x>.
- Tram, V.N.Q., Somura, H., Moroizumi, T., 2021. The impacts of land-use input conditions on flow and sediment discharge in the Dakbla watershed, Central highlands of Vietnam. *Water (Switzerland)* 13(5), 627. <https://doi.org/10.3390/w13050627>.
- Vu, M.T., Raghavan, S.V., Liong, S.Y., 2012. SWAT use of gridded observations for simulating runoff - A Vietnam river basin study. *Hydrology and Earth System Sciences* 16(8), 2801–2811. <https://doi.org/10.5194/hess-16-2801-2012>.
- Wagner, P.D., Bhallamudi, S.M., Narasimhan, B., Kumar, S., Fohrer, N., Fiener, P., 2019. Comparing the effects of dynamic versus static representations of land use change in hydrologic impact assessments. *Environmental Modelling and Software*, 122, 103987. <http://dx.doi.org/10.1016/j.envsoft.2017.06.023>.
- Yang, Q., Almendinger, J.E., Zhang, X., Huang, M., Chen, X., Leng, G., Zhou, Y., Zhao, K., Asrar, G.R., Srinivasan, R., Li, X., 2018. Enhancing SWAT simulation of forest ecosystems for water resource assessment: A case study in the St. Croix river basin. *Ecological Engineering*, 120, 422–431. <https://doi.org/10.1016/j.ecoleng.2018.06.020>.
- Yang, X., Liu, Q., Fu, G., He, Y., Luo, X., Zheng, Z., 2016. Spatiotemporal patterns and source attribution of nitrogen load in a river basin with complex pollution sources. *Water Research* 94, 187–199. <https://doi.org/10.1016/j.watres.2016.02.040>.
- Zeng, Z., Estes, L., Ziegler, A.D., Chen, A., Searchinger, T., Hua, F., Guan, K., Jintrawet, A., Wood, E.F., 2018. Highland cropland expansion and forest loss in Southeast Asia in the twenty-first century. *Nature Geoscience* 11, 556–562. <https://doi.org/10.1038/s41561-018-0166-9>.
- Zettam, A., Taleb, A., Sauvage, S., Boithias, L., Belaidi, N., Sánchez-Pérez, J.M., 2017. Modelling hydrology and sediment transport in a semi-arid and anthropized catchment

using the SWAT model: The case of the Tafna River (Northwest Algeria). *Water (Switzerland)* 9(3), 216. <https://doi.org/10.3390/w9030216>.

Zhao, S., Peng, C., Jiang, H., Tian, D., Lei, X., Zhou, X., 2006. Land use change in Asia and the ecological consequences. *Ecological Research* 21(6), 890–896. <https://doi.org/10.1007/s11284-006-0048-2>.

APPENDIX

Neitsch, S.L., Arnold, J.G., Kiniry, J.R., Williams, J.R., 2011. Soil and Water Assessment Tool theoretical documentation, version 2009. Texas Water Resources Institute, USA. <https://doi.org/10.1016/j.scitotenv.2015.11.063>.

Tam, N.V., 2012. A Simple tool for creating txtinout files for simulating land use change with SWAT. https://github.com/tamnva/SWAT_LUC (accessed June 20 2020).